800026

TNO

AD [illegible] DDC FILE COPY

MECHANICAL PROPERTIES OF HIGHLY FILLED ELASTOMERS V

Influence of filler characteristics on tensile cree at large deformations, on rupture properties and on tensile strain recovery.

Reported by

L.C.E. Struik, H.W. Bree and F.R. Schwarzl

DDC
SEP 5 1966

CENTRAAL LABORATORIUM
T.N.O.

Best Available Copy

[redacted]
(ACCESSION NUMBER) (THRU)
R 109 (PAGES) (CODE)
(NASA CR OR TMX OR AD NUMBER) (CATEGORY)
FACILITY FORM 602

TNO

MECHANICAL PROPERTIES OF HIGHLY FILLED ELASTOMERS V

Influence of filler characteristics on tensile creep at large deformations, on rupture properties and on tensile strain recovery.

Reported by

L.C.E. Struik, H.W. Bree and F.R. Schwarzl

DDC
SEP 5 1966

132 JULIANALAAN · DELFT · TELEPHONE 01730-37000 · THE NETHERLANDS

CENTRAL LABORATORY TNO

CENTRAAL LABORATORIUM TNO
DELFT
(Holland)

077 700

(14) TR-5

~~Report No.~~ CL/66/61
~~Order No. 1507~~

(6) MECHANICAL PROPERTIES OF HIGHLY FILLED ELASTOMERS V.

Influence of filler characteristics on tensile creep at large deformations, on rupture properties and on tensile strain recovery.

(9) Technical Report

~~Reported by~~

(10) L.C.E. Struik, H.W. Bree and F.R. Schwarzl

The work reported here was carried out by:

H.W. Bree, assisted by Miss M.P. van Duijkeren	Preparation of filled polyurethanes; determination of swelling behaviour; measurement of packing density and fluidity.
C.W. v.d. Wal, G.A. Schwippert and L.C.E. Struik, assisted by R.H.J.W.A. Drent, N. v.d. Wees, G.H.J. van Velzen and J.A.M. van Veldhoven	Development of the experimental technique for tensile creep measurements.
L.C.E. Struik, assisted by Miss A.H. Bos, Miss C. Zoetewei j and J. Seffelaar	Measurement of tensile creep properties; determination of density.
J. Isings, assisted by F. Slokker	Determination of particle size distribution of fillers; microscopic investigation of vacuole formation.
R. Nauta, assisted by A. de Beukelaar	Machining of specimens.
B. de Goede (Central Technical Institute TNO, The Hague)	Classification of filler substance by sieving and air separation.

(15) ~~Office of Naval Research~~ ~~Contracts~~ N 62558-3884, N 62558-4375

(11) ~~Dated~~ April 1966

(12) 11

Technical Report No. 5

TABLE OF CONTENTS

*) Appendix I will be distributed on request.

SUMMARY

About 60 polyurethane - sodium chloride composites were prepared. The content for materials filled with single fractions ranged from 0 to 55 per cent by volume; the size of these fractions from 1 µm to 300 µm. Materials with a content of 50 to 70 per cent by volume were made by using a mixture of a coarse and a fine fraction.

For these materials, primary tensile creep and rupture properties, both at various constantly high stress levels, were determined at room temperature. Further recovery after primary creep was investigated. The filled rubbers showed a typical tensile creep behaviour, related to the growth of vacuoles in the material (de-wetting). Definite relationships were found between, respectively:

uniformity of creep over the gauge length and content of filler;
location of considerable creep on time scale and particle size as well as stress level;
shape of the creep curve and content of filler;
recovery behaviour and final strain during primary creep as well as particle size;
rupture stress and particle size, filler content and rupture time;
rupture elongation and content of filler.

Generally, the processes of de-wetting, recovery and rupture were considerably delayed by a decrease in particle size (reinforcement). The effect of de-wetting on creep, much depended on the content of filler.

1. INTRODUCTION

In the design of solid rocket motors, great importance is attributed to the mechanical behaviour of solid propellant grains. This is due to the fact that the presence or occurrence of cracks in the propellent during the ignition stage may lead to irregularities in the burning process and to malfunction of the rocket motor. Stress cracking in the propellant may occur during the storage period, as a result of shrinkage or of thermal stresses, or during the combustion period, due to the action of the combustion pressure or that of the acceleration forces.

For the proper understanding of the behaviour of solid propellant grains under those circumstances, detailed knowledge of the mechanical properties of highly filled elastomers is essential. The work described here, was started to investigate the influence of filler characteristics, such as size, shape, content and surface treatment, on the mechanical behaviour of the filled elastomers.

To avoid complications in the preparation and handling of samples, this investigation was performed on inert filled materials. The composite propellant we have in mind, consists of polyurethane rubber filled with ammonium perchlorate. The model materials investigated consisted of the same type of rubber, which, however, was filled with sodium chloride. Of course, it is realized that significant differences could exist between live and inert filled materials with respect to mechanical properties, especially to those influenced by rubber-filler interaction. It is, therefore, planned to verify general trends and conclusions found for these polyurethane - sodium chloride composites, by investigating other model materials and real propellants at a later stage.

During this investigation, model substances were prepared on a kg-scale. Only one type of polyurethane rubber was used throughout. It was filled with various amounts of several fractions of sodium chloride. The size of these fractions was varied between 1 μm and 480 μm. The amounts could be varied between 0 and 55 per cent. by volume. A filler content up to 70 per cent. by volume could be obtained by using a bimodal filler, treated with a surfactant.

As a first step, the thermo-mechanical properties of these model substances were investigated in dependence on temperature and frequency in the small deformation region of linear response. A comprehensive discussion of the influence of particle size and content of filler on shear moduli at 1 Hz, thermal expansion and bulk moduli, was given in preceding Technical Reports[1)2)3)], and in publications[4)5)6)]. Work is still in progress on shear and bulk moduli at high and very low frequencies (wave propagation and torsional creep), and will be reported later.

The small deformation elastic moduli and Poisson's ratio could be described by a simple macroscopic theory (Fröhlich-Sack-Van der Poel). According to this theory, the mechanical properties of the composite material are determined only by those of the pure filler and binder, and the filler content. Filler size slightly affected the results at very small particle size ($< 30\ \mu m$) only. Another important result is the invariance of the α-relaxation (glass-rubber transition) for content and size of filler.

A further step was the investigation of the mechanical properties of these model materials in the non-linear response range, including its upper boundary (ultimate properties), and of the applicability of knowledge of the small deformation behaviour to this technically important region. An experimental study was performed concerning the influence of particle size, content of filler and stress level on tensile creep and rupture properties at large deformations. Part of this work was described previously[7)], the completed programme will be discussed in this report. All creep measurements were carried out at room temperature. An extension of this work to other temperatures, as well as to the measurement of stress-strain diagrams at various temperatures and strain rates all on the same materials, is still in progress.

2. MATERIALS

2.1. Preparation of polyurethane rubbers

All samples of filled and unfilled polyurethane rubbers prepared for tensile creep measurements, were based on a linear (polypropylene ether)glycol (Desmophen 3600*) with a molecular weight of about 2,000. The molecules of this polyether were lengthened with toluene diisocyanate and crosslinked by means of trimethylol propane in the presence of a catalyst. Full details concerning the chemistry of the preparation of these rubbers were given in previous Technical Reports[1)2)]; they are not repeated here. Neither do we repeat a description of a systematic method for the preparation of highly filled rubbers; this method was described in detail in the most recent Technical Report[7)].

2.2. Survey of the materials prepared; routine control measurements

The aim of the tensile creep programme was to determine the influence of filler characteristics on the tensile creep properties of sodium chloride - polyurethane composites by systematic variation of content, particle size and particle size distribution of the filler. The influence of surfactants should furthermore be analyzed.

A survey of the materials prepared for this tensile creep programme is given in Fig. 1 (general) and Table 1 (detailed). Polyurethane rubbers were filled with 0, 10, 20, 30, 40, 50 and 55 per cent. by volume of single sodium chloride fractions. The particle sizes of these fractions were: 210-300 μm (fraction no. 2), 90-105 μm (no. 4), 33-40 μm (no. 6), 8-20 μm (no. 7) and < 8 μm (no. 8). Further, six materials were filled with bimodal filler substance no. 9. This filler was a mixture, in a weight ratio of 65/35 of coarse fraction no. 2 (210-300 μm) and fine fraction no. 6 (33-40 μm). The filler concentration of these bimodal filled materials ranged from 50 to 70 per cent. by volume.

Fig. 1 shows that many materials were made in duplicate or triplicate. This was done to investigate the batch-to-batch variability, or, in some cases, to replace partly inhomogeneous batches. Further, for most of the compositions, one of the materials was prepared with, and another without, use of the surfactant Asolectin**).

---

*) Farben Fabriken Bayer, Leverkusen, Germany.

**) Asolectin (Associated Concentrates Inc., New York). Filler substance treated with a solution of Asolectin in chloroform-methanol 2:1, followed by drying in vacuo at 40 °C.

Details of each batch are given in Table 1*). This table contains, for each batch, the chemical composition of the prepolymer; the content of filler, as calculated from the weights of the ingredients used, and as calculated from the density; the size and the fraction number of the filler; the concentration of surfactant, calculated as weight per cent. with respect to filler; the equilibrium swelling ratio (% vol. increase) in two different solvents (chloroform and trichloroethylene); the density, d. Details of these routine control measurements were given earlier[2].

From Table 1 it is seen that the chemical composition of the rubbery binder was approximately the same for all samples prepared (columns 2, 3, 4). This uniformity of the binder reflected itself in the swelling data (columns 10, 11). From columns 5 and 6 we see that the differences between the volume concentration as calculated from the weights of the ingredients used and as calculated from the density are smaller than 0.4 vol.% (except for samples 3600/123, 131, 133, 134, 225, 242 A and 202 A). Differences in this order were found to be of no importance in the interpretation of the tensile creep measurements.

*) See page 25

3. EXPERIMENTAL TECHNIQUE FOR THE DETERMINATION OF TENSILE CREEP

The principle of the measurement was as follows: A hanging specimen in the form of a bar-bell, was subjected to a tensile stress by loading it with a constant weight. The square cross-section in the prismatic part of the specimen was about 8.0 x 8.0 mm^2, and its length roughly 250 mm. Time-dependent tensile strain was measured by registration of the position of well-defined marks on the specimen, with regard to a precision millimeter-scale, parallel to it at a distance less than 0.5 mm.

The registration was performed automatically with a photographic camera system. In most cases, photographs were made at 2, 4, 8, 16 ..... 2^k, etc. seconds after the beginning of the creep experiment. This series of observation times is equidistant on a logarithmic time scale. By using three marks on the specimen, at a mutual distance of 75 mm, the strain could be measured over different pieces of its prismatic part. In this way, uniformity of tensile creep over the gauge length was checked. Finally, rupture time was measured by switching off a time counter by the falling weight.

All measurements have been performed in a temperature and humidity conditioned room (21 $\pm$ $\frac{1}{2}$ °C, rel. hum. 65 $\pm$ 1 %). For these creep experiments, the errors were less than:

0.2 % strain (absolute strain error);
0.1 % $\pm$ 1 second in the elapsed time;
0.02 hrs in the rupture time, if it exceeded 0.1 hrs;
$\pm$ 2 sec. in the rupture time, if it was smaller than 0,1 hrs;
0,5 % in the weight (stress).

Full details concerning the technique of grinding and further preparation of specimens, automatic recording of strain and rupture time and the procedure of the measurements were given previously[7].

4. THE RELATIONSHIP BETWEEN TENSILE CREEP, FILLER CHARACTERISTICS AND STRESS LEVEL

4.1. Tensile creep data of filled and unfilled rubbers

Two types of routine measurements have been performed: primary creep and tensile strain recovery. Here we only present data of primary creep experiments; those of the recovery measurements will be given and discussed in Chapter 5.

The complete set of 195 experimental creep curves is given in Appendix I*). Each figure gives creep curves under various high stress levels**) for one or two materials with the same filler characteristics; however, in some cases differing in the amount of surfactant used. As symbols for fracture and unloading, respectively crosses and arrows were used. Subscript g of a cross indicates that fracture was likely to be premature, due to holes visible in the fracture surface.

In view of the mastercurve representation discussed in section 4.5, it is not necessary to have all the figures of Appendix I at one's disposal. Only three typical results, given in Figs 2, 3 and 4, are presented in this report; these three figures are sufficiently illustrative.

Figs 2 and 3 show tensile strain ε vs time t under various high stress levels for polyurethane rubbers 3600/108 and 3600/134, respectively. Material 3600/108 is an unfilled rubber, 3600/134 contains 50 per cent. by volume of sodium chloride fraction no. 2 (210 - 300 μm). Finally, Fig. 4 shows tensile creep curves for polyurethane rubbers filled with various amounts of coarse sodium chloride fraction no. 2 (210 - 300 μm), under the same stress level of 3.00 kg/cm^2. The meaning of symbols in Figs 2, 3 and 4 is the same as discussed above.

4.2. Uniformity of tensile creep over the gauge length; reproducibility of the measurements within one batch

It is an important question whether the creep phenomena observed were uniform over the gauge length of the specimen, or not. If so, the strain should approximately be the same at all places of the specimen. If not, the material would be highly strained until rupture in one or more small regions, and

---

*) Appendix I will be distributed on request.

**) In this report tensile stress σ is always calculated with regard to the original cross-section of the specimen. Further, creep curves are always plotted on a logarithmic time scale.

relatively less deformed at other places of the specimen. Clearly, this non-uniformity would highly complicate the interpretation of tensile creep data.

Non-uniformity of tensile creep is illustrated in Fig. 5. Tensile creep curves are given for polyurethane rubbers filled with various amounts of sodium chloride fraction no. 6 (33 - 40 μm). Symbols like dots, triangles and rectangles, denote strain values as found over the entire gauge length. Vertical bars indicate the differences between strain measured over the upper and that over the lower half of the gauge length.

Fig. 5 demonstrates that non-uniformity chiefly occurred in the steeply rising parts of the creep curves. It increased with an increase of the content of filler. This behaviour was observed for all polyurethane rubbers investigated, not only for those represented in Fig. 5.

By analyzing all creep data available, we found that the non-uniformity was less than 1 to 2 % strain for materials with a content of filler smaller than 40 per cent. by volume. For materials filled with 40 and 50 vol.%, strain values lost their significance during the steep ascent of the creep curve. However, considerable creep was present and its location on the time-scale was very well defined, due to the high value of the slope (see Fig. 5).

For materials filled with 55 to 70 vol. %, creep phenomena became essentially non-uniform. The specimen showed creep only in small regions. The overall strain of the specimen became smaller and smaller, the higher the content of filler was. This is demonstrated by Fig. 6. It concerns polyurethane rubbers filled with bimodal sodium chloride filler substance no. 9, a mixture of coarse fraction no. 2 (210 - 300 μm) and fine fraction no. 6 (33 - 40 μm). Fig. 6 gives tensile creep curves for materials with a volume concentration of 50, 60, 65 and 70 vol. %, all under the same stress level of 4.0 kg/cm^2. Creep phenomena completely disappeared at a filler content of 70 per cent. by volume. As a consequence, we shall discuss the behaviour of this last group of materials separately (see section 6.4).

Strictly speaking, the non-uniformity should be compared with the reproducibility of the measurements for specimens originating from the same batch. This, because upper and lower half of the specimen, compared for non-uniform-

ity, came from different parts of the batch, just as do two different specimens. Typical results for duplicate measurements were discussed previously[7] (see also Appendix I, Figs 10, 18, 19, 36 and 38). It was found that the variability of the results within one batch was of the same order as the differences in creep between upper and lower half of the gauge length.

It is still an unanswered question whether non-uniformity of creep either originates from the high value of the content of filler alone, or also depends on the properties of the rubbery binder. A detailed discussion of this technically important question has been given previously by Bills and Wiegand[8]. To obtain some information, we compared the behaviour of our materials with that of "Model Substance B"*). This is a polyurethane - potassium chloride - aluminum composite with a content of filler of 61 per cent. by volume (52 vol. % KCl, 9 vol. % Al). Creep curves for this material are given in Fig. 7. Essentially non-uniform creep was observed, just as for our materials with approximately the same content of filler. However, this question of non-uniformity of tensile creep is far from being clarified. It will need further attention. Especially such conditions as type of rubbery binder, ambient temperature and humidity should be varied systematically to obtain adequate information.

4.3. The mechanism responsible for tensile creep; general structure of a primary tensile creep curve

In the most recent Technical Report[7] it was shown that the tensile creep phenomena observed were related to vacuole formation in the material. These vacuoles are caused by stress concentrations in the vicinity of the filler particles. It is not sure whether these vacuoles were formed at the rubber-filler interface (de-wetting), or in the rubbery component itself (internal cracking), or at both places simultaneously. However, we continue identifying vacuole formation with the somewhat obscure word "de-wetting".

De-wetting is a destructive non-reversible phenomenon. Once de-wetted, the mechanical properties of the material are permanently changed. This fact is demonstrated by the results of a simple experiment, summarized in Fig. 8. It concerns a test on one and the same specimen of polyurethane rubber 3600/215 A, filled with 50 vol. % of sodium chloride fraction no. 4 (90 - 105 μm). Fig. 8 is divided into two subfigures, the left one, Fig. 8 A gives

*) Aerojet General, obtained through Prof. Frudenthal (Columbia University, New York).

creep and recovery curves in terms of strain ε, and the right one, Fig. 8 B, gives creep curves in terms of tensile compliance ε/σ.

The test consisted of various experiments carried out in succession. First, the virginal specimen was subjected to the low stress level of 3.00 kg/cm^2 (curve 1). No considerable creep occurred and the recovery was instantaneous and complete (curve 1 A). During this experiment, the material properties did not change creep and recovery curves reproduced when the experiment was repeated (data not shown). We call this virginal state of the material the "non-dewetted" state. All small deformation measurements reported earlier, had been performed when the material was in this non-dewetted state.

After this first part of the test, the material was subjected to a higher stress level of 3.75 kg/cm^2. Strain ε and compliance ε/σ considerably increased with time (curve 2). After unloading, recovery was not instantaneous (curve 2 A). Finally, the specimen was reloaded to the original low stress level of 3.00 kg/cm^2 (curve 3). Compared with the original curve at 3.00 kg/cm^2, the compliance was increased over a factor of 10. It was in the order of the value at the end of the second creep experiment (curve 2).
This behaviour was not only representative for special material 3600/215 A, but was found to be characteristic for all the filled polyurethane rubbers investigated. Furthermore the duration of the experiment, short in Fig. 8, did not influence the picture.

With this de-wetting mechanism in mind, we constructed a general tensile creep curve as given in Fig. 9. At short times, the material is in the non-dewetted state. The low (constant) strain level is controlled by the stress-strain relationships corresponding to this state. Its mechanical properties are discussed in section 4.4. After some time, de-wetting becomes noticeable as an increase of strain with time. The effect of the de-wetting process on strain, and its location on the time scale, will depend on stress level, size and content of filler (sections 4.5 and 4.6).

The de-wetting disorganizes the material. It is possible that the rubbery cinder cannot endure this, so that the specimen breaks somewhere in the steeply increasing part of the creep curve before de-wetting is complete. This behaviour was actually found for all the materials investigated. Clearly, the rupture properties are, in this case, largely connected with the de-

wetting properties (see 6.2. and 6.3.). However, when the rubbery binder is strong enough to endure the disorganization due to de-wetting, a constant end level for the strain should be found (dotted line in Fig. 9). As stated above, a completely de-wetted state before rupture has never been found for our materials.

4.4. The mechanical properties in the non-dewetted state

The small deformation as well as the short time*) tensile creep measurements concerned the non-dewetted state. It is an interesting question whether for this non-dewetted state, stress-strain relationships and their dependence on filler characteristics for large deformations can be predicted from the corresponding knowledge about small deformation moduli. To check this, the relative Young's modulus+) E_r of the non-dewetted material was calculated in two ways: First, from small deformation shear modulus G and bulk modulus K, both at 21 °C; and, secondly, from the approximately constant level of tensile creep curves at short times.

Results are given in Fig. 10, where the relative modulus E_r is plotted vs the particle size of the filler, with the content of filler as a parameter. Horizontal bars give values for E_r from tensile measurements. The length of the bars corresponds to the size width of the filler fraction. Small deformation moduli are given by symbols like triangles etc., placed at the logarithmic size mean of the corresponding filler fractions.

From Fig. 10 it is clear that both moduli fairly well agree with each other. Consequently, the constant strain (level) at the beginning of tensile creep curves can be predicted from small deformation moduli. We refer to previous work[1)2)3)4)6)] for a detailed discussion of the influence of filler characteristics on these moduli.

---

*) Of course, the time that the material stays in the non-dewetted state depends on the stress level.

+) The relative modulus of a filled material is the ratio of the modulus of the filled to that of the unfilled material. This relative measure of the influence of the filler was introduced to avoid complications due to differences in experimental conditions between shear, bulk and tensile measurements (rel. humidity).

4.5. The influence of the stress level on the development of tensile creep; a time-stress shifting procedure for data reduction

Tensile creep curves of filled polyurethane rubbers largely depended on the stress level; this is illustrated by the set of creep curves under various high stresses for material 3600/134, given in Fig. 3. We observe an enormous influence of the stress level on the location of the creep process in time scale. A change in stress from 2.0 to 3.5 kg/cm^2 induced an acceleration by a factor of 10^4. However, we got the impression that the shape of the creep curves only slightly depended on the stress level. Furthermore, this dependence almost vanished when creep curves were replotted as tensile compliance F vs the logarithm of time.

This fact, i.e. the shifting by variation of stress without considerable change in shape, forms the basis of a time-stress shift procedure used for data reduction. It was presented previously, and could be explained by a qualitative theoretical discussion[7]. The procedure is analogous to the well-known time-temperature reduction method[9] used for mechanical and dielectrical relaxation data of amorphous polymers in the glass to rubber transition.

Fig. 11 demonstrates the method. It concerns polyurethane rubber 3600/133, filled with 40 vol. % of coarse sodium chloride fraction no. 2 (210 - 300 μm). Tensile compliance F is plotted vs log t. Full lines are the experimental curves, measured at various stress levels. We choose the stress σ_o of 3.00 kg/cm^2 and the corresponding creep compliance curve as references. Curves at other stress levels are then shifted to best overlap with the reference curve. Those shifted curves are given in Fig. 11 as thin dotted lines. The shift factors used, in decades of time, are noted above the arrows connecting original and shifted lines. A subfigure in Fig. 11 (top left) gives the shift log a (σ,σ_o) as a function of the stress σ.

The usefulness of this procedure is measured by the maximum width of the strip in the compliance-time plane in which all best overlapping curves are situated. In Fig. 11, this maximum width is indicated by capital S. For material 3600/133, this scatter S was large. Much better results were obtained for other materials. We only chose material 3600/133 to illustrate

clearly in which manner S has been defined.

This method was applied to reduce all tensile creep data of Appendix I. The "true stress" formula

$$F = \frac{\varepsilon}{\sigma(1 + \varepsilon)} \qquad (1)$$

was used for the calculation of the compliance. Results are given in Figs 12-18. Figs 12-16 present the mastercurves. Each figure concerns materials filled with the same amount of various sodium chloride fractions. The sequence of the figures is that of increasing content of filler. Materials with different batch numbers are distinguished from each other. The reference stress σ_o in all figures is 6.00 kg/cm^2. Numerical data for scatter S are given in Appendix II, Table II,6 for each mastercurve.

Shift-stress relationships are given in Figs 17 and 18, numerical data in Appendix II. Fig. 17 is divided into 5 subfigures, each concerning materials filled with various amounts of the same fraction. Values for log $a(\sigma,\sigma_o)$ as found for materials with different values of the content of filler are distinguished by different characters. From Figs 17,A to 17,E we observe no systematic influence of the content of filler on the shift-stress functions. The absence of a large influence of filler size is illustrated in Fig. 18. All data of Fig. 17 were replotted in this single figure. Values for log $a(\sigma,\sigma_o)$ as found for materials filled with different fractions are distinguished. The scatter in Fig. 18 is somewhat greater than that in each subfigure of Fig. 17. The maximum deviations from the mean curve are about one time decade. However, compared with the total variation in log $a(\sigma,\sigma_o)$ from -7 to +4, this scatter is small.

Finally, we observed that the scatter S in the mastercurves, due to the time-stress reduction was smaller than the batch-to-batch variability. This justifies the data reduction method. As a consequence, we shall further discuss the influence of filler characteristics on the development of tensile creep by using these mastercurves only.

4.6. The influence of size and content of filler on the development of tensile creep

The mastercurves of Figs 12-17 were replotted in Figs 19-23. Now each figure concerns materials filled with various amounts of the same sodium chloride fraction. The sequence of the figures is that of increasing filler size. The reference stress level again is 6.00 kg/cm^2. Mastercurves for materials of the same composition but different batch numbers are not distinguished. Each curve gives the mean course of the creep curve for the corresponding filler characteristics.

We observe the influence of filler size from the first set of figures (Figs 12-16) and that of the content of filler from the second set (Figs 19-23). We make the following remarks:

(a) Creep phenomena became more and more pronounced, the higher the content of filler was; see for example Figs 4 and 21. This effect is connected with two others. First, the compliance F_u in the non-dewetted state largely decreased with increasing content of filler (see section 4.4). Second, the mean compliance at break $\overline{F_{br}}$ equalled the value for the unfilled rubber within a factor of 2 for all materials investigated (see section 6.4). Both facts are given in Fig. 24 for materials filled with 0 to 50 vol. % of coarse sodium chloride fraction no. 2 (210 - 300 μm). The compliance range covered during de-wetting equals the difference between $\overline{F_{br}}$ and F_u (see Fig. 24). We clearly see from Fig. 24 that it considerably increased with an increase of the content of filler. For materials filled with other sodium chloride fractions, analogous results were obtained.

(b) The slope of the creep curves largely increased with increasing filler concentration; this can be seen clearly from Fig. 4. At a low content of filler, the creep curve was approximately a straight line vs log t (see Fig. 12). At a high content of filler, the creep curve consisted of a constant strain (compliance) level at short times and a very steep upward part just before break (see Fig. 16). This effect implies that the logarithmic time interval in which most of the de-wetting occurred became narrower, the higher the content of filler was. (Compare, for in-

stance, Fig. 11 with Fig. 16.) It is therefore possible to define a characteristic de-wetting time τ for materials with a high content of filler. We define τ as the time at which F reached the value of 0.025 kg/cm^2, approximately halfway between non-dewetted state and break. We see from Figs 15 and 16 that the time interval in which most of the de-wetting occurred lies around τ and has a width smaller than 0.5 to 1 time decade. This was true for rubbers filled with 40 and 50 vol. % of sodium chloride; τ lost its significance for materials filled with less than 30 vol. %.

(c) The location of considerable creep on time scale largely shifted to shorter times with an increase of filler size (see Figs 12-16); the influence of filler content was much smaller (see Figs 19-23). A further illustration of both facts is given in Fig. 25. For rubbers filled with 30, 40 and 50 vol. % of sodium chloride, characteristic de-wetting time τ is plotted vs particle size in a double logarithmic diagram. Again we observe that τ did not depend much on the content of filler; however, the influence of filler size was very large. From fine fraction no. 8 (< 8 μm) to coarse fraction no. 2 (210 - 300 μm), τ changed 8 to 9 decades in time. This delaying effect of the smallest particles implies reinforcement. This is demonstrated in Fig. 26. Stress σ, necessary to produce a τ-value of 0.1 hrs is plotted vs the particle size of the filler for materials filled with 40 vol. % of sodium chloride. Going from coarse to fine fraction, we observe a reinforcement by a factor of 3.

5. TENSILE STRAIN RECOVERY

Part of the primary creep experiments were finished by unloading of the specimen. After that, its recovery was studied as a function of time. Results are given in Fig. 27, and data about the corresponding primary creep experiments in Appendix III. Fig. 27 is divided into 4 subfigures. Each of these concerns polyurethane rubbers filled with various amounts of the same fraction of sodium chloride. Note the nomenclature ε' for strain during recovery.

Recovery curves, given in Fig. 27, were plotted in double logarithmic diagrams. In this way, we easily observe an important feature. All the curves of Fig. 27 are approximately parallel to each other. They can be superposed by a vertical shift. This shift along the logarithmic strain scale means division or multiplication on a linear scale. Consequently, normalized creep curves, obtained by dividing strain ε' by its value at a characteristic time t_1, must reduce to one single mastercurve.

The choice of t_o is arbitrary. We used a value of 1 h, and denote strain ε' at that time by ε_1'. The mastercurve is given in Fig. 28*). Data concerning different filler fractions are distinguished by different characters. The scatter around this curve, representing the 30 recovery curves of Fig. 27, turns out to be 10 to 20 % (relative error). The mastercurve is independent of size and content of the filler, and of the history of the specimen during primary creep prior to recovery. This means that a recovery curve is completely determined by the strain value ε_1' at a recovery time of 1 h. Multiplication of the mastercurve given in Fig. 28 by this parameter ε_1' results in the actual recovery curve.

Consequently, we can restrict ourselves to ε_1' for studying the influence of filler characteristics and history of the specimen on tensile strain recovery.

---

*) In practice we initially shifted all recovery curves to best overlap. After that, we shifted the mastercurve obtained in this manner to be 1 at a recovery time of 1 h.

This parameter ε_i' is related to the history of the specimen and to particle size. This is demonstrated in Fig. 29, where ε_i' is plotted vs the contribution ε_d of de-wetting during primary creep. ε_d was calculated as the difference between ε_{max} at unloading and strain ε_o in the non-dewetted state. From Fig. 29 we observe distinct correlations between ε_i' and ε_d *). Within 1 to 2 % strain, ε_i' was proportional to ε_d. However, the proportionality constant $\varepsilon_i'/\varepsilon_d$ depended on particle size. It was observed that the recovery after a recovery time of 1 h was the more complete, the larger the particle size was. This means that, just as was found for primary creep (section 4.6) and for rupture (section 6.3), also recovery was considerably delayed for rubbers filled with the finest fractions. However, we believe that for the case of creep and rupture and the case of recovery, the reasons for this effect are different. At a later stage of this investigation it is planned to return in more detail to the recovery behaviour of filled rubbers.

*) Somewhat better correlations could be found between ε_i' and the contribution of de-wetting to the tensile compliance at unloading. We restricted ourselves to ε_d for simplicity.

6. RUPTURE PROPERTIES IN RELATION TO FILLER CHARACTERISTICS

6.1. Data of rupture stress

Rupture stress, σ_{br}, depended on size and content of filler and on rupture time, t_{br}. The experimental data varied from batch to batch and might be influenced by the concentration of surfactant Asolectin. We investigated the influence of all these variables by using a method illustrated in Fig. 30. It concerns polyurethane rubbers filled with various amounts of coarse sodium chloride fraction no. 2 (210 - 300 μm). Rupture stress, σ_{br}, is plotted vs rupture time, t_{br}, for various values of the content of filler. We determined σ_{br} for 4 fixed values of t_{br} by graphical interpolation. These standard values were 10^{-1}, 10^{0}, 10^{1} and 10^{2} hrs. Figures like Fig.30 were constructed for all materials investigated, and the same interpolation method has been followed.

Numerical results are given in Appendix IV. It was found that the influence of surfactant Asolectin was in the order of the batch-to-batch variations*). We therefore neglected it and averaged all data available for materials of the same filler characteristics.

6.2. The relationship between rupture time and rupture stress

From the experimental results given in Appendix IV we derived 4 figures. One of these is given in Fig. 31. Rupture stress, σ_{br}, is plotted vs content of filler, c, at various values of the filler size, δ. The rupture time for Fig. 31 was 10^{1} hrs. Analogous results were obtained for the other values selected for t_{br} (10^{-1}, 10^{0} and 10^{2} hrs). Rupture stress, σ_{br}, was found to depend linearly on the logarithm of rupture time, t_{br}. This is demonstrated by Figs 32 and 33 in the following way. We chose a rupture time of 1 h as a reference. σ_{br} at other values of t_{br} could be found from the corresponding value at the reference time, by adding a quantity $S(t_{br})$, given in Fig. 32. In formula:

$$\sigma_{br}(t_{br}) = \sigma_{br}(1) + S(t_{br}). \qquad (2)$$

---

*) Also for moduli at small deformation, no significant influence of surfactant Asolectin was found; see Report CL/65/88, Quarterly Progress Report, March 1, 1965, through May 31, 1965.

The result of this reduction method is given in Fig. 33. This figure contains all superposed data for rupture times of 10^{-1}, 10^{0}, 10^{1} and 10^{2} hrs.

In Fig. 33 we observe a scatter in stress of about 0.25 kg/cm^2. This scatter is 5 times smaller than the maximum value of $S(t_{br})$ (1.25 kg/cm^2) used for the superposition.

The principal result of this superposition method is that we can now see from Fig. 33 that the influence of size and content of filler on rupture stress is nearly independent of the influence of rupture time. This at least holds for the experimental time range from 10^{-1} to 10^{+2} hrs (3 decades).

6.3. The fluence of size and content of filler on rupture stress

We clearly see from Fig. 33 that there exists a relationship between σ_{br}, the content of filler, c, and the particle size, δ. For coarse fraction no. 2 (210 - 300 μm), σ_{br} decreased monotonically with increasing content of filler, c. For materials filled with fractions with a size smaller than about 100 μm, σ_{br} showed a maximum at a content of filler between 20 and 30 per cent. by volume. Finally, we observe that for bimodal filled rubbers with a content of filler exceeding 50 vol. %, σ_{br} was approximately independent of the content of filler.

The rupture stresses for the filled rubbers could be higher than those for the unfilled rubbers. This reinforcement became the more effective, the smaller the particle size was. This is demonstrated by Fig. 34. The ratio ν of the maximum stress σ_{br} over σ_{br} for the unfilled rubber is plotted vs particle size. The reinforcement amounted to a factor of 2 for the smallest particles. Note that the results given in Fig. 34 are nearly independent of the rupture time.

Finally, we plotted σ_{br} vs particle size δ at various values of the content of filler in Fig. 35. The value of t_{br} for this figure was 10^{1} hrs. Results shown in this figure are experimental data, without use of the reduction method of formula (2). Results for other values of t_{br} can be found by using the shift function of Fig. 32. We conclude from Fig. 35 that the particle size is at least equally important for the ultimate strength of the filled polyurethanes as the content of filler.

6.4. The influence of size and content of filler on rupture strain

For strain at break ε_{br}, it was not possible to construct figures like Fig. 30, and to derive from those relationships between ε_{br}, the filler characteristics and the rupture time t_{br}. The spread in the results was too large. The same was found to be true for the compliance F_{br} at break, defined by

$$F_{br} = \frac{\varepsilon_{br}}{\sigma_{br}(1 + \varepsilon_{br})} \qquad (3)$$

Therefore we used a rough measure for these two quantities. All experimental values of ε_{br} for the various materials of the same filler characteristics, found for several values of the rupture stress, were averaged. This results in an arithmatic mean $\overline{\varepsilon_{br}}$. In the same manner we found the mean $\overline{F_{br}}$ for the compliances at break. From experimental evidence, $\overline{\varepsilon_{br}}$ and $\overline{F_{br}}$ give the mean levels of both quantities for fracture between 10^{-2} and 10^{2} hrs. Further it was observed that the actual values of ε_{br} and F_{br} dit not differ more than a factor of 2 from $\overline{\varepsilon_{br}}$ and $\overline{F_{br}}$.

Results are given in Fig. 36 for $\overline{\varepsilon_{br}}$ and in Fig. 37 for $\overline{F_{br}}$. Both quantities are plotted on a logarithmic scale vs the content of filler. Results as found for materials filled with different sodium chloride fractions are distinguished from each other by different characters. The dotted line in Fig. 37 denotes the compliance F_u of the non-dewetted material.

For filler concentrations smaller than 50 vol. %, $\overline{\varepsilon_{br}}$ and $\overline{F_{br}}$ did not vary more than a factor of 2 with a change in the content and the size of the filler. However, for filler contents exceeding 50 vol. %, both quantities drop over about 1.5 decade. This considerable decrease in $\overline{\varepsilon_{br}}$ and $\overline{F_{br}}$ probably will not be due to the bimodality of the filler but due to the high filler concentration. This because the "bimodal" point at 50 vol. % lies between the points found for "unimodal" filled rubbers and the "unimodal" point at 55 vol. % lies between the "bimodal" points at 50, 60, 65 and 70 vol. %.

The reason for this strong decrease in the ultimate strain and compliance with increasing filler content is as follows: For highly filled rubbers, the specimen creeps non-uniformly (section 4.2). There is only de-wetting followed by rupture in small regions. The total strain of the specimen remains small

and becomes approximately equal to that of the non-dewetted material. This can be seen from Fig. 37. Consequently, for rubbers filled with 65 and 70 vol. % of sodium chloride, $\overline{F_{br}}$ equals F_u. We thus find that non-uniform creep is the reason of the large decrease in ultimate strain.

This behaviour of highly filled polyurethane rubbers helps us to predict the compliance $\overline{F_{br}}$ at break. As $\overline{F_{br}}$ equals the compliance F_u of the non-dewetted material (see Fig. 37) and F_u equals the value as found from small deformation measurements (see section 4.4), we can consequently predict $\overline{F_{br}}$. The only variable not known is the time of break t_{br}. Its dependence on the stress level and filler characteristics will be investigated extensively in a later stage.

Further it is an unsolved problem how to predict shear modulus G, and also Young's modulus E, for these highly bimodal filled rubbers. As mentioned previously[6], actual values for G differed 50 to 100 % at a content of 70 vol. % from the values as predicted by Van der Poel's theory from filler content only. A revised theory, taking into account the bimodality of the filler, i.e. the mixing ratio of coarse to fine fraction, is in development.

CONCLUSIONS

1. Polyurethane rubbers filled with 0 to 55 per cent. by volume of single sodium chloride fractions could be prepared. The size of these fractions ranged from 1 to 300 μm. Materials containing 50 to 70 vol. % could be made by using a filler with a bimodal size distribution.

2. A semi-automatic method was developed for the determination of tensile creep, tensile strain recovery and rupture properties under high constant stresses, at controlled temperature of 21 $\pm \frac{1}{2}$ °C and relative humidity of 65 $\pm$ 1 %.

3. The strain within the gauge length of the specimen was uniform for polyurethane rubbers filled with 40 per cent. by volume or less. Non-uniformity increased considerably when the filler content exceeded 50 vol. %. Essentially non-uniform creep behaviour was found for rubbers filled with 65 and 70 per cent. by volume.

4. The variability of creep properties was much smaller for specimens from the same batch than for specimens from different batches of the same composition. This batch-to-batch variation was smaller than the differences between materials differing one step in the experimental series of values for the content of filler (0, 10, 20, 30, 40, 50, 55 vol. %) or for the particle size of the filler (210-300 μm, 90-105 μm, 33-40 μm, 8-20 μm, and < 8 μm).

5. Tensile creep phenomena observed could be related to vacuole formation in the material (de-wetting). At shorttimes, the material was in a non-dewetted state. After some time, de-wetting became visible as a monotonical increase with time of strain and compliance. Mostly the de-wetting process was interrupted by break of the specimen. An obvious end level for strain at long times was never found.

6. De-wetting is a destructive, non-reversible phenomenon. Once de-wetted, the mechanical properties of the material have permanently changed.

7. The tensile properties of the non-dewetted material could be predicted from small deformation moduli.

8. Creep compliances, relating to the same material under various stresses, could be reduced to a single mastercurve by a time-stress shifting procedure. The time-stress shift functions turned out to be independent of content or size of the filler.

9. The position of the de-wetting process on the time scale largely depended on size and slightly depended on content of filler. The change in strain induced by de-wetting, ε_d, considerably depended on content and slightly depended on size of filler.

10. When all tensile strain recovery curves were normalized, i.e. divided by the strain value ε_1' at a recovery time of 1 h, all experimental points lie on one single mastercurve. This mastercurve was independent of size and content of filler and of the conditions of the primary creep experiment preceding the recovery. Strain ε_1' was proportional to the contribution ε_d of de-wetting to the strain during primary creep. However, $\varepsilon_1'/\varepsilon_d$, the fraction of the strain not recovered after 1 h, much increased with decreasing filler size, i.e. the recovery was delayed for the small particles.

11. Rupture stresses, σ_{br}, depended on size and content of filler, and on rupture time. The influence of filler characteristics on rupture stress was independent of the influence of rupture time on rupture stress. For a coarse filler (210-300 μm), σ_{br} decreased monotonically with increasing content of filler, for finer fractions a maximum value for σ_{br} was found at a filler content of about 25 vol. %. This reinforcement amounted to 100 % for rubbers filled with the finest fraction ($< 8\ \mu$m). Further, there was a slight, linear dependence of rupture stress on the logarithm of rupture time.

12. For highly bimodal filled rubbers, rupture stress was found to be independent of the content of filler.

13. The strains and compliances at break did not vary more than a factor of 2 for rubbers filled with less than 50 per cent. by volume. For higher filler concentrations, rupture compliances dropped over 1.5 decade. Values equal to those of the non-dewetted material were reached at a filler content of 65 to 70 vol. %. The reason for this effect was the non-uniformity of creep.

REFERENCES

1. F.R. Schwarzl, Mechanical Properties of Highly Filled Elastomers, Technical Report No. 1, Contract N 62558-2822 Office of Naval Research, Central Laboratory T.N.O., Delft, July, 1962.

2. F.R. Schwarzl, Mechanical Properties of Highly Filled Elastomers II, Influence of particle size and content of filler on tensile properties and shear moduli, Technical Report No. 2, Contracts N 62558-2822 and N 62558-3243 Office of Naval Research, Central Laboratory T.N.O., Delft, April, 1963.

3. F.R. Schwarzl, Mechanical Properties of Highly Filled Elastomers III, Influence of particle size and content of filler on thermal expansion and bulk moduli, Technical Report No. 3, Contracts N 62558-3581 and N 62558-3884 Office of Naval Research, Central Laboratory T.N.O., Delft, June, 1964.

4. F.R. Schwarzl, H.W. Bree and C.J. Nederveen, Mechanical Properties of Highly Filled Elastomers I, Proc. 4th Int. Congr. Rheology (Providence, 1963), E.H. Lee (Ed.), Interscience/Wiley, N.Y. (1965) Vol. 3, 241-263.

5. C.W. van der Wal, H.W. Bree and F.R. Schwarzl, Mechanical Properties of Highly Filled Elastomers II, J. Appl. Polymer Sci. 9 (1965) 2143-2166.

6. F.R. Schwarzl et al, On Mechanical Properties of Unfilled and Filled Elastomers, Proc. Int. Conf. on Mech. and Chem. of Solid Propellants, Lafayette, 1965, in press.

7. H.W. Bree, F.R. Schwarzl and L.C.E. Struik, Mechanical Properties of Highly Filled Elastomers IV, Influence of particle size and content of filler on tensile creep at large deformations, Technical Report No. 4, Contracts N 62558-3884 and N 62558-4375 Office of Naval Research, Central Laboratory T.N.O., Delft, July, 1965.

8. K.W. Bills and J.H. Wiegand, Relation of Mechanical Properties to Solid Rocket Motor Failure, A.I.A.A. Journal, 1 (1963) 2116-2123.

9. J.D. Ferry, Viscoelastic Properties of Polymers, John Wiley & Sons, Inc., New York, 1961.

Table 1 Composition and properties of NaCl filled samples p

1	2	3	4	5	6	7	8	9	1
sample no.	composition prepolymer g/100 g polyether Desmophen 3600			filler content vol. % NaCl		fraction No.	NaCl-filler particle size	surfactant concentration (weight % on NaCl)	(%
	TDI	TMP	DB	from ingredients	from d		µm		chl for
3600/108	20.4	4.0	1.5	-	-	-	-		4
3600/227	19.7	4.0	-	-	-	-	-		3
3600/138	20.4	4.0	3.5	9.8	9.9				3
3600/123	20.4	4.0	4.0	19.5	20.3				4
3600/131	20.4	4.0	3.5	29.5	30.2				3
3600/133	20.4	4.0	2.5	39.6	40.4				4
3600/222	19.7	4.1	3.0	39.5	39.9	2	210-300		3
3600/230 A	19.8	4.0	2.5	39.6	39.6			0.11	3
3600/134	20.4	4.0	2.0	49.6	51.1				4
3600/223	19.7	4.1	2.0	49.7	50.0				3
3600/231 A	19.7	4.0	2.0	49.7	49.5			0.11	3
3600/176	19.7	4.0	1.5	54.8	54.0				3
3600/177 L	19.7	4.0	1.5	54.5	54.4			0.55	3
3600/203 A	19.7	4.1	2.0	54.7	54.9			0.02	3
3600/204	19.8	4.1	2.0	54.7	54.9				3
3600/210	19.7	4.1	3.0	19.9	19.9				3
3600/211	19.7	4.1	2.0	29.8	29.9				3
3600/214 A	19.8	4.1	2.0	29.8	29.8			0.04	3
3600/212	19.7	4.1	1.5	39.9	39.7	4	90-105		3
3600/216 A	19.7	4.1	1.5	39.8	39.8			0.04	3
3600/213	19.7	4.0	1.5	49.8	49.4				3
3600/215 A	19.7	4.1	1.5	49.8	49.7			0.04	3
3600/164	19.7	4.0	3.0	9.8	9.8				3
3600/217	19.8	4.0	3.0	9.8	9.7	6	33-40		3

*) At 20 °C except as stated otherwise.

A = Acolectin L = Lecithin

1 Composition and properties of NaCl filled samples prepared

5	6	7	8	9	10	11	12	
filler content vol. % NaCl		fraction No.	NaCl-filler particle size	surfactant concentration (weight % on NaCl)	swelling 23 °C (% vol.increase)		d*) (g/cm³)	
from ingredients	from d		µm		chloroform	trichloroethylene		
-	-	-	-		412	310	1.0715	
-	-	-	-		383	292	1.0722	
9.8	9.9				396	300	1.1792	(23°)
19.5	20.3				402	304	1.2928	(23°)
29.5	30.2				394	305	1.4016	(23°)
39.6	40.4				410	310	1.5140	(23°)
39.5	39.9	2	210-300		370	282	1.5092	
39.6	39.6			0.11	391	291	1.5068	
49.6	51.1				410	301	1.6309	(23°)
49.7	50.0				365	273	1.6200	
49.7	49.5			0.11	385	295	1.6155	
54.8	54.0				324	256	1.6865	
54.5	54.4			0.55	376	285	1.6689	
54.7	54.9			0.02	385	285	1.6744	
54.7	54.9				340	265	1.6740	
19.9	19.9				365	281	1.2902	
29.8	29.9				345	265	1.3996	
29.8	29.8			0.04	386	293	1.3988	
39.9	39.7	4	90-105		389	294	1.5070	
39.8	39.8			0.04	381	297	1.5084	
49.8	49.4				370	276	1.6142	
49.8	49.7			0.04	385	287	1.6170	
9.8	9.8				380	291	1.1797	
9.8	9.7	6	53-40		378	289	1.1787	

se.

B

Table 1 (Continued)

1	2	3	4	5	6	7	8
sample no.	composition prepolymer g/100 g polyether Desmophen 3600			filler content vol. % NaCl		fraction no.	NaCl-f partic size
	TDI	TMP	DB	from ingredients	from d		
3600/166	19.7	4.0	2.0	19.7	19.6		
3600/218	19.7	4.0	2.0	19.8	19.8		
3600/168	19.7	4.1	1.5	29.8	29.7		
3600/219	19.7	4.0	1.5	29.8	29.9		
3600/239 A	19.7	4.0	1.5	29.8	29.4	6	33-
3600/170	19.7	4.0	1.5	39.8	39.7		
3600/175	19.8	4.0	1.5	39.6	39.3		
3600/240 A	20.1	4.0	1.6	39.8	39.7		
3600/220	19.7	4.1	1.5	39.8	39.9		
3600/205 A	19.7	4.1	1.5	39.8	39.6		
3600/206 A	19.7	4.1	1.5	49.8	49.5		
3600/178	19.7	4.0	3.0	9.7	9.9		
3600/224	19.7	4.0	3.0	10.4	10.6		
3600/232 A	19.7	4.0	3.0	9.8	9.5		
3600/180	19.7	4.0	2.0	19.8	19.4	7	8-
3600/225	19.7	4.2	2.0	19.9	18.2		
3600/233 A	19.7	4.0	2.0	19.8	19.8		
3600/181	19.6	4.1	1.5	29.9	29.8		
3600/234 A	19.7	4.0	1.5	29.8	29.7		
3600/235 A	19.7	4.0	1.5	39.8	39.7		
3600/185	19.7	4.0	3.1	9.9	9.7		
3600/236 A	19.7	4.0	3.0	9.8	9.8		
3600/190	19.7	4.0	3.0	9.9	9.7		
3600/186	19.7	4.0	2.0	19.8	19.8	8	< 8
3600/237 A	19.8	4.0	2.0	19.8	19.8		
3600/188	19.7	4.0	1.5	29.7	29.7		
3600/238 A	19.7	4.0	1.5	29.8	29.7		
3600/191 L	19.7	4.0	1.5	39.8	39.5		
3600/208 A	19.8	4.1	2.0	49.7	49.8	9	{65:21
3600/241	20.1	4.0	2.0	50.0	49.8		{35: 3
3600/209 A	19.8	4.1	1.4	59.8	59.6		
3600/242 A	20.1	4.0	1.5	64.8	64.2		
3600/202 A	19.8	4.1	1.5	70.0	69.3		
3600/207 A	19.7	4.1	1.5	70.0	69.6		

*) At 20 °C except as stated otherwise.

A = Asolectin L = Lecithin

A

(Continued)

5	6	7	8	9	10	11	12
filler content vol. % NaCl		fraction no.	NaCl-filler particle size	surfactant concentration (weight % on NaCl)	swelling 23 °C (% vol. increase)		d*) (g/cm³)
from ingredients	from d		µm		chloroform	trichloroethylene	
19.7	19.6				370	282	1.2871
19.8	19.8				365	276	1.2890
29.8	29.7				365	277	1.3980
29.8	29.9				360	268	1.3995
29.8	29.4	6	33-40	0.05	380	273	1.3944
39.8	39.7				341	265	1.5070
39.6	39.3				337	261	1.5036
39.8	39.7			0.05	378	266	1.5089
39.8	39.9				356	265	1.5090
39.8	39.6			0.1	377	278	1.5061
49.8	49.5			0.05	383	281	1.6144
9.7	9.9				363	271	1.1804
10.4	10.6				362	274	1.1878
9.8	9.5			0.05	372	281	1.1766
19.8	19.4	7	8-20		367	279	1.2854
19.9	18.2				365	275	1.2719
19.8	19.8			0.05	372	275	1.2896
29.9	29.8				331	260	1.3990
29.8	29.7			0.05	367	265	1.3982
39.8	39.7			0.05	371	261	1.5079
9.9	9.7				351	270	1.1783
9.8	9.8			0.06	370	277	1.1796
9.9	9.7				339	261	1.1782
19.8	19.8	8	< 8		336	262	1.2888
19.8	19.8			0.06	360	256	1.2892
29.7	29.7				340	264	1.3977
29.8	29.7			0.06	355	246	1.3984
39.8	39.5			1.9	403	308	1.5058
49.7	49.8	9	65:210-300	0.02	374	276	1.6182
50.0	49.8		35: 33-40		310	245	1.6188
59.8	59.6			0.02	375	278	1.7258
64.8	64.2			0.02	315	235	1.7766
70.0	69.3			0.02	348	266	1.8321
70.0	69.6			0.02	349	266	1.8246

erwise.

thin

B

LEGEND TO FIGURES

Fig. 1. Survey of the materials prepared and investigated for tensile creep properties.

Fig. 2. Tensile creep under various high stress levels and tensile strain recovery for unfilled polyurethane rubber 3600/108; temp. 21 °C; rel. hum. 65 %.

Fig. 3. Tensile creep under various high stress levels for polyurethane rubber 3600/134, filled with 50 vol. % of sodium chloride fraction no. 2 (210 - 300 µm); temp. 21 °C; rel. hum 65 %.

Fig. 4. Tensile creep for polyurethane rubbers filled with various amounts of coarse sodium chloride fraction no. 2 (210 - 300 µm) under the stress level of 3.00 kg/cm^2; temp. 21 °C; rel. hum 65 %. The curve shown for the unfilled rubber was interpolated from results given in Fig. 2.

Fig. 5. Tensile creep curves for several materials as measured over different parts of the specimen. Symbols concern strain values as found over the entire gauge length. Vertical bars denote the differences between strain values found over the upper and lower halves of the gauge length.
Temp. 21 °C; rel. hum. 65 %.

Fig. 6. Tensile creep for polyurethane rubbers filled with 50, 60, 65 and 70 vol. % of bimodal sodium chloride substance no. 9 (210 - 300 µm, 33 - 40 µm) under the stress level of 4.0 kg/cm^2. Temp. 21 °C; rel. hum. 65 %.

Fig. 7. Tensile creep under various high stress levels for "Model Substance B", a polyurethane rubber filled with 52 vol. % KCl and 9 vol. % Al. Temp. 21 °C; rel. hum. 65 %.

Fig. 8. Mechanical test series of specimen 3600/215 A, no. 5, containing 50 vol. % of sodium chloride fraction no. 4 (90 - 105 µm); temp. 21 °C; rel. hum. 65 %.
Curve 1 : tensile creep of the virginal specimen under the stress level of 3.00 kg/cm^2, unloading after 0.044 hrs.

Curve 1 A : recovery stopped after 0.24 h.

Curve 2 : tensile creep at a high stress level of 3.75 kg/cm^2; unloading after 0.2 h.

Curve 2 A : recovery stopped after 0.55 h.

Curve 3 : tensile creep under the original low stress level of 3.00 kg/cm^2; unloading after 0.1 h.

The experiments were performed one directly after the other.

Fig. 9. Schematic tensile creep curve for a filled polyurethane rubber.

Fig. 10. Relative Young's modulus E_r of non-dewetted materials vs particle size; content of filler as parameter. Horizontal bars give E_r calculated from tensile creep measurements. Characters like circles etc. denote E_r, calculated from small deformation shear measurements reported earlier[2)4)6)].
Temp. 21 °C; rel. hum. 65 % for tensile creep and 0 % for shear measurements.

Fig. 11. Illustration of the time-stress shift procedure on creep data of material 3600/133, filled with 40 vol. % of NaCl fraction no. 2 (210 - 300 μm); temp. 21 °C; rel. hum. 65 %.
Full lines represent the original creep compliances; thin dotted lines the shifted creep compliances; the dashed line is the master curve.

Fig. 12. Tensile compliance F vs time for polyurethane rubbers filled with 10 per cent. by volume of various sodium chloride fractions.
Temp. 21 °C; rel. hum. 65 %; reference stress level σ_o = 6.00 kg/cm^2.

1 : 185/190

2 : 236

3 : 178/224

4 : 232 A

5 : 217

6 : 164

7 : 138

Fig. 13. Ditto but 20 per cent. by volume.

1 : 186
2 : 237 A
3 : 180
4 . 225/233 A
5 : 218
6 : 166
7 : 210
8 : 123

Fig. 14. Ditto but 30 per cent. by volume.

1 : 188
2 : 238 A
3 : 181
4 : 234 A
5 : 168
6 : 219
7 : 239 A
8 : 214 A
9 : 211
10: 131

Fig. 15. Ditto but 40 per cent. by volume.

1 : 191 L
2 : 235 A
3 : 170
4 : 220
5 : 240
6 : 205 A
7 : 212
8 : 216 A
9 : 133
10: 222
11: 230 A

Fig. 16. Ditto but 50 per cent. by volume.
1 : 206 A
2 : 213
3 : 215 A
4 : 134
5 : 223
6 : 231 A

Fig. 17. Time-stress shift relationship for tensile creep of polyurethane rubbers filled with various amounts of several sodium chloride fractions.
A : no. 8 (< 8 μm)
B : no. 7 (8 - 20 μm)
C : no. 6 (33 - 40 μm)
D . no. 4 (90 - 105 μm)
E : no. 2 (210 - 300 μm)
Reference stress σ_o = 6.00 kg/cm^2; temp. 21 °C; rel. hum. 65 %.

Fig. 18. Time-stress shift relationship for tensile creep of polyurethane rubbers filled with various amounts of several fractions of sodium chloride. Reference stress σ_o = 6.00 kg/cm^2; temp. 21 °C; rel. hum. 65 %.

Fig. 19. Tensile compliance F vs reduced time for polyurethane rubbers filled with various amounts of sodium chloride fraction no. 8 (< 8 μm); temp. 21 °C; rel. hum. 65 %; reference stress σ_o = 6.00 kg/cm^2.

Fig. 20. No. 7 (8 - 20 μm) ditto

Fig. 21. No. 6 (33 - 40 μm) ditto

Fig. 22. No. 4 (90 - 105 μm) ditto

Fig. 23. No. 2 (210 - 300 μm) ditto

Fig. 24. Compliances F_u and $\overline{F_{br}}$, respectively for the non-dewetted state and at break, vs the content of filler, for polyurethane rubbers filled with sodium chloride fraction no. 2 (210 - 300 μm). Temp. 21 °C; rel. hum 65 %; $\overline{F_{br}}$ defined according to section 6.4.

Fig. 25. Characteristic de-wetting time τ, vs particle size for polyurethane rubbers filled with 30, 40 and 50 vol. % of various sodium chloride fractions; temp. 21 °C; rel. hum. 65 %; stress level $\sigma = 6.00$ kg/cm^2.

Fig. 26. Stress level σ, necessary to produce a characteristic de-wetting time of 0.1 h, vs the particle size for polyurethane rubbers filled with 40 vol. % of various sodium chloride fractions; temp. 21 °C; rel. hum. 65 %.

Fig. 27. Tensile strain ε', during recovery vs log. time for materials filled with various amounts of several sodium chloride fractions.
A : no. 8 (< 8 μm)
B : no. 7 (8 - 20 μm)
C : no. 6 (33 - 40 μm)
D : no. 4 (90 - 105 μm)
Temp. 21 °C; rel. hum. 65 %

Numbers written near each curve indicate batch and specimen. For each specimen, the corresponding primary creep data are summarized in Table III,1 of Appendix III.

Fig. 28. Normalized recovery strain $\varepsilon'/\varepsilon'_1$ vs log. time for polyurethane rubbers filled with several sodium chloride fractions. ε'_1 denotes the strain at a recovery time of 1 h. Temp. 21 °C; rel. hum. 65 %.

Fig. 29. Strain ε'_1 at a recovery time of 1 h vs the contribution ε_d of de-wetting to strain at unloading. Temp. 21 °C; rel. hum. 65 %.

Fig. 30. Rupture stress σ_{br} vs rupture time t_{br} for polyurethane rubbers filled with various amounts of coarse sodium chloride fraction no. 2 (210 - 300 μm). Temp. 21 °C; rel. hum. 65 %.

Fig. 31. Rupture stress σ_{br}, necessary to produce rupture after 10 hrs as a function of content and particle size of the filler. Temp. 21 °C; rel. hum. 65 %.

Fig. 32. Time-stress shift relation $S(t_{br})$ for polyurethane rubbers filled with various amounts of different fractions of sodium chloride. Reference rupture time 1 h; temp. 21 °C; rel. hum. 65 %.

Fig. 33. All data of rupture stress, shifted to a reference rupture time of 1 h, plotted vs content of filler. Temp. 21 °C; rel. hum. 65 %. The quantity plotted on the ordinate is σ_{br} (1) from formula (2).

Fig. 34. Reinforcement factor v vs particle size of the filler, δ. Temp. 21 °C; rel. hum. 65 %.

Fig. 35. Rupture stress σ_{br} vs particle size δ of the filler for various values of the filler concentration. Rupture time t_{br} for this figure was 10^1 hrs. Temp. 21 °C; rel. hum. 65 %.

Fig. 36. Average rupture strain $\overline{\varepsilon_{br}}$ vs content of filler for polyurethane rubbers filled with various sodium chloride fractions. Temp. 21 °C; rel. hum. 65 %.

Fig. 37. Average rupture compliance $\overline{F_{br}}$ vs content of filler for polyurethane rubbers filled with various sodium chloride fractions. The dotted line is the compliance F_u of the non-dewetted material. Its strange course for filler contents higher than 50 vol. % originates from the bimodality of the filler (a mixture of 65 % coarse and 35 % fine particles). Temp. 21 °C; rel. hum. 65 %.

Fig.1

Fraction no. / size / Content	210–300 µm	80–105 µm	33–40 µm	8–20 µm	< 8 µm	210–300 µm 33–40 µm
0 %	108,227					
10 %	138		164,217	173,224 232A	185,190 238A	
20 %	123	210	166,218	180,225 233A	180,237A	
30 %	131	211,214A	168,219 239A	181,234A	188,238A	
40 %	133,222 230A	212,216A	170*), 175*), 240A 220,205A	235A	191L*)	
50 %	134,223 231A	213,215A	206A			241,208A
55 %	178*), 177L*) 203A*), 204*)					
60 %						209A
65 %						242A
70 %						202A*), 207A*)

A = Asolectin L = Lecithin *) partly inhomogeneous.

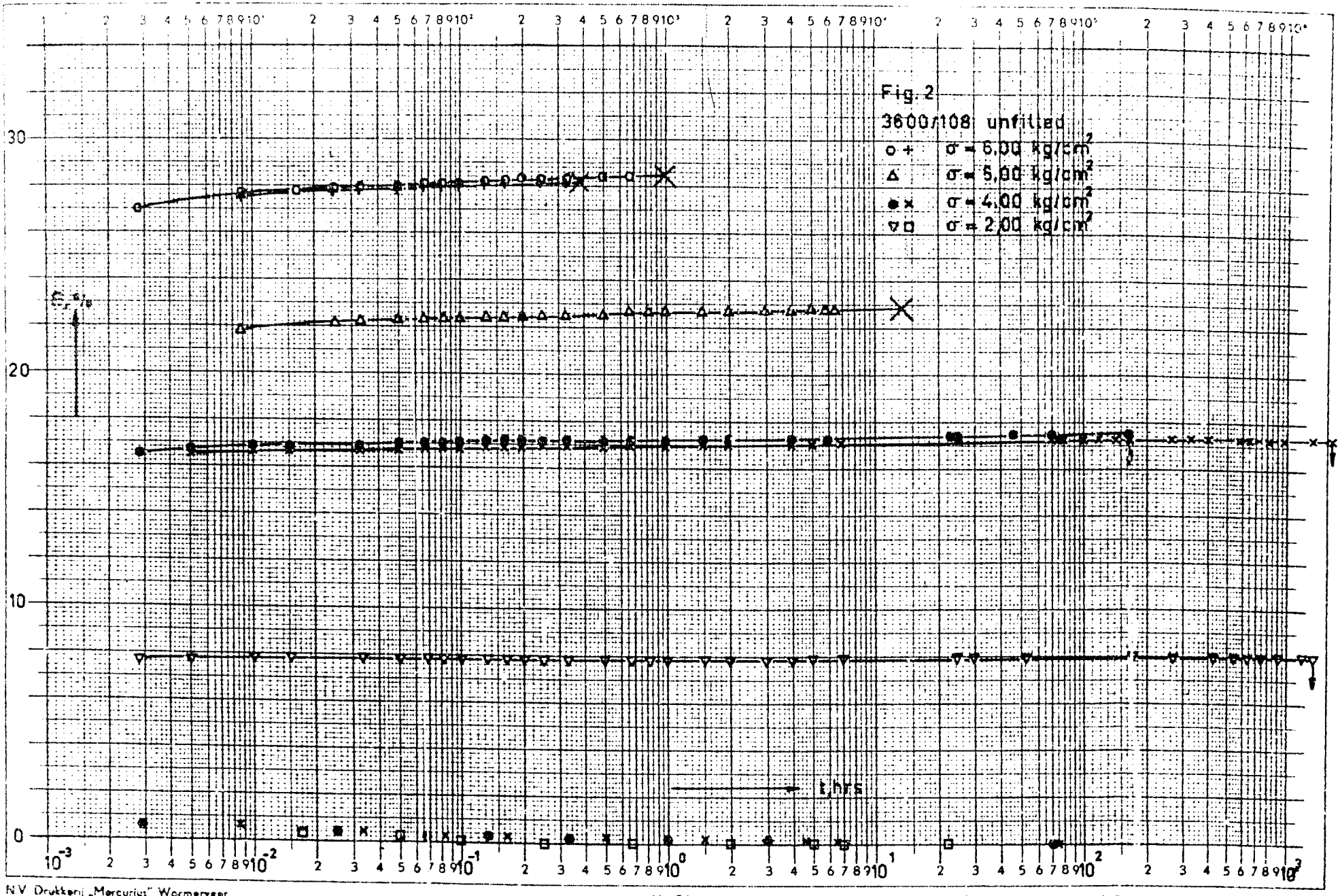

N.V. Drukkerij „Mercurius" Wormerveer

X-as loger verdeeld 1-10⁴ Eenheid 45 mm Y-as verdeeld in mm.

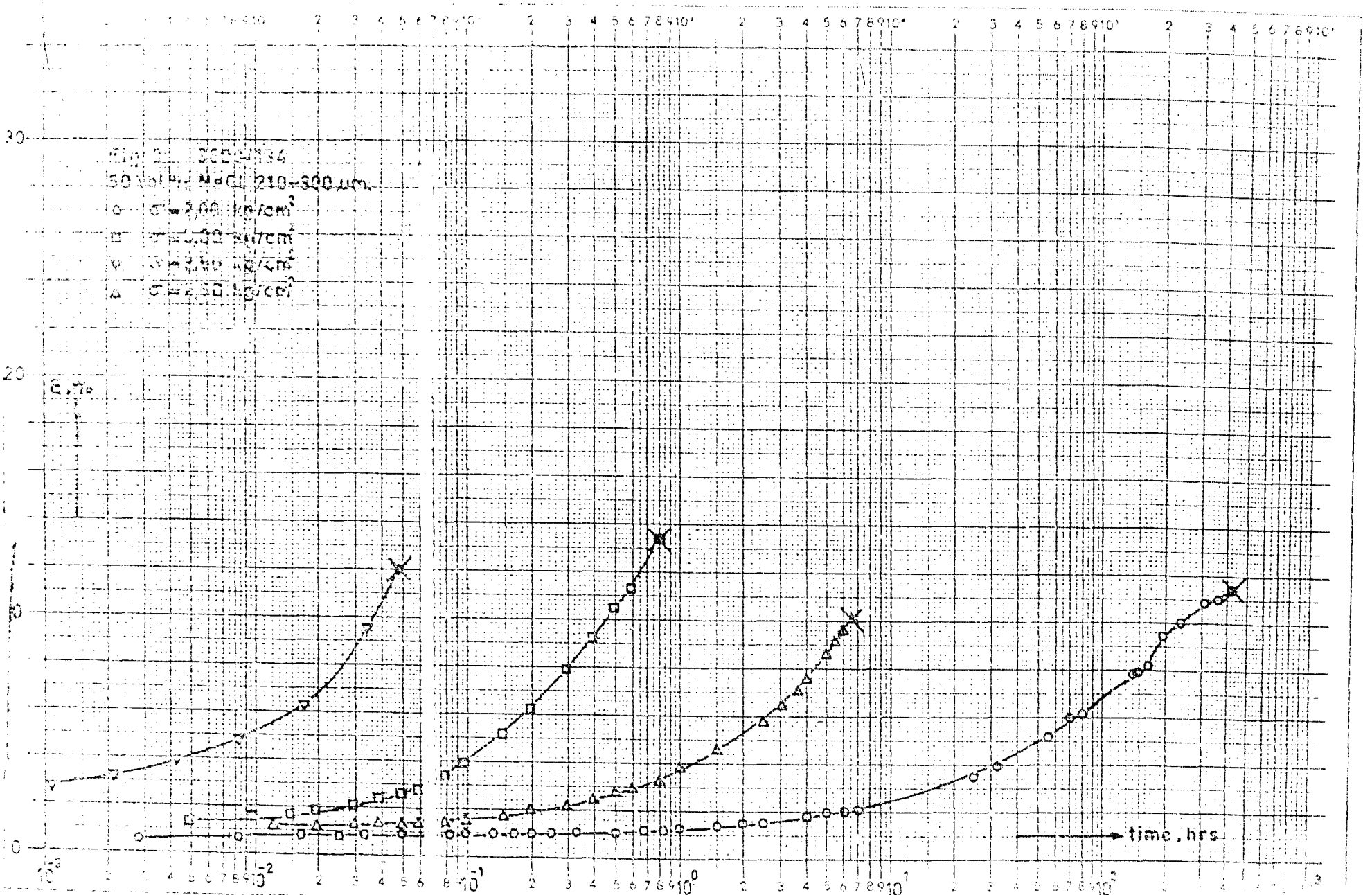

No 34

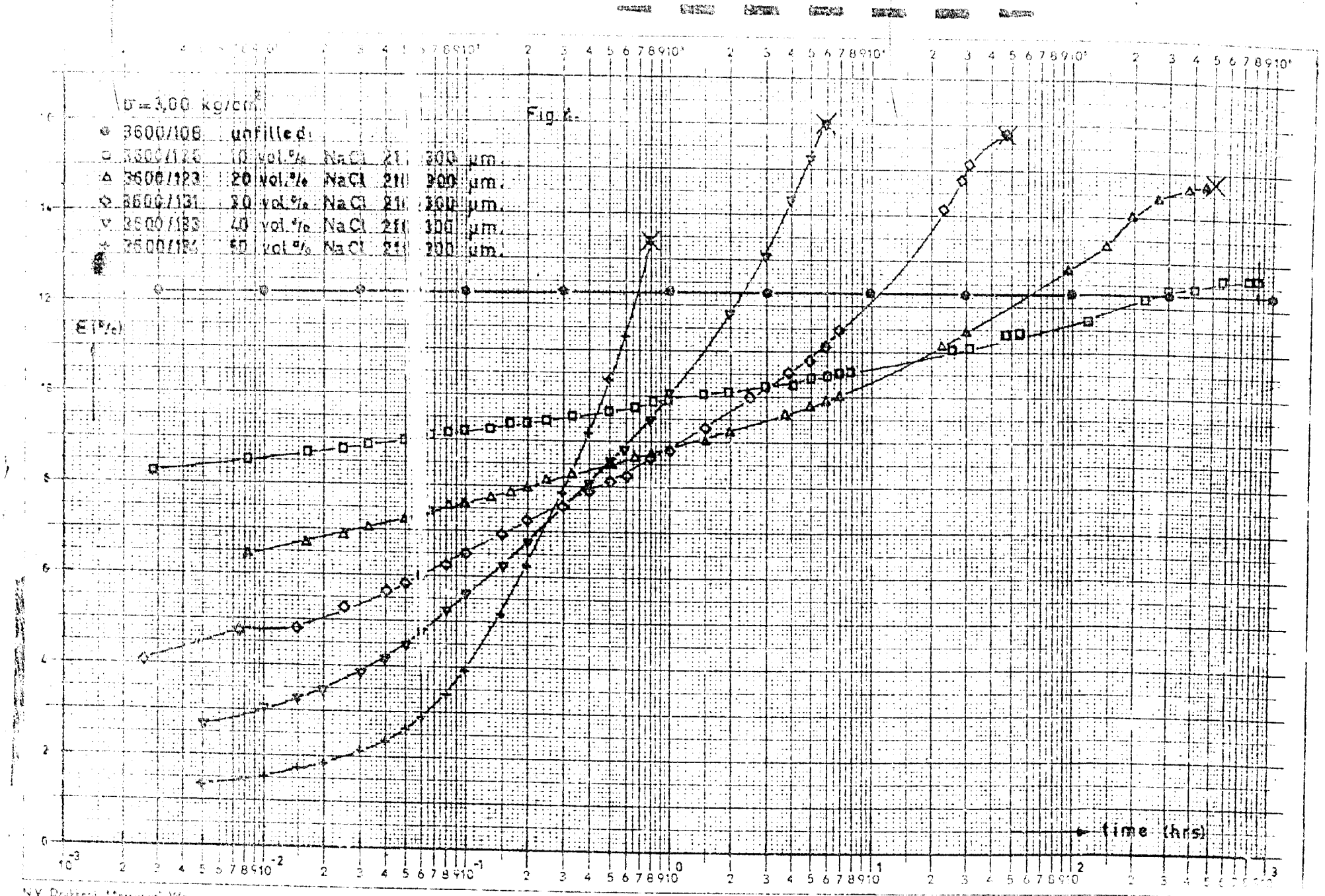
σ = 3,00 kg/cm²
3600/108 unfilled
3600/123 20 vol.% NaCl 211 300 µm.
3600/131 30 vol.% NaCl 211 300 µm.
3600/183 40 vol.% NaCl 211 300 µm.
3600/184 50 vol.% NaCl 211 300 µm.
ε (%)
time (hrs)

Fig. 4.

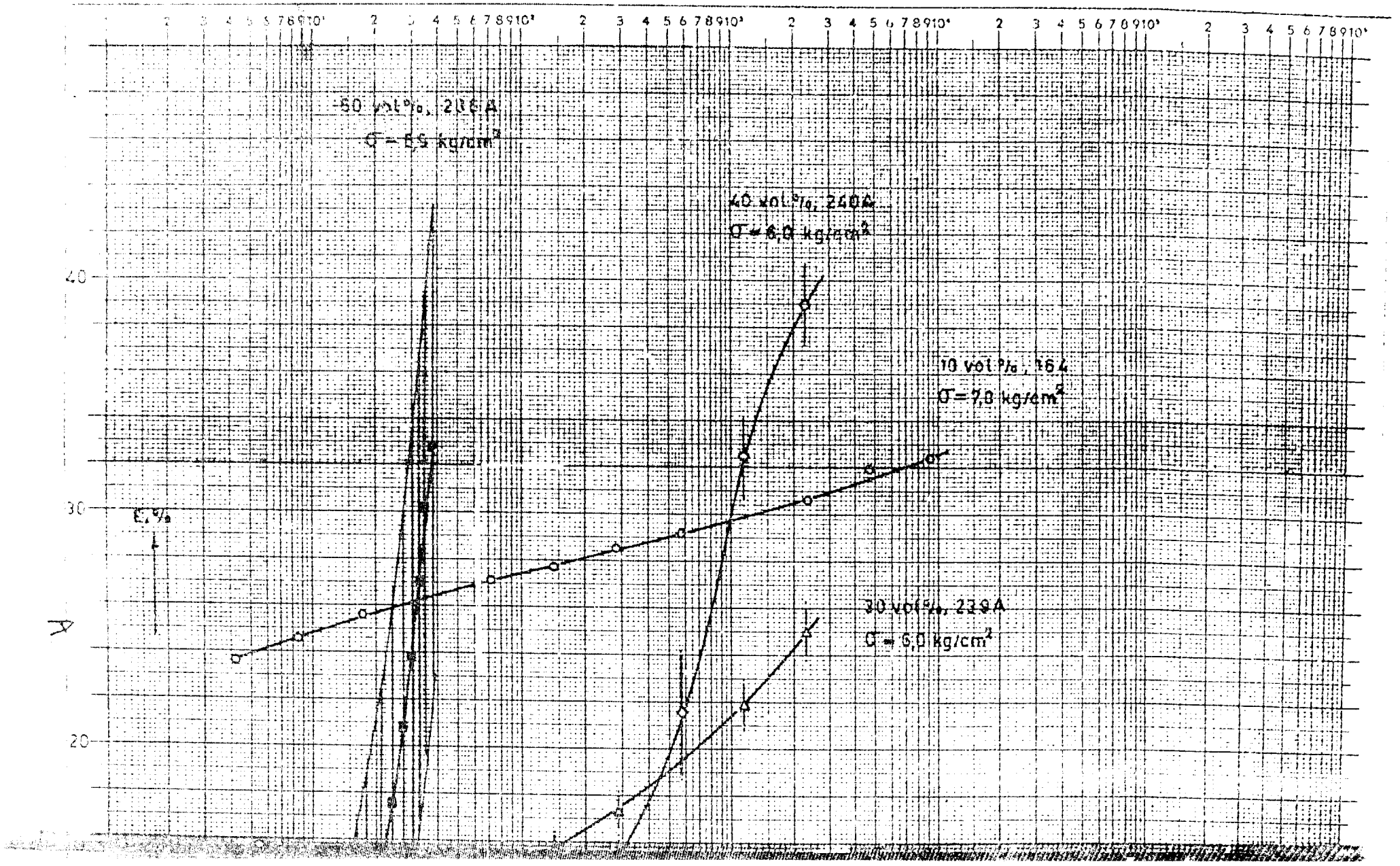
50 vol%, 238 A
σ = 6,5 kg/cm²
40 vol%, 240 A
σ = 6,0 kg/cm²
10 vol%, 164 A
σ = 7,8 kg/cm²
30 vol%, 239 A
σ = 6,0 kg/cm²
ε, %
40
30
20

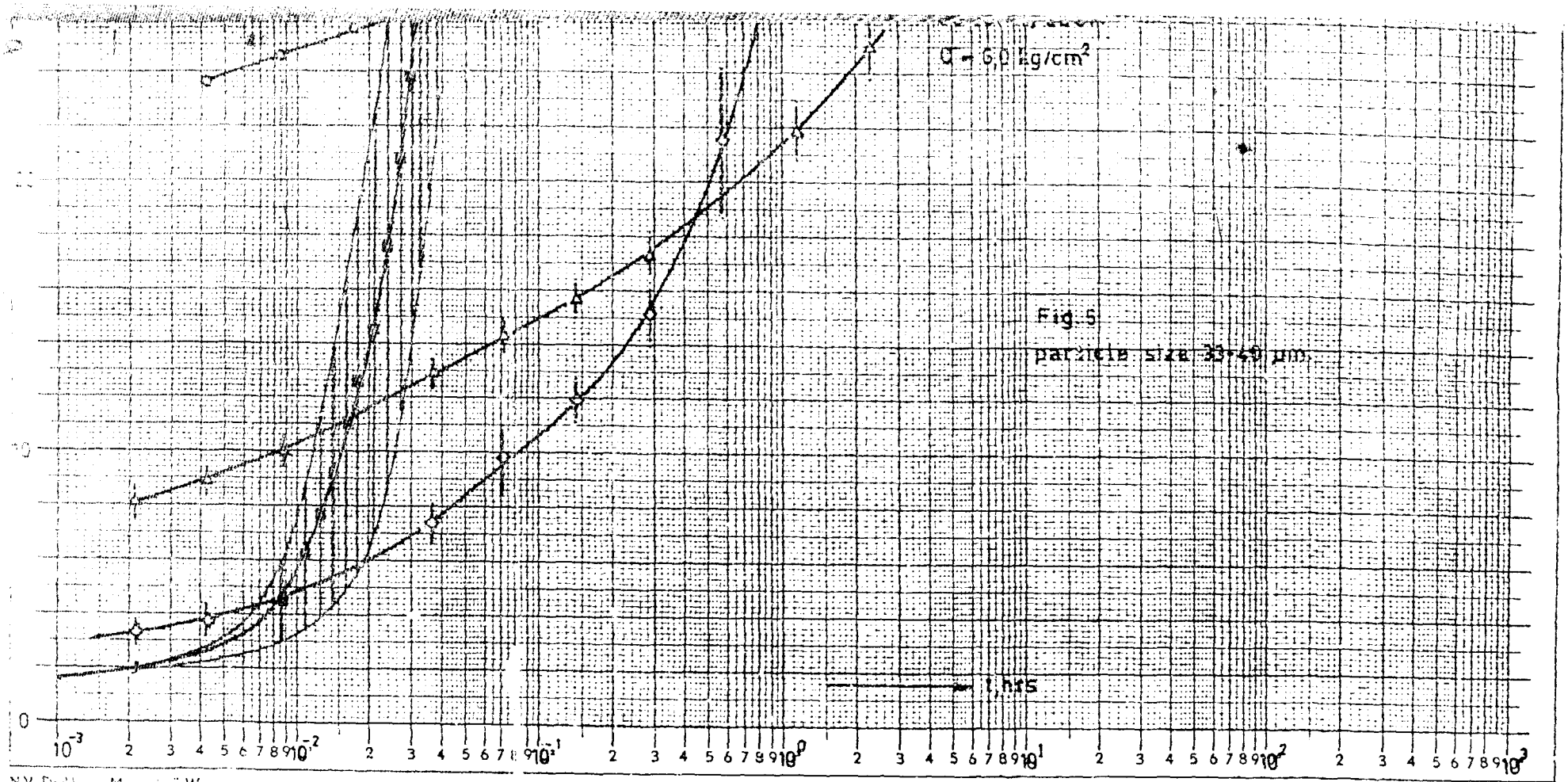

Fig. 6

particle size 33÷49 µm.

N.V. Drukkerij „Mercurius" Wormerveer

X-as logar. verdeeld 1-10⁴ Eenheid 45 mm. Y-as verdeeld in mm

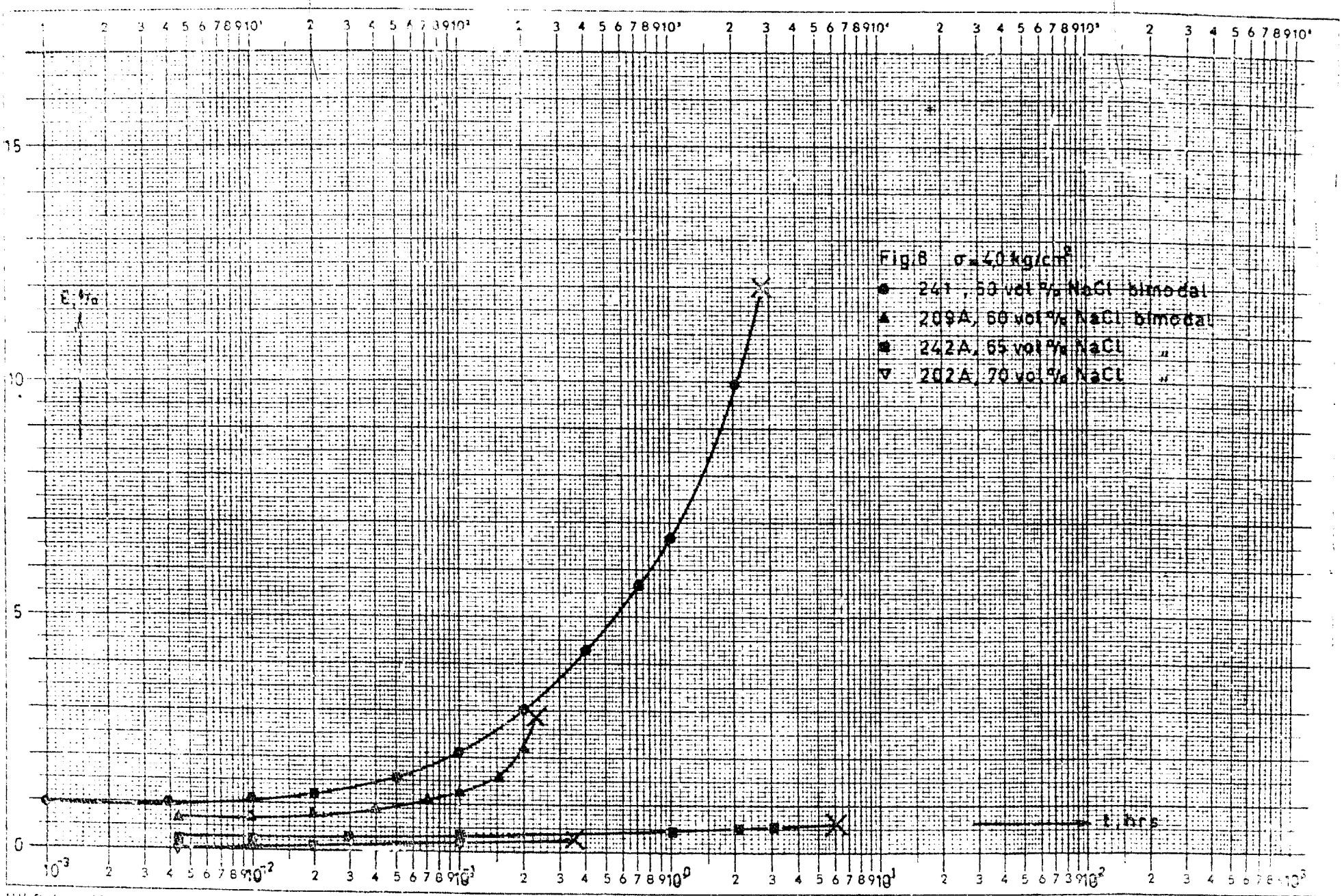

N.V. Drukkerij „Mercurius" Wormerveer

X-es logar. verdeeld 1-10⁴ Eenheid 45 mm. Y-as verdeeld

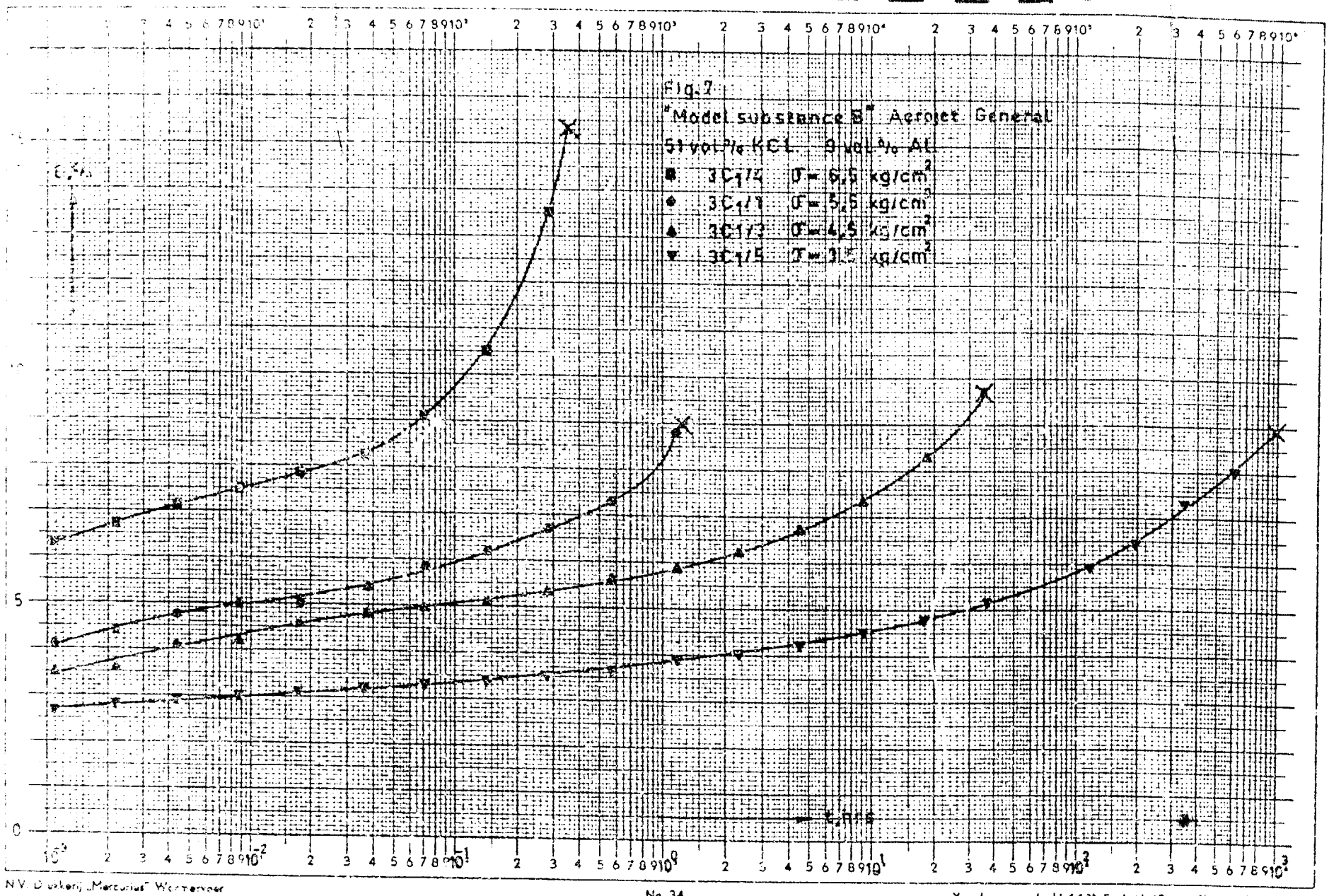

N.V. Drukkerij „Mercurius" Wormerveer

No. 34

X-as logar. verdeeld 1:10⁸ Eenheid 45 mm. Y-as verdeeld in mm.

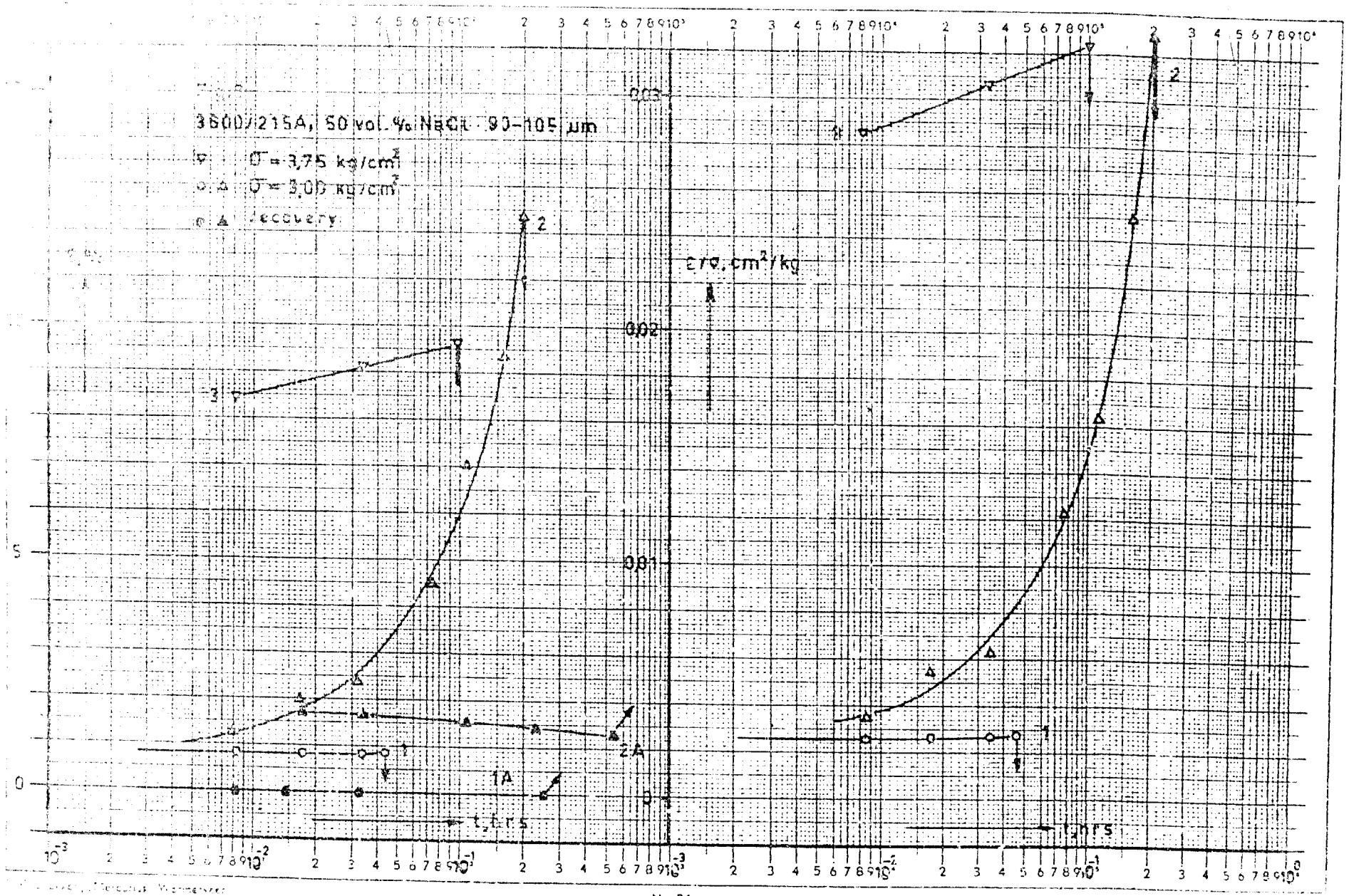

X-as logar. verdeeld 1-10¹ Eenheid 45 mm. Y-as verdeeld in mm.

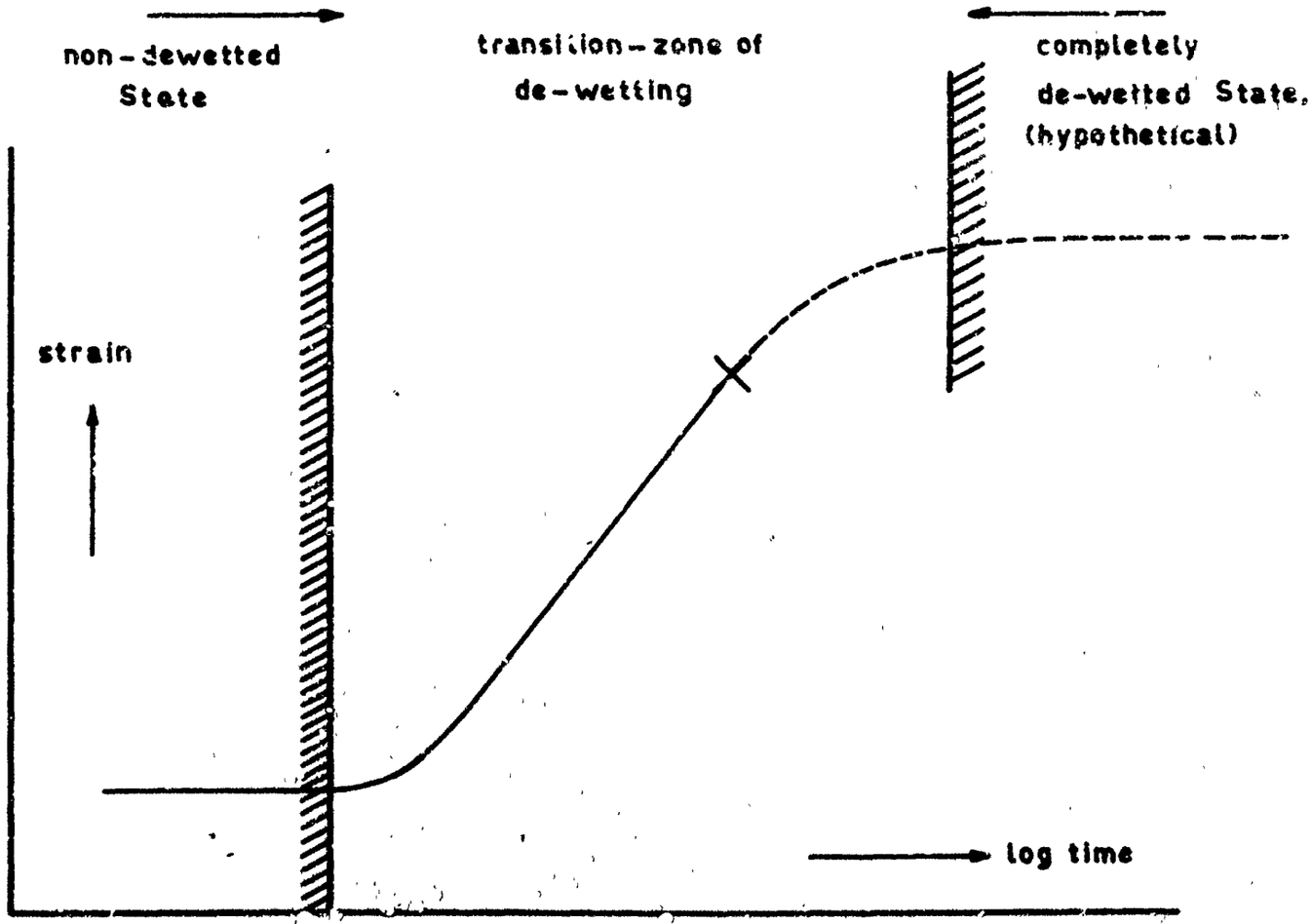
non-dewetted
State
transition-zone of
de-wetting
completely
de-wetted State.
(hypothetical)
strain
log time

Fig. 9

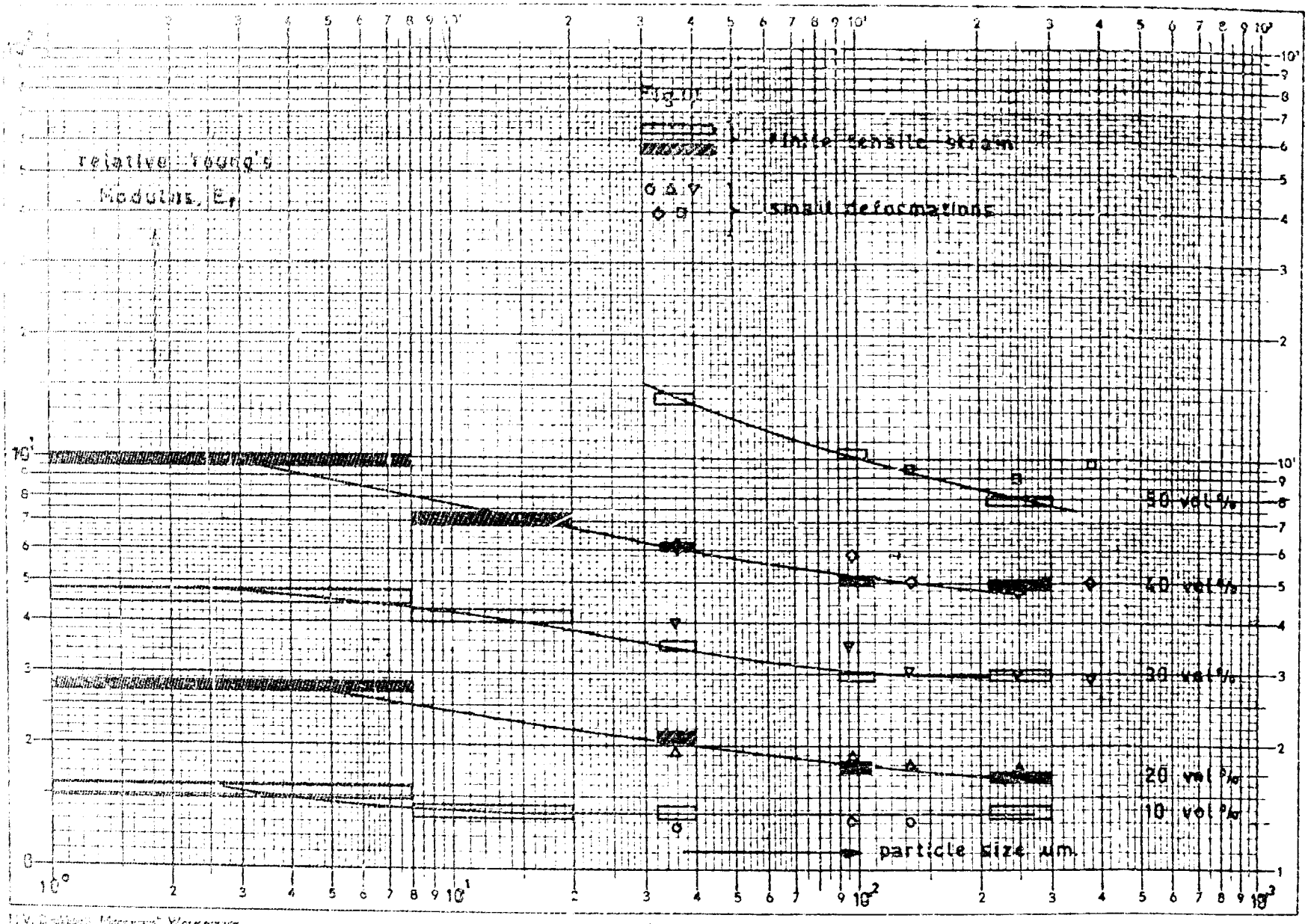
relative Young's Modulus, E_r
finite tensile strain
small deformations
50 vol %
40 vol %
30 vol %
20 vol %
10 vol %
particle size µm.

No. 20

0,05
0,04
0,03
0,02
0,01
F, cm²/kg
log
2
1
0
-1
-2
vg
g /cm²
2,5 kg /cm²
σ = 2,0 kg /cm²
Shrink-slip
log
Fig. 11
S600/133
25 vol.% NaCl
210–300 µm

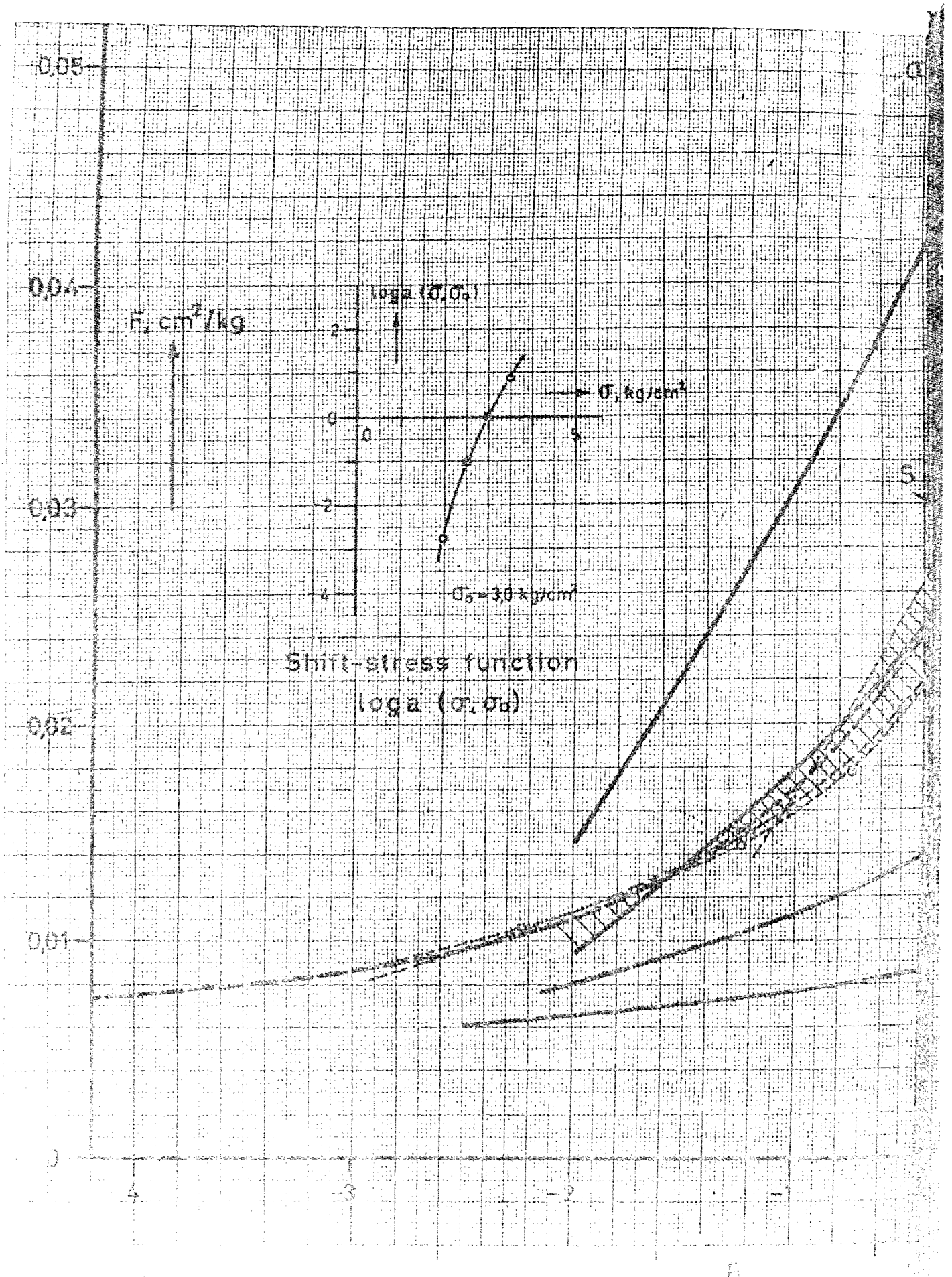
0,05
0,04
0,03
0,02
0,01
F, cm²/kg
log a (σ, σ₀)
σ, kg/cm²
σ₀ = 3,0 kg/cm²
Shift-stress function
log a (σ, σ₀)

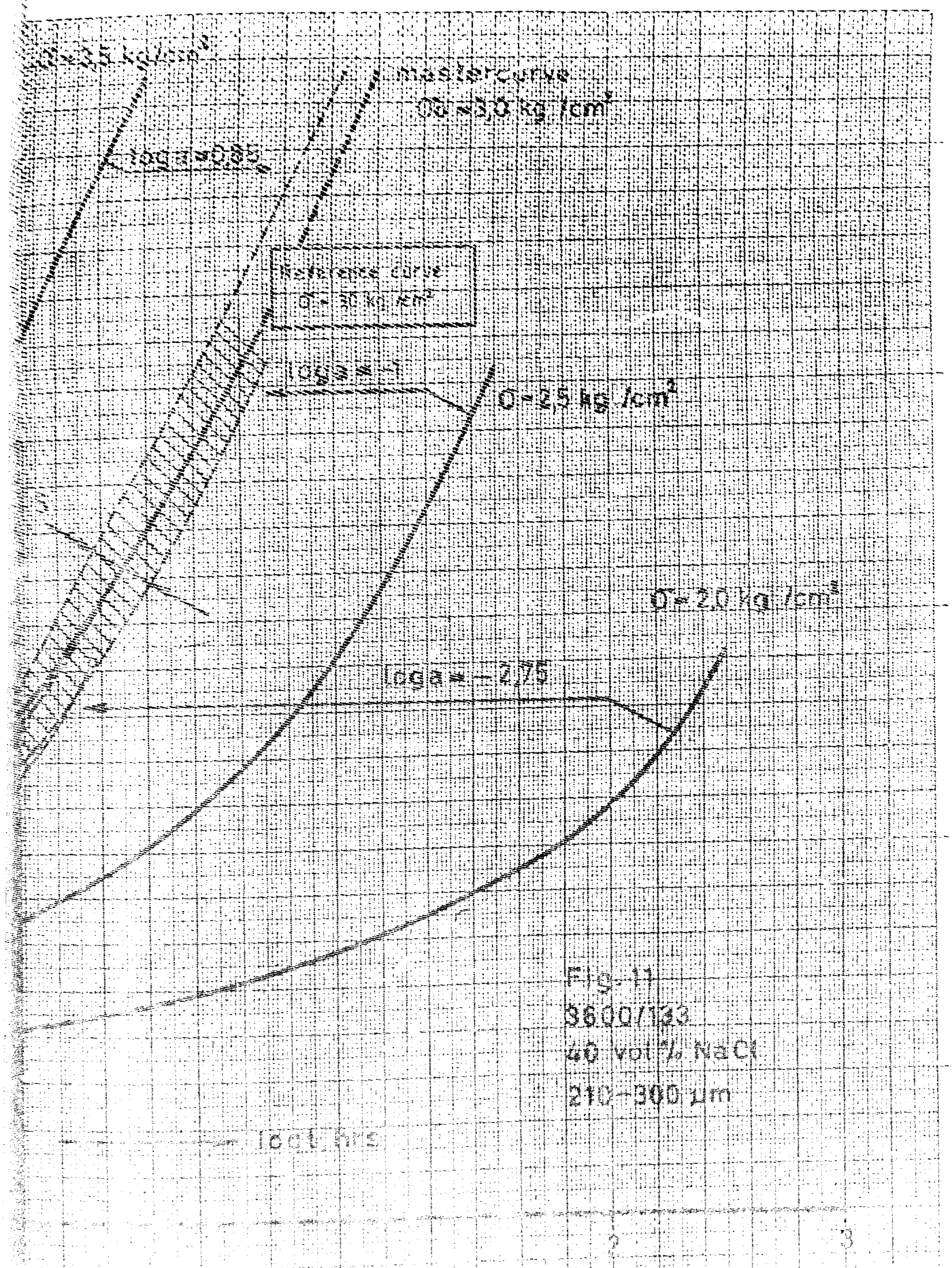
σ = 3,5 kg/cm²
mastercurve
σ₀ = 3,0 kg/cm²
log a = 0,88
Reference curve
σ = 3,0 kg/cm²
log a = -1
σ = 2,5 kg/cm²
σ = 2,0 kg/cm²
log a = -2,75
Fig. 11
3600/133
40 vol% NaCl
210-300 µm
log t, hrs
2
3

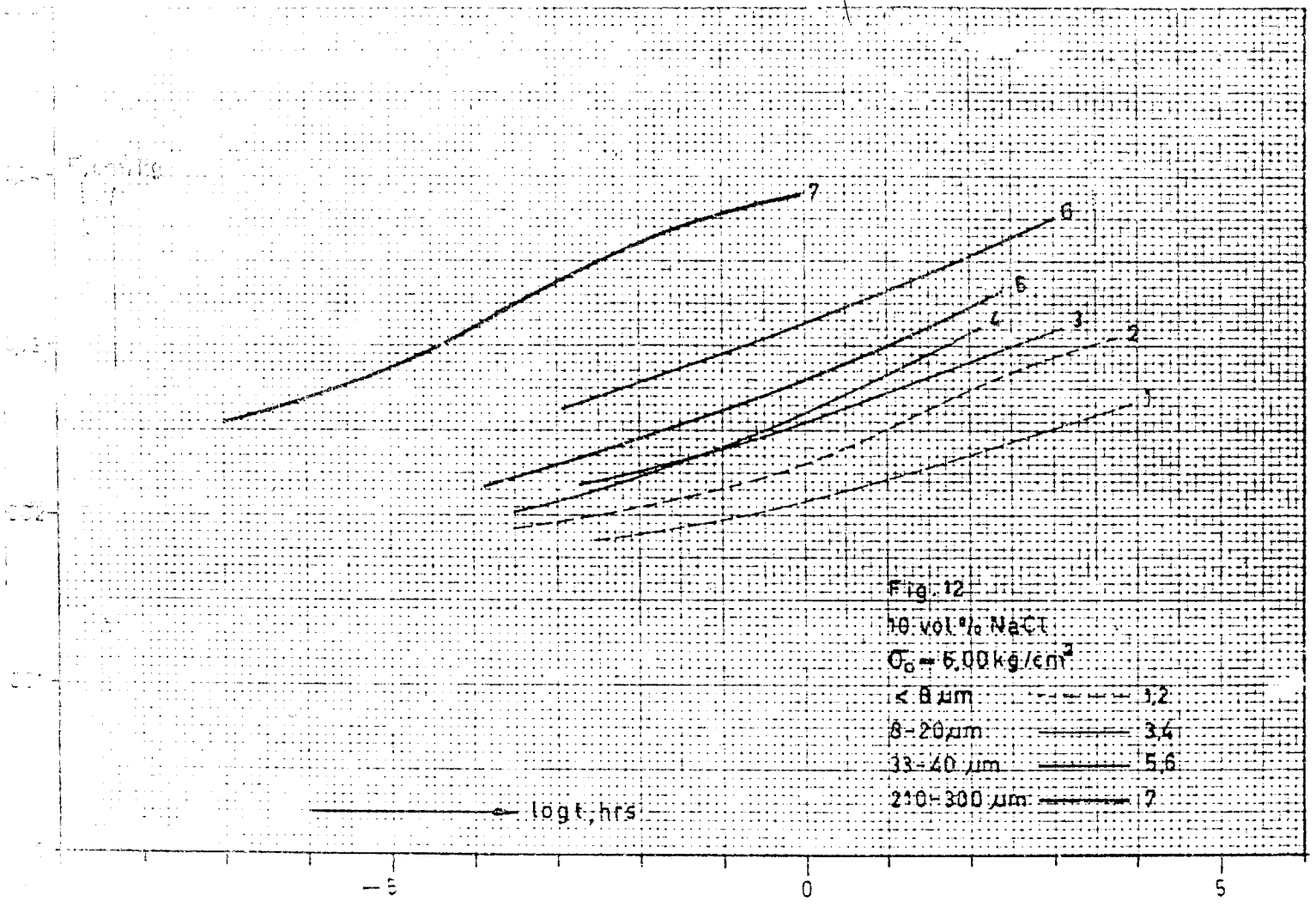

Fig. 12
10 vol.% NaCl
σ_o = 6.00 kg/cm^2
< 8 µm 1,2
8-20 µm 3,4
33-40 µm 5,6
210-300 µm 7

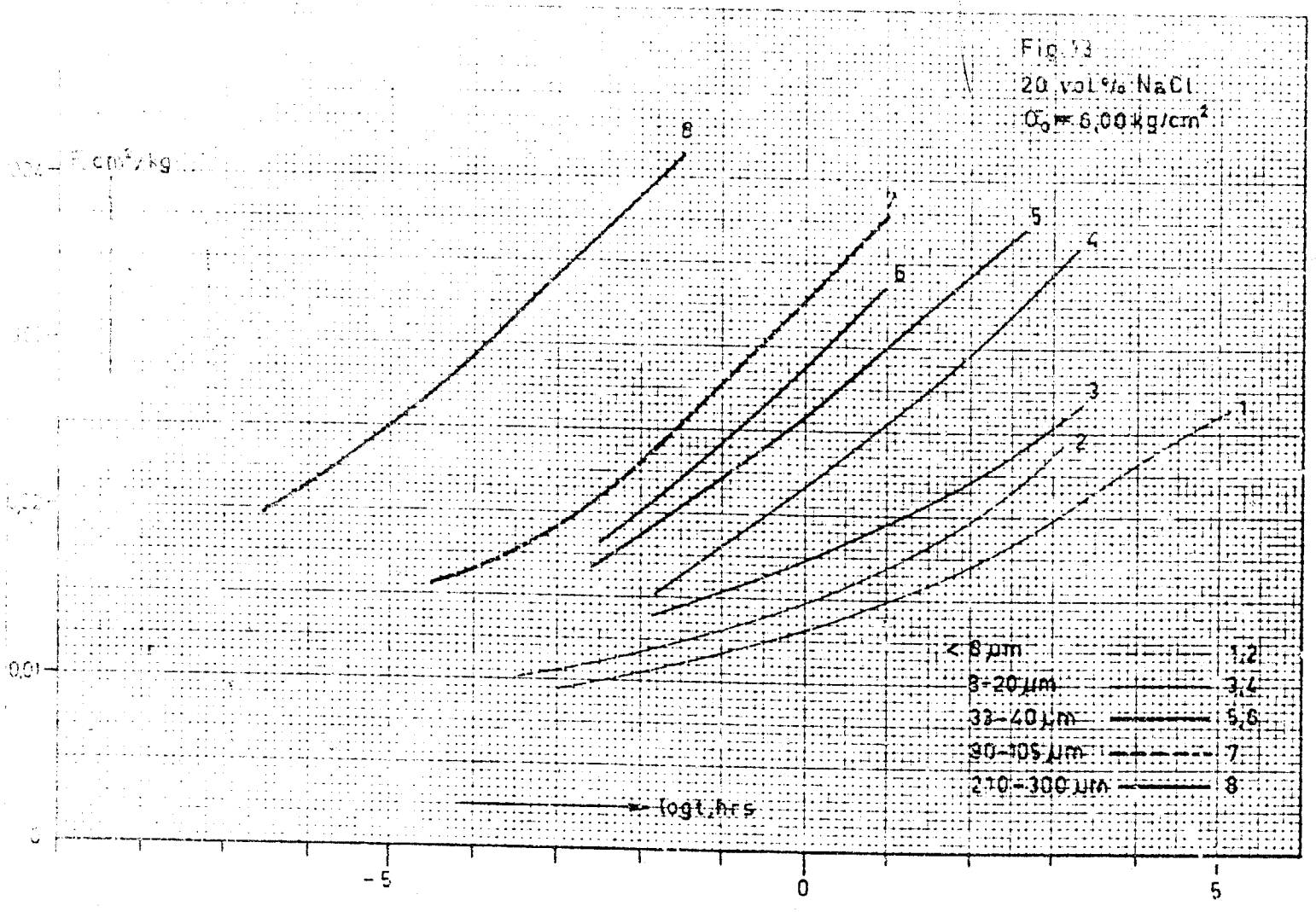

10 Deelstrepen is 15 m.m.

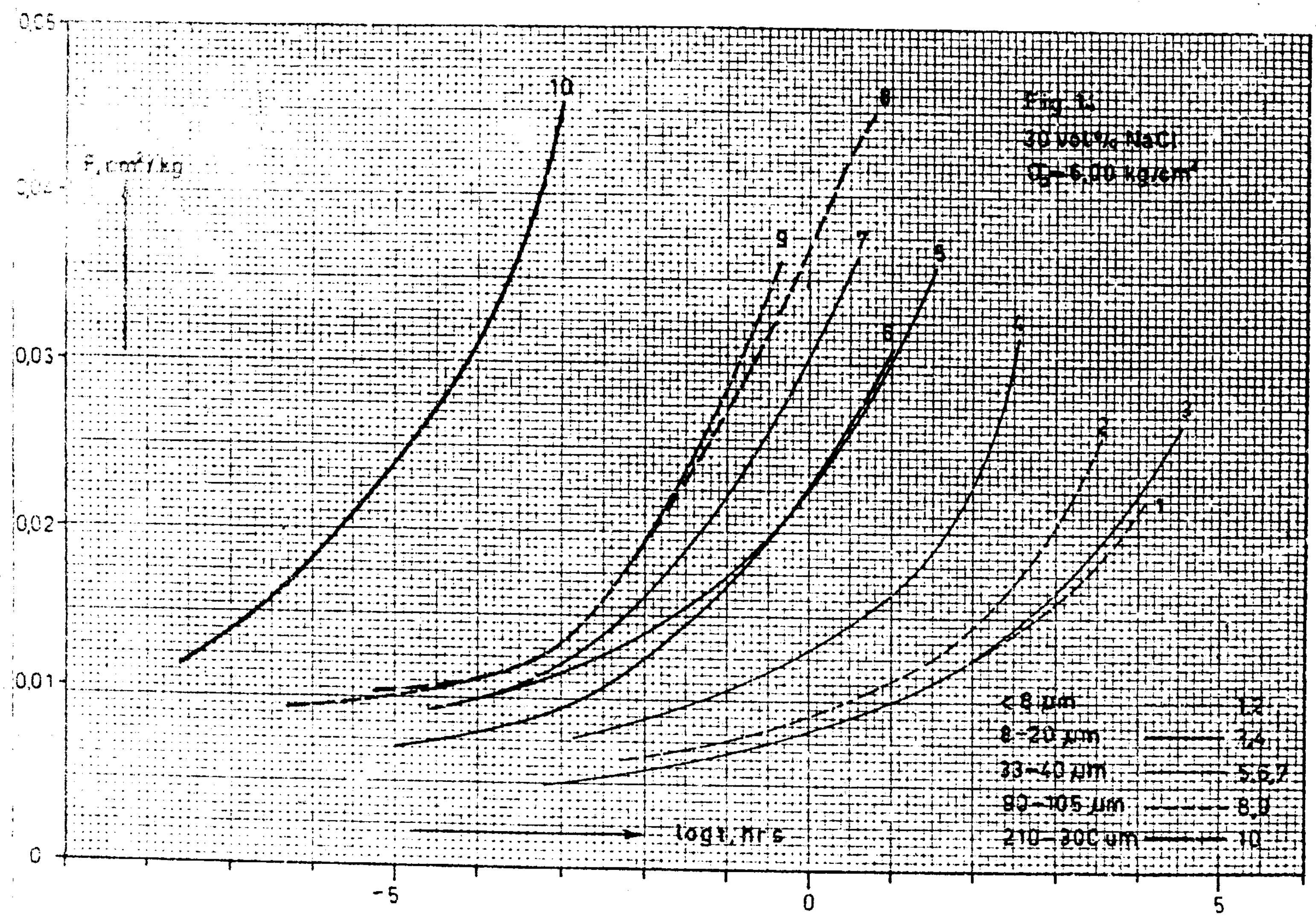

NV Drukkerij „Mercurius" Wormerveer
10 Deelstreepen is 15 m.m.

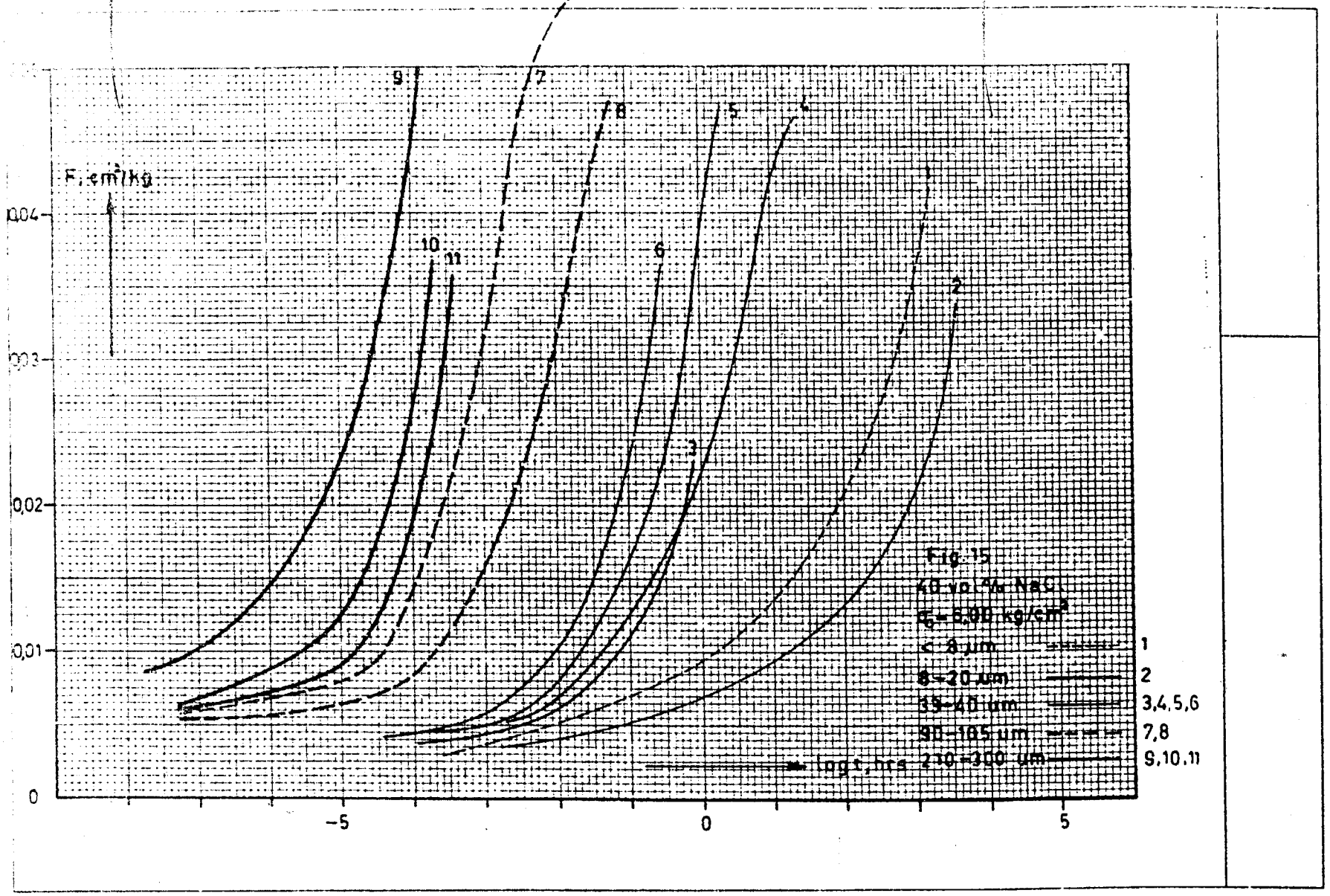

10 Deelstrepen is 15 m.m.

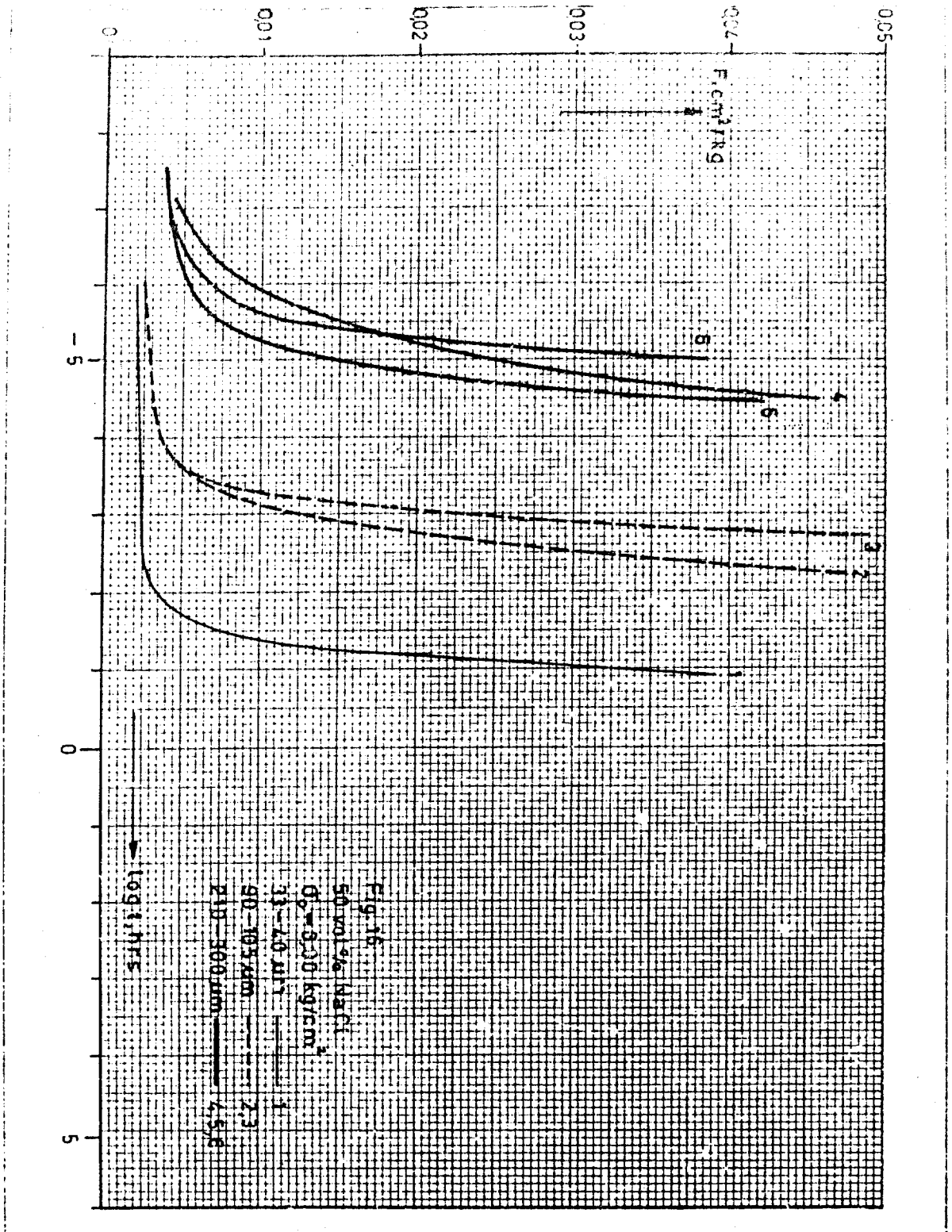

10 Deelstrepen is 15 m.m.

N.V. Drukkerij „Mercurius" Wormerveer

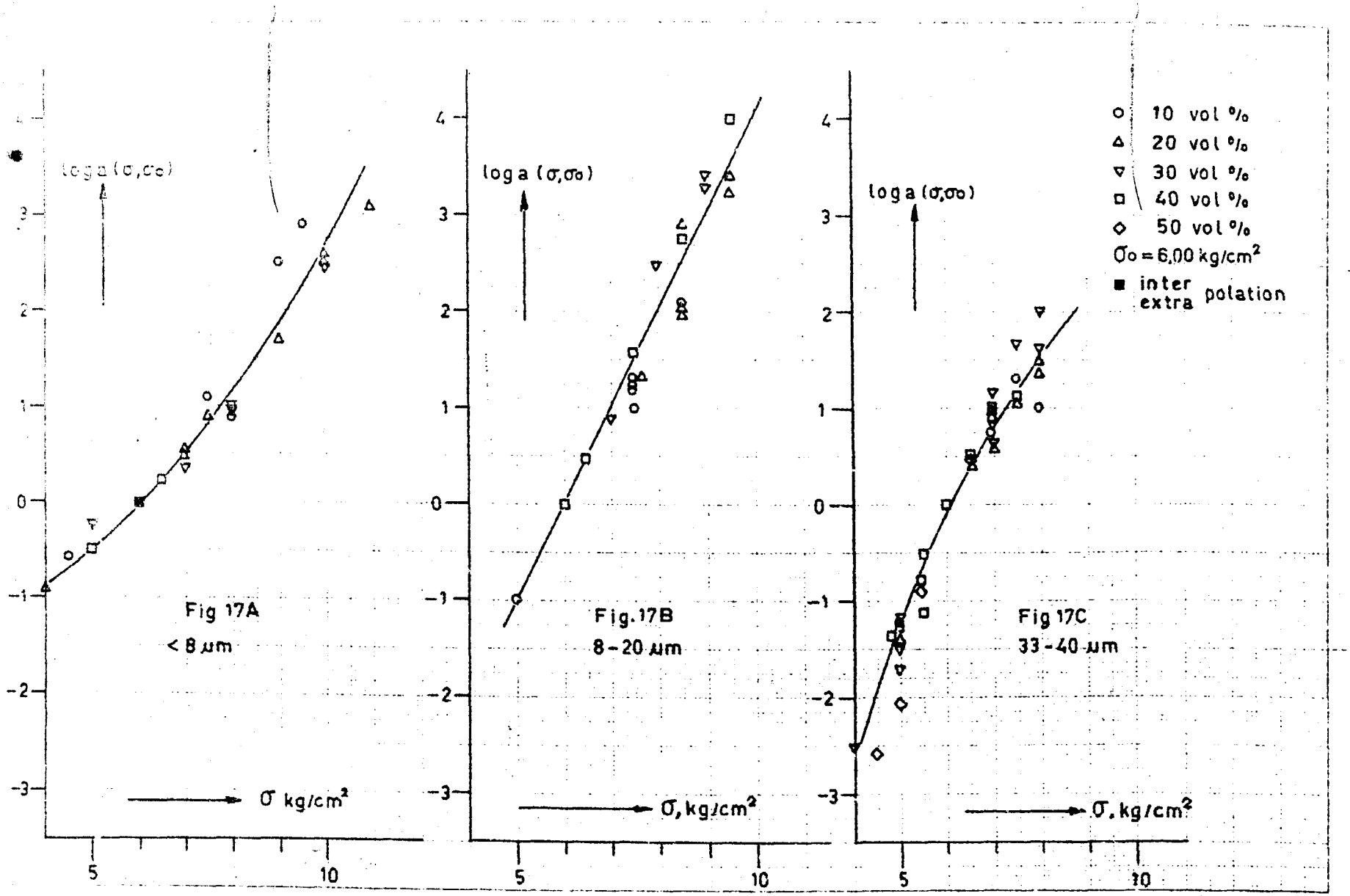
log a (σ,σo)
Fig 17A
< 8 µm
σ kg/cm²
log a (σ,σo)
Fig.17B
8 - 20 µm
σ, kg/cm²
log a (σ,σo)
Fig 17C
33 - 40 µm
σ, kg/cm²
10 vol %
20 vol %
30 vol %
40 vol %
50 vol %
σo = 6,00 kg/cm²
inter polation
extra

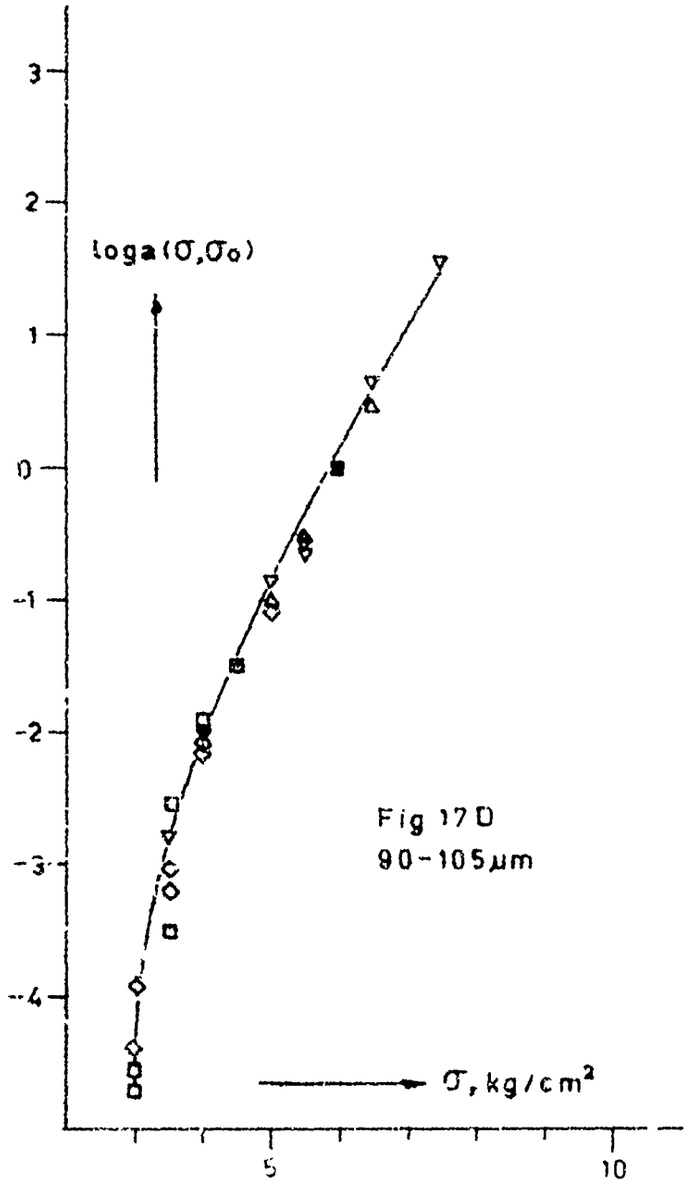

Fig 17 D
90-105 µm

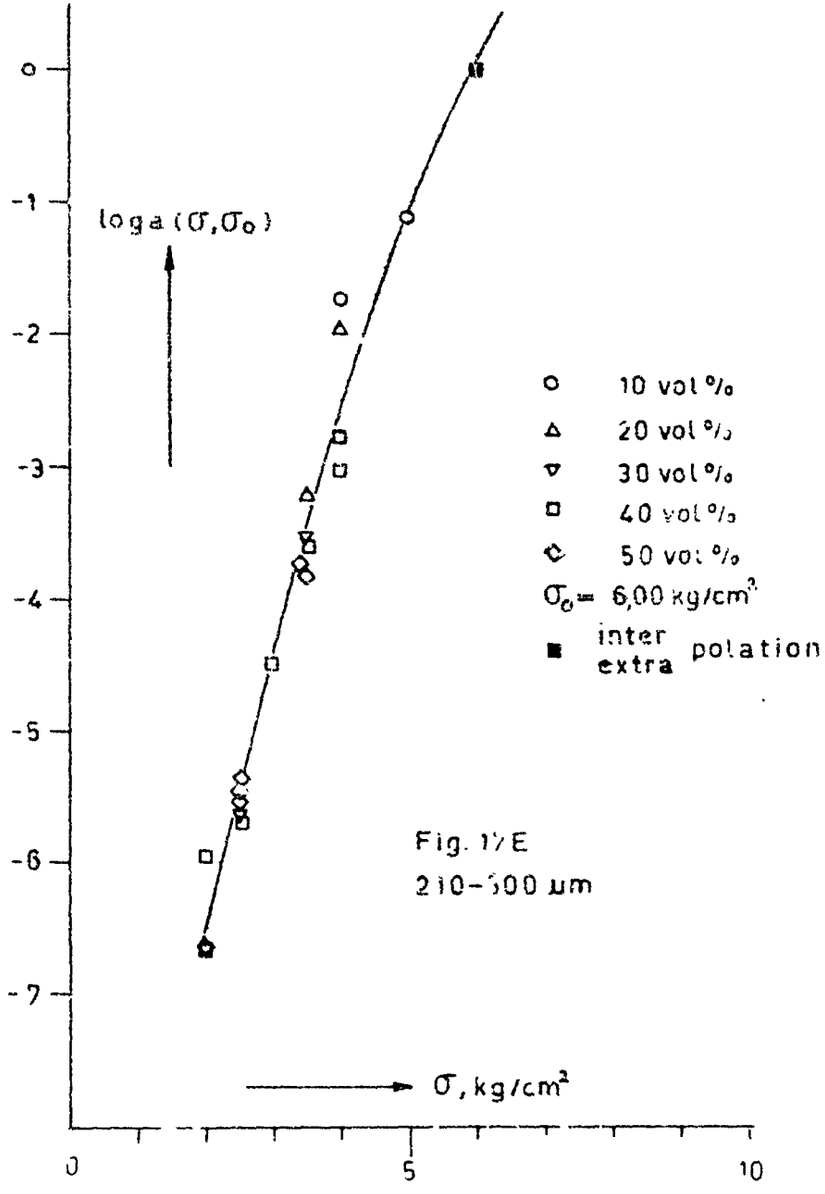

Fig. 17 E
210-300 µm

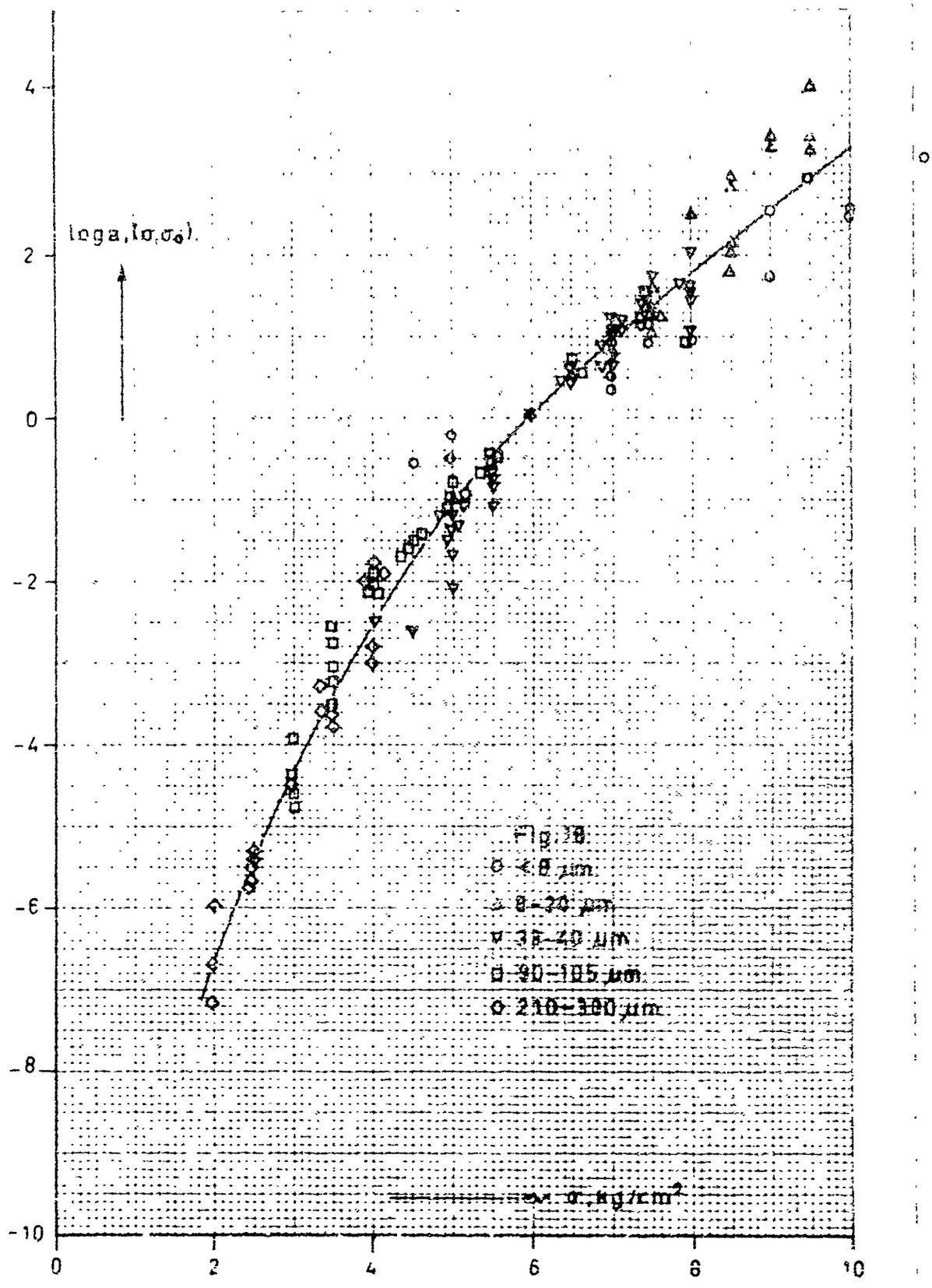
log a, [σ, σ₀]
4
2
0
-2
-4
-6
-8
-10
0
2
4
6
8
10
σ, kg/cm²
< 8 µm
8–20 µm
35–40 µm
90–105 µm
210–300 µm

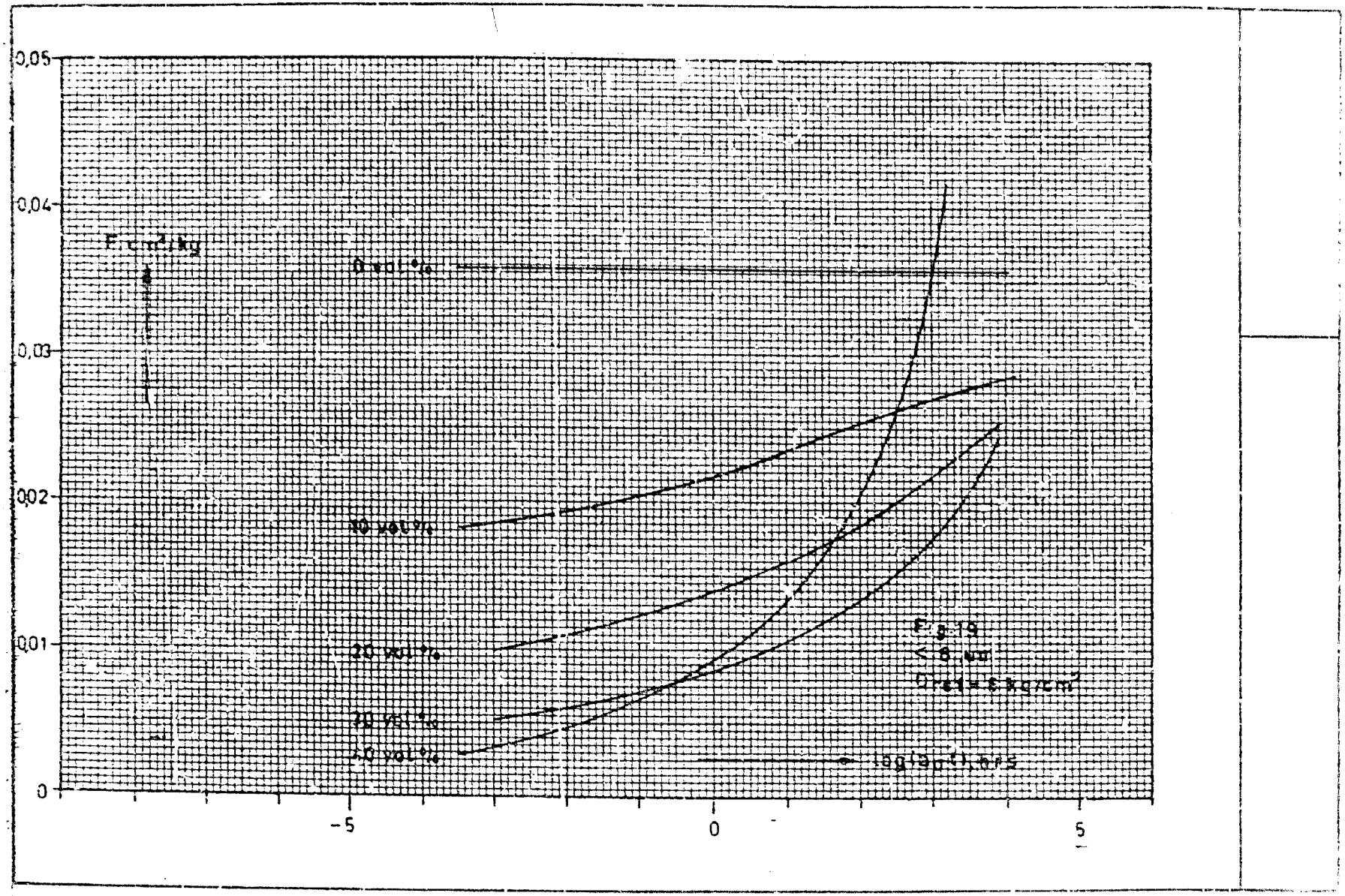
0,05
0,04
0,03
0,02
0,01
0
F cm²/kg
0 vol %
10 vol %
20 vol %
30 vol %
40 vol %
F: 8-19
< 8 µm
-5
0
5
log(ap.t), h/s

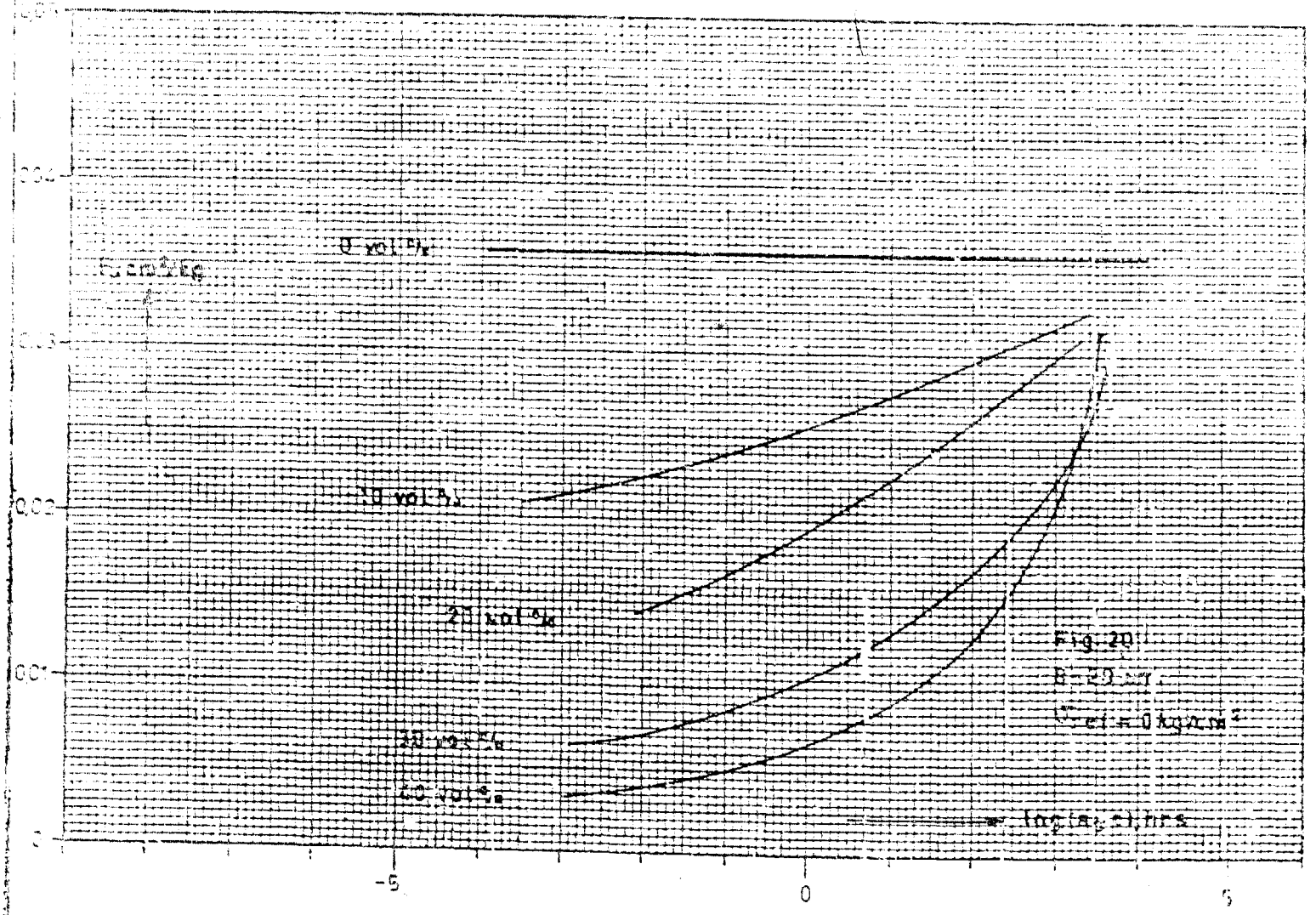

Fig. 20

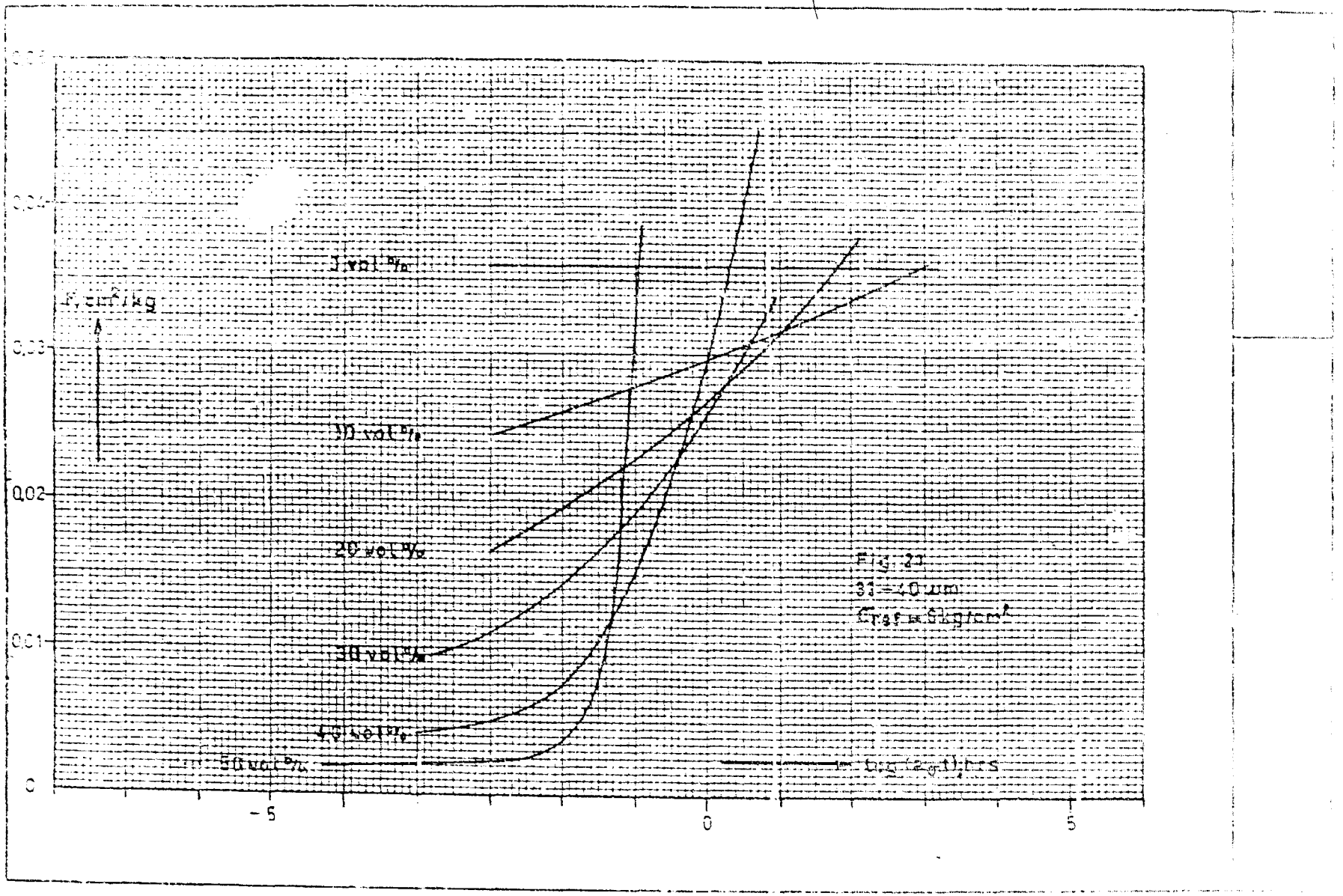

Fig 21
31 - 40 μm
$\sigma_{ref} = 5 kg/cm^2$

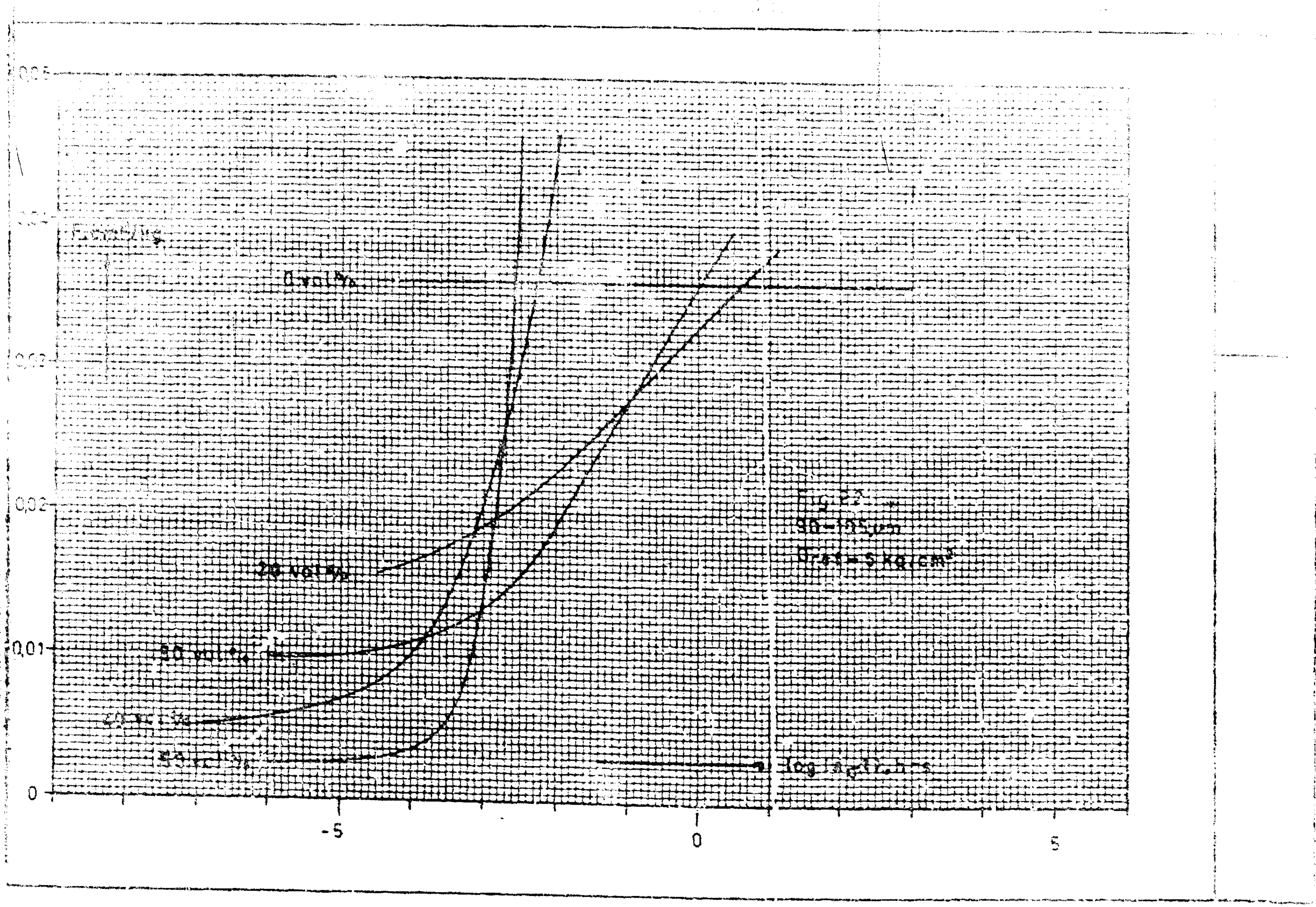

0,05
0,04
0,03
0,02
0,01
0
-5
0
5
0 vol%
20 vol%
30 vol%
90–105 μm
log

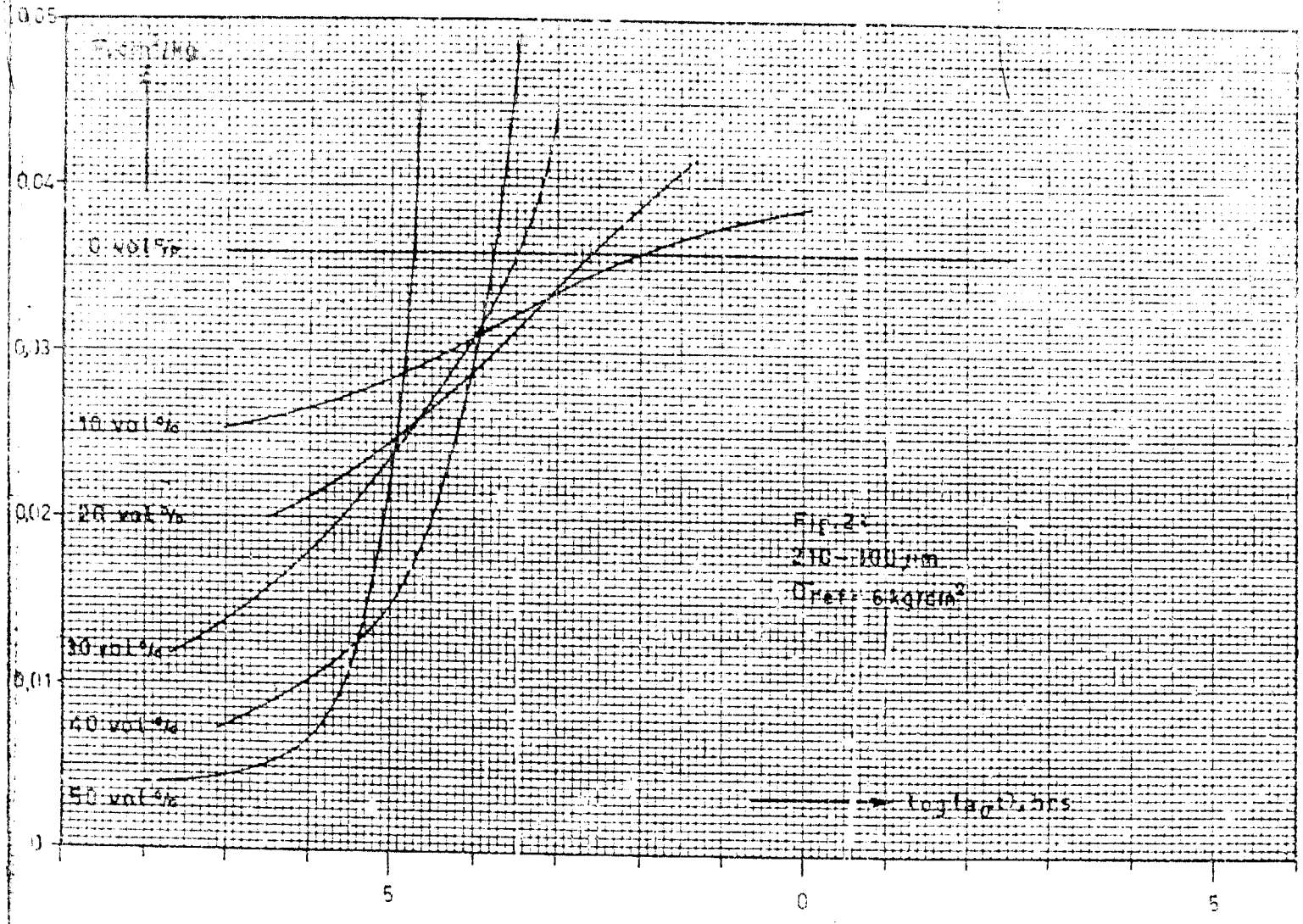
0,05
0,04
0,03
0,02
0,01
0
0 vol%
10 vol%
20 vol%
30 vol%
40 vol%
50 vol%
5
0
5

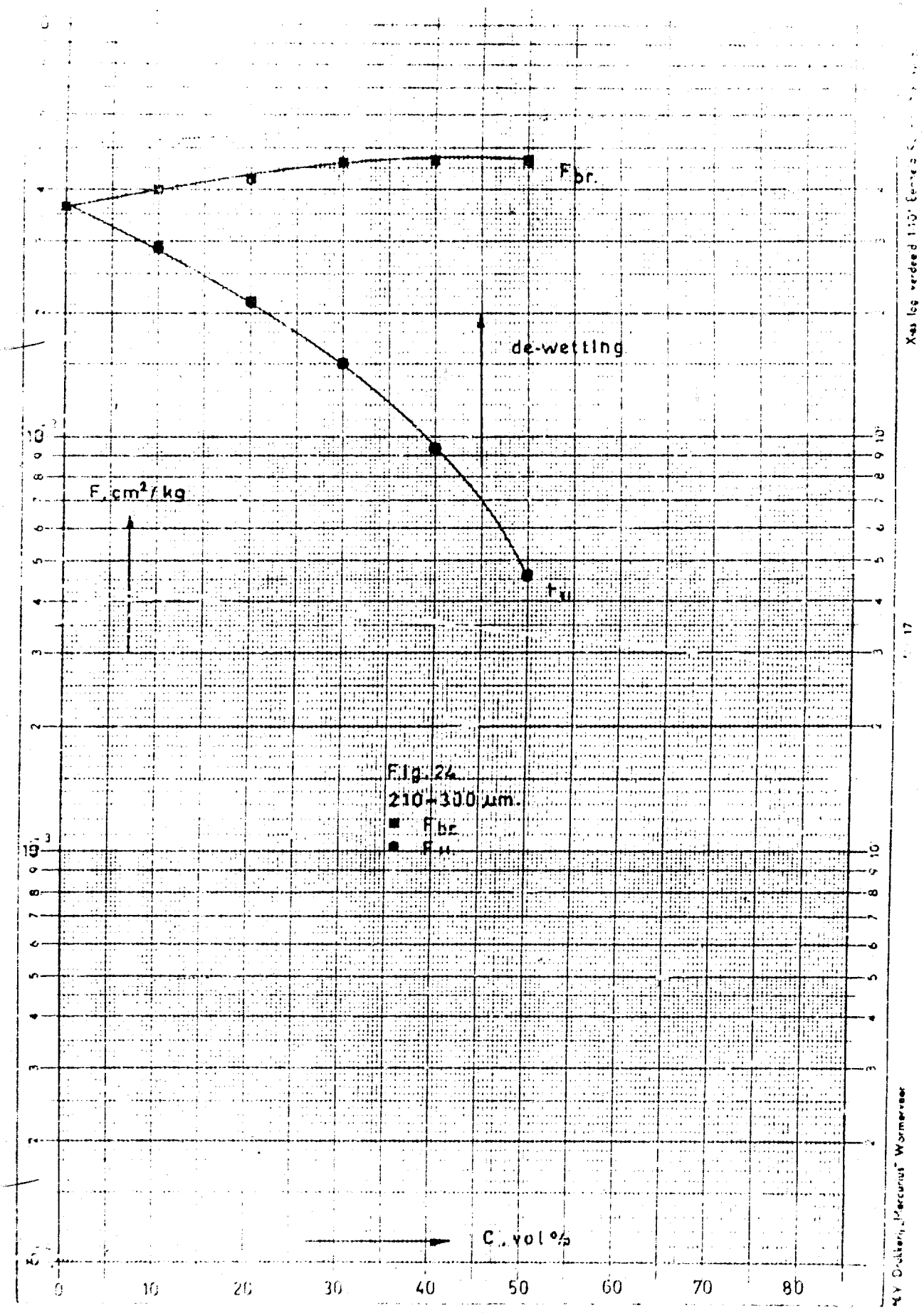

Fig. 24.
210–300 µm.
■ F br.
● F tt.

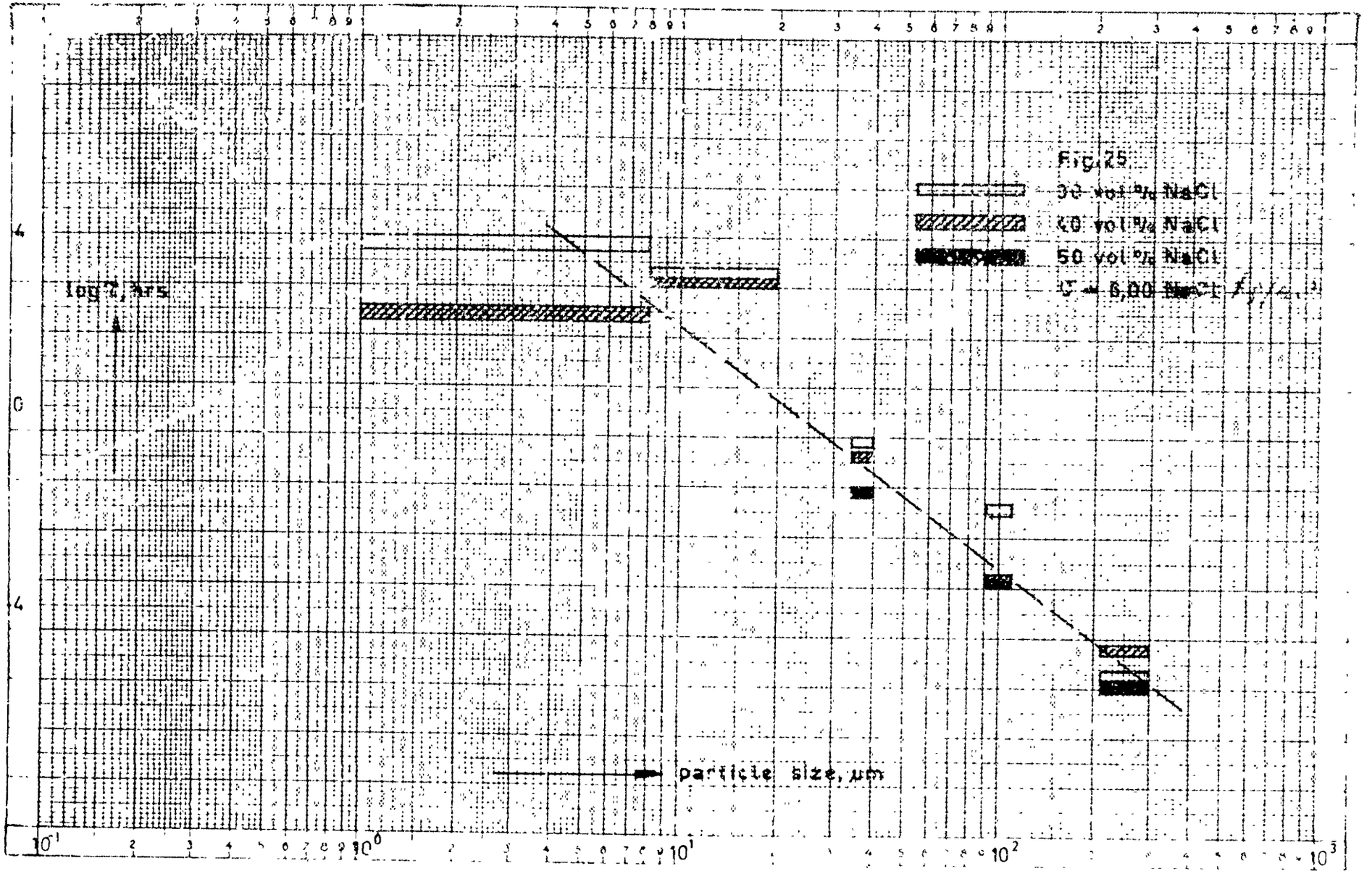
Fig. 25
30 vol % NaCl
40 vol % NaCl
50 vol % NaCl
log t, hrs
particle size, µm

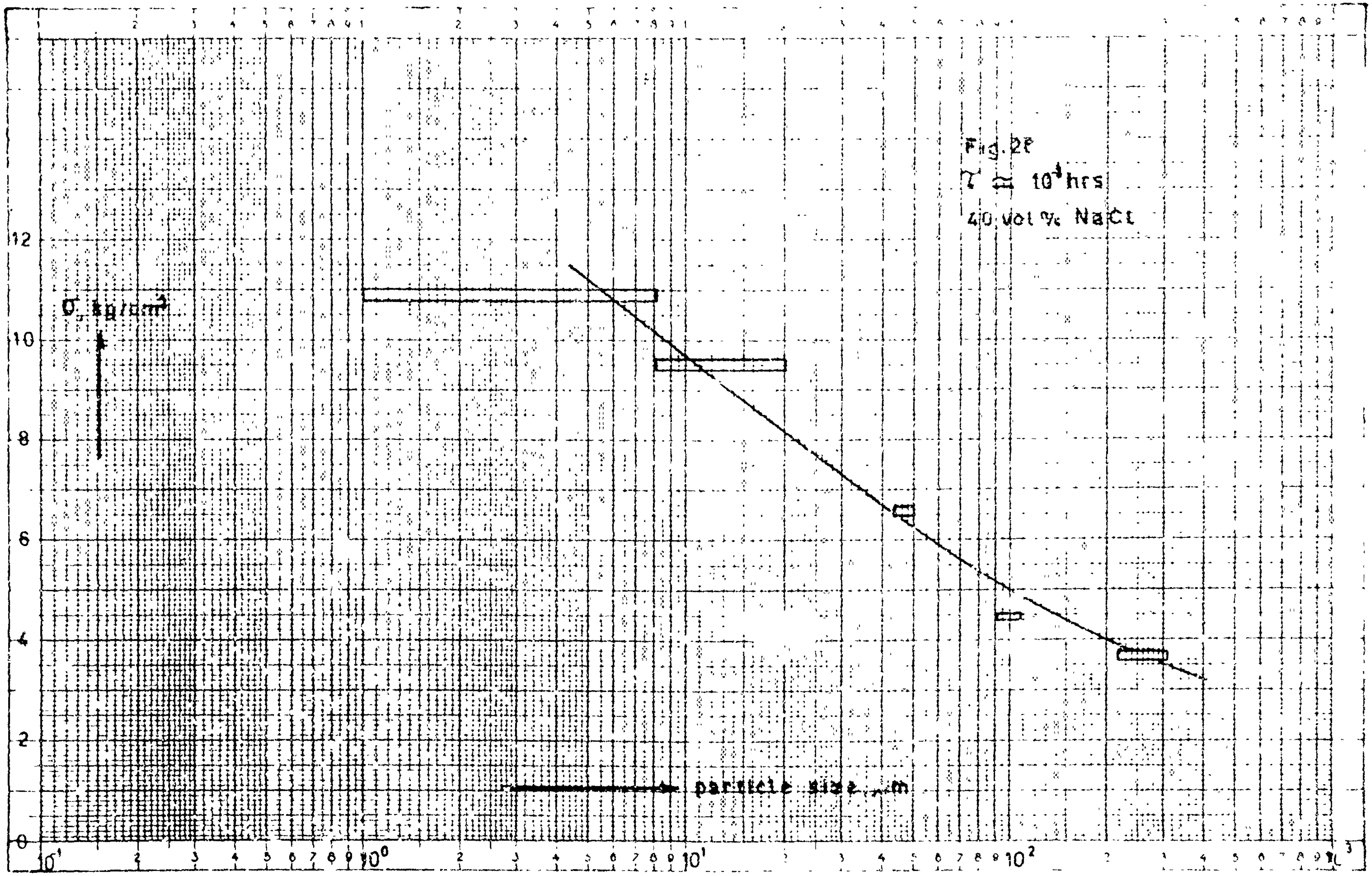

DRUKKERIJ MERCURIUS WORMERVEER No. 12

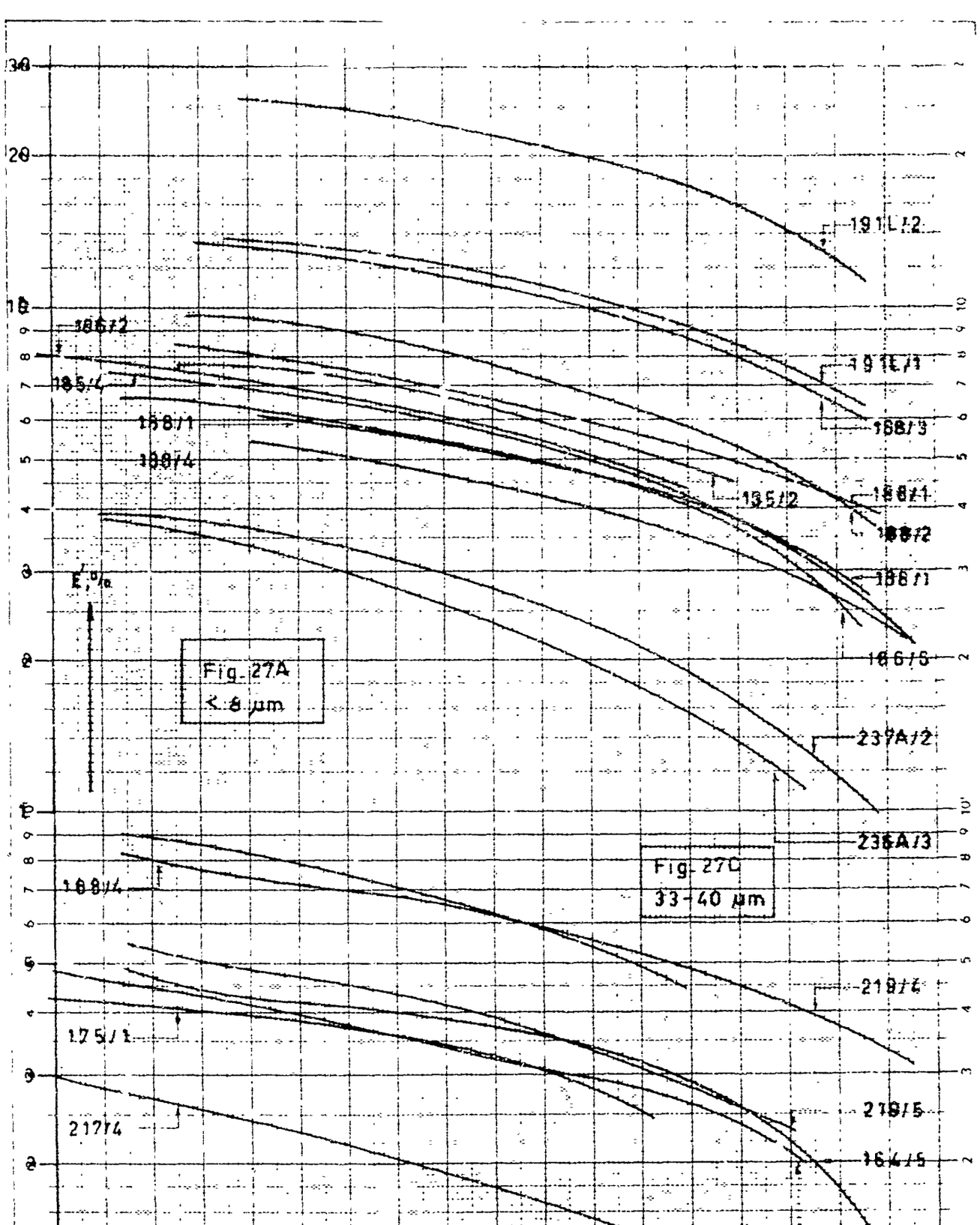
191L/2
188/2
191E/1
185/4
188/3
188/1
188/4
185/2
188/1
188/2
188/1
E, %
Fig. 27A
< 8 µm
166/5
237A/2
236A/3
Fig. 27C
33-40 µm
188/4
219/4
175/1
219/5
217/4
164/5
219/2
log t, hrs
-3
-2
-1
0
1
2
3

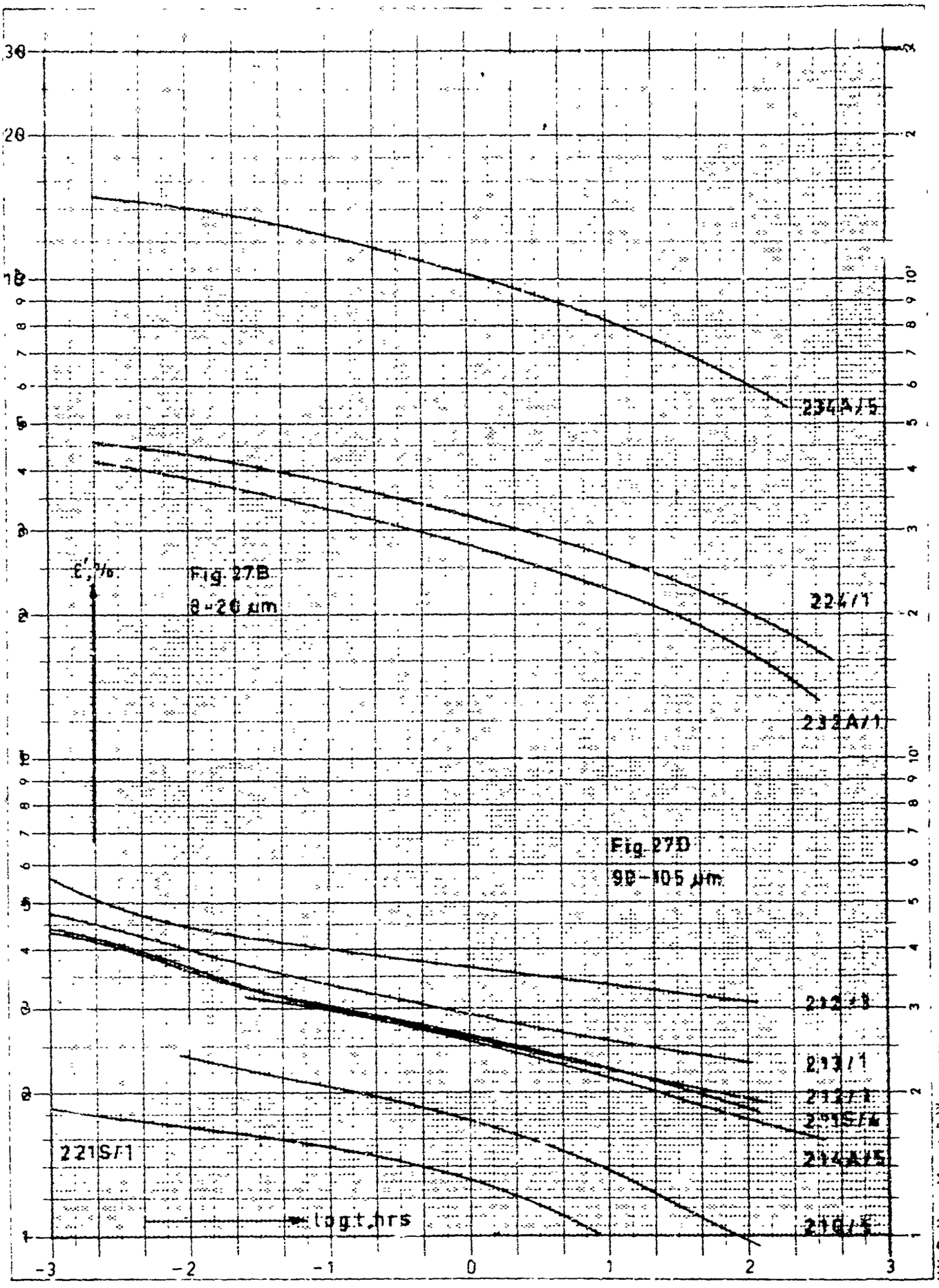
ε', %
Fig. 27B
8-20 µm
Fig. 27D
90-105 µm
234A/5
224/1
232A/1
212+8
213/1
212/1
221S/1
214A/5
216/5
log t, hrs
-3
-2
-1
0
1
2
3

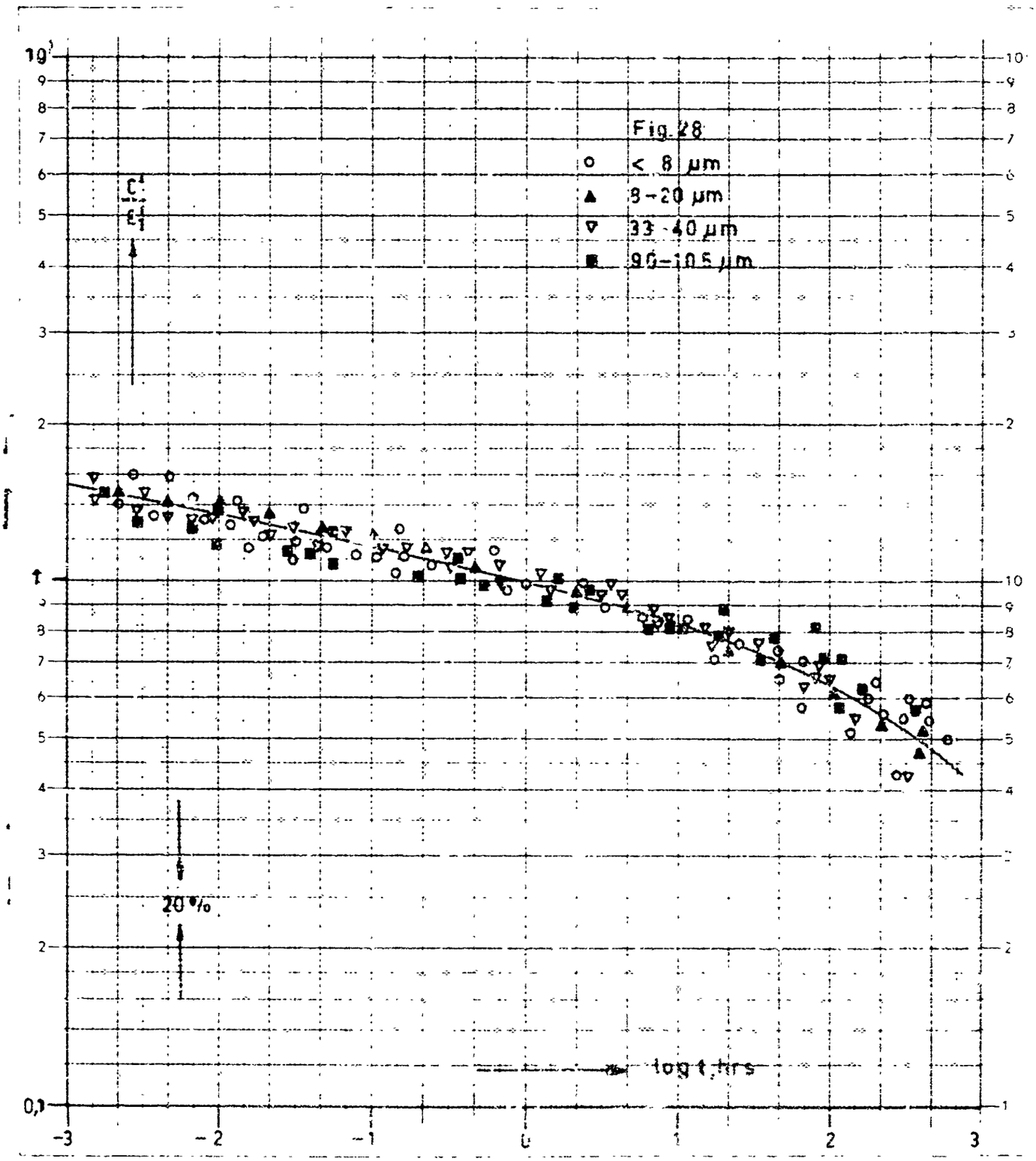

N.V. Drukkerij Mercurius Wormerveer No. 31 TR 60 mm

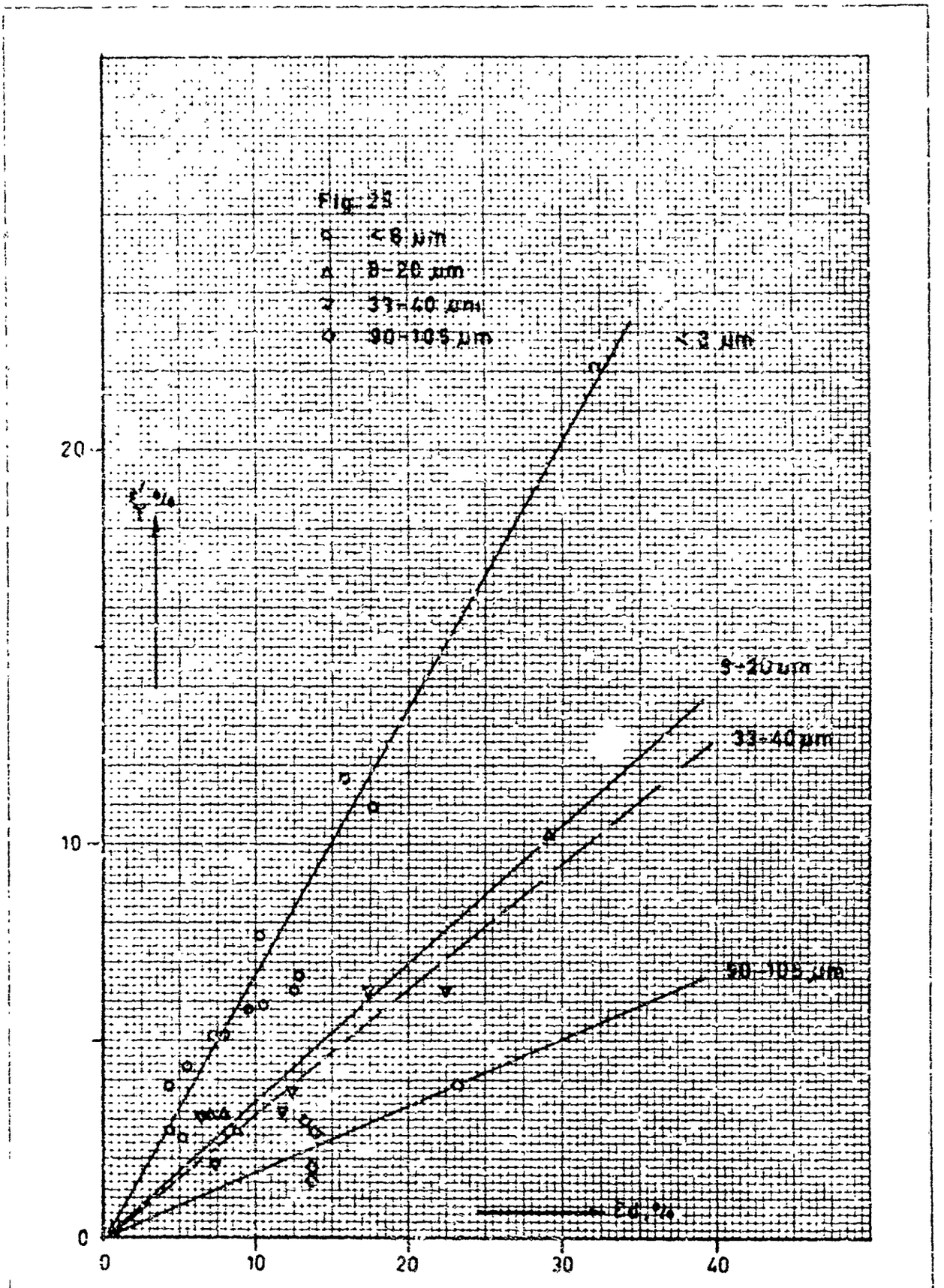

1Q Deelstrepen is 15 m m.

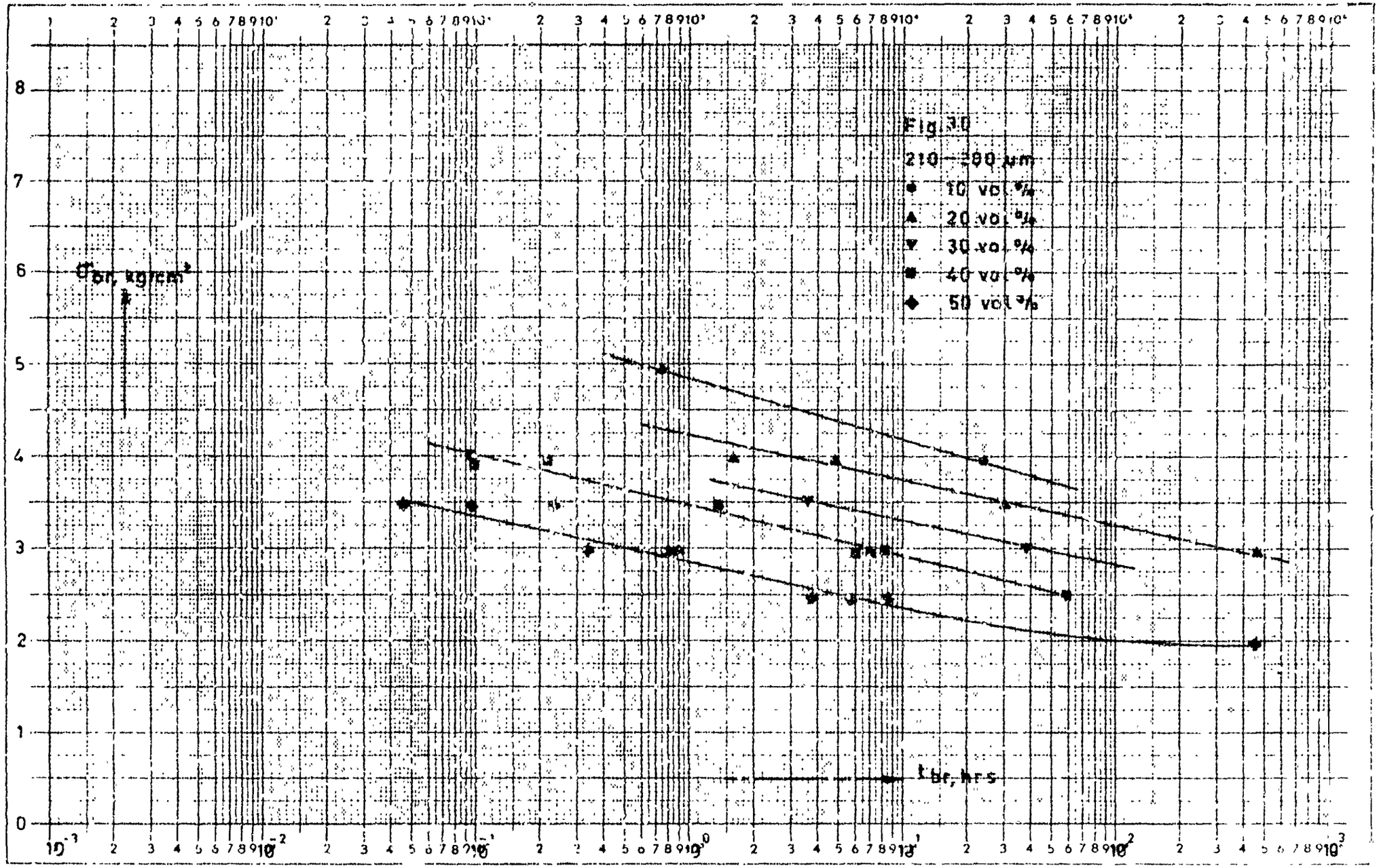
Fig. 30
210—300 µm
10 vol. %
20 vol. %
30 vol. %
40 vol. %
50 vol. %
σbr, kg/cm²
tbr, hrs

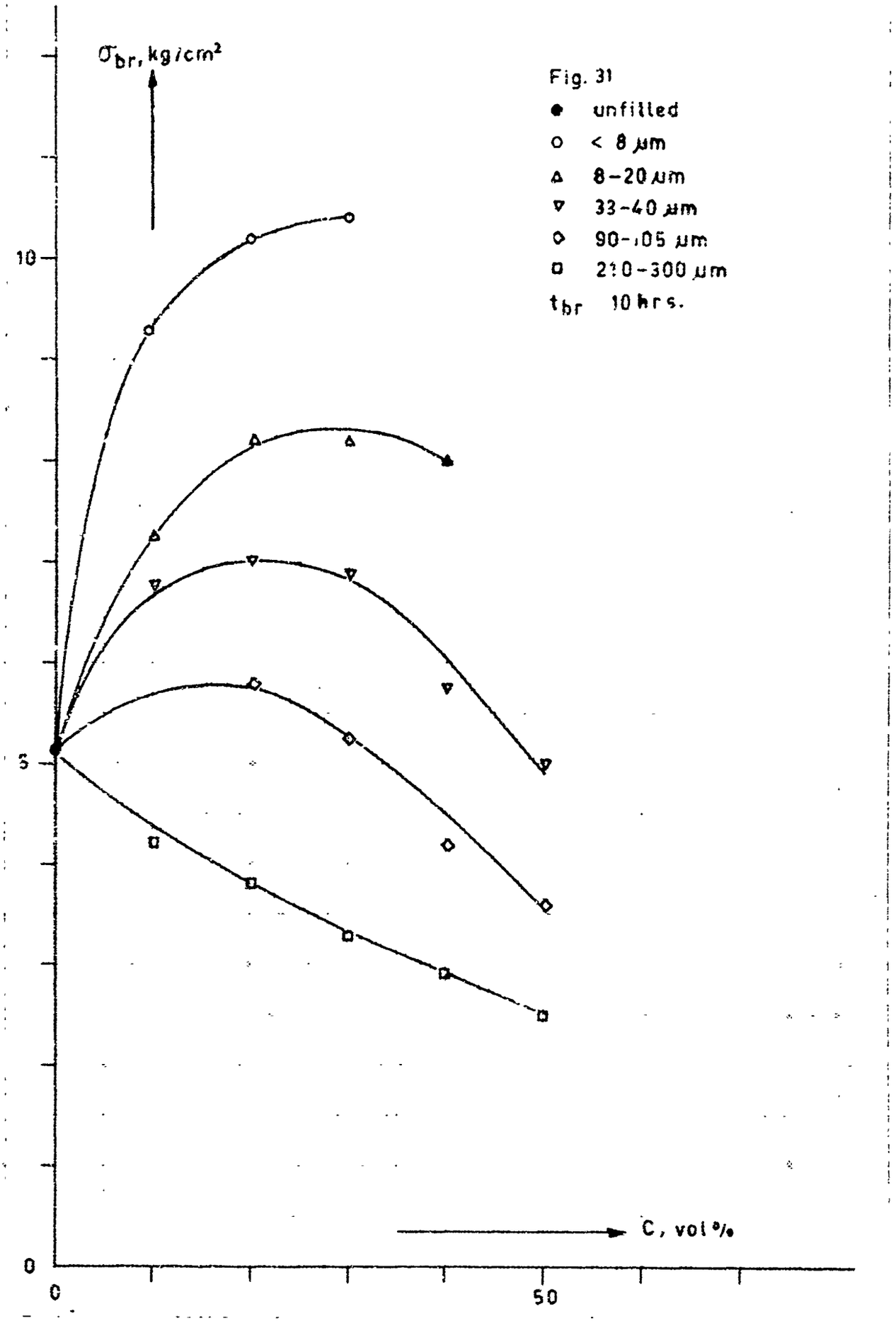
σ_{br}, kg/cm²
10
5
0
0
50
C, vol %
Fig. 31
unfilled
< 8 µm
8–20 µm
33–40 µm
90–105 µm
210–300 µm
t_{br} 10 hrs.

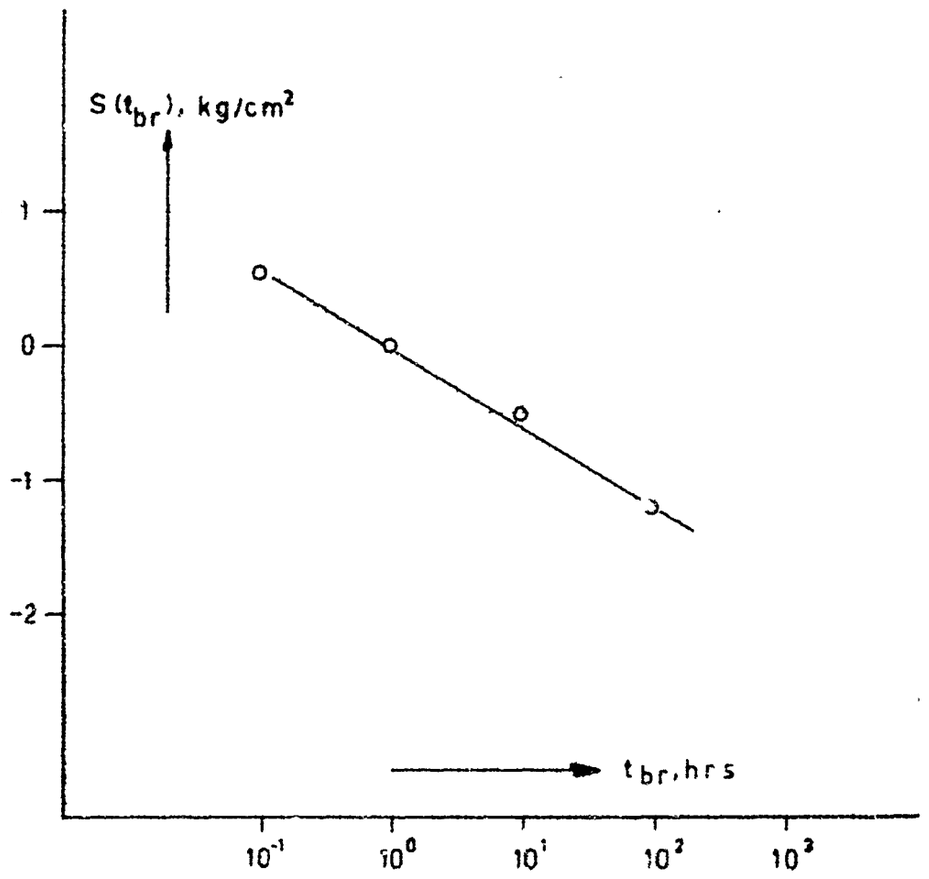

Fig.32

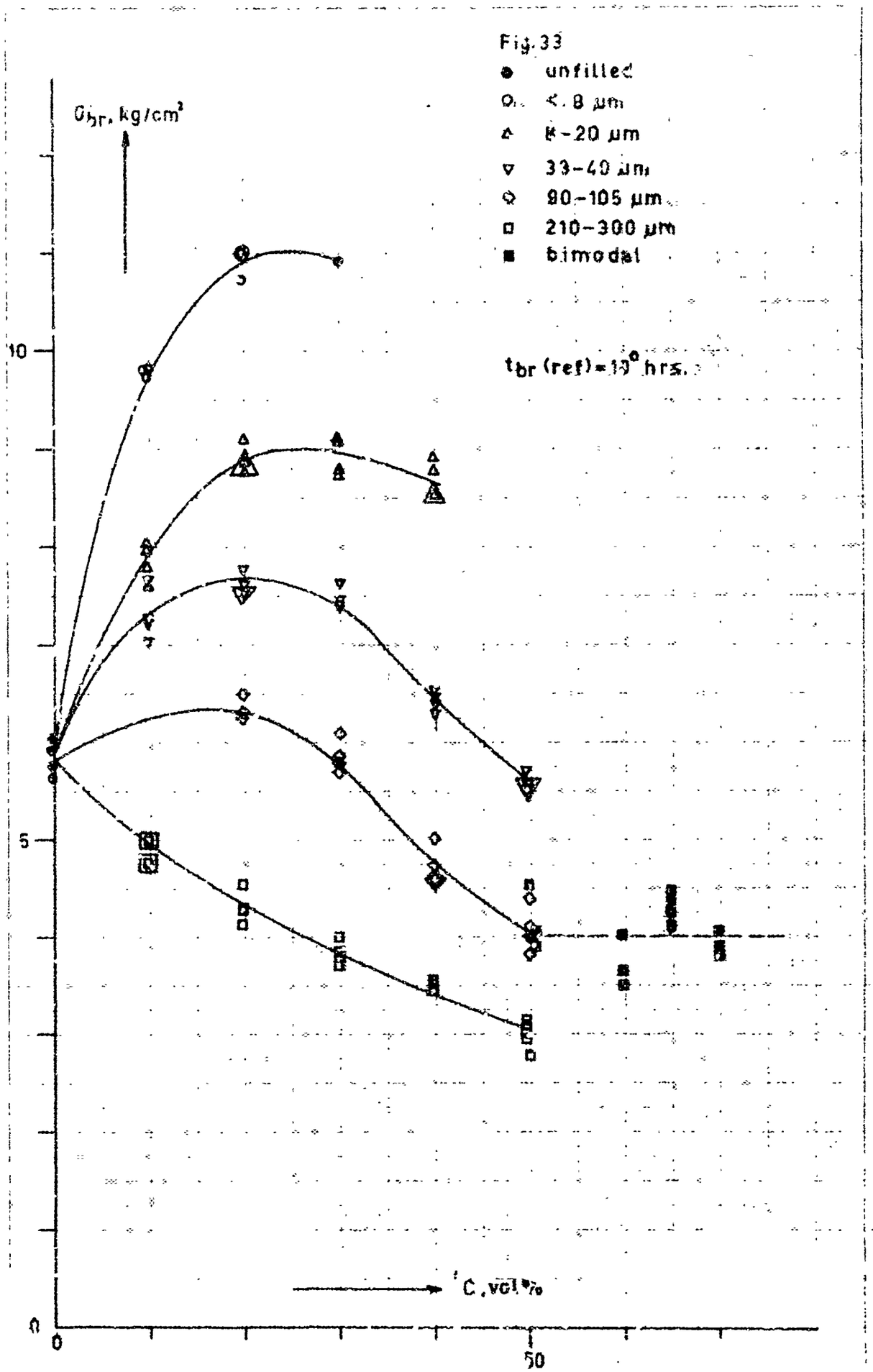
Fig.33
unfilled
< 8 µm
8-20 µm
33-40 µm
80-105 µm
210-300 µm
bimodal
σ_{br}, kg/cm²
t_{br} (ref) = 10^6 hrs.
10
5
1
0
50
C, vol %

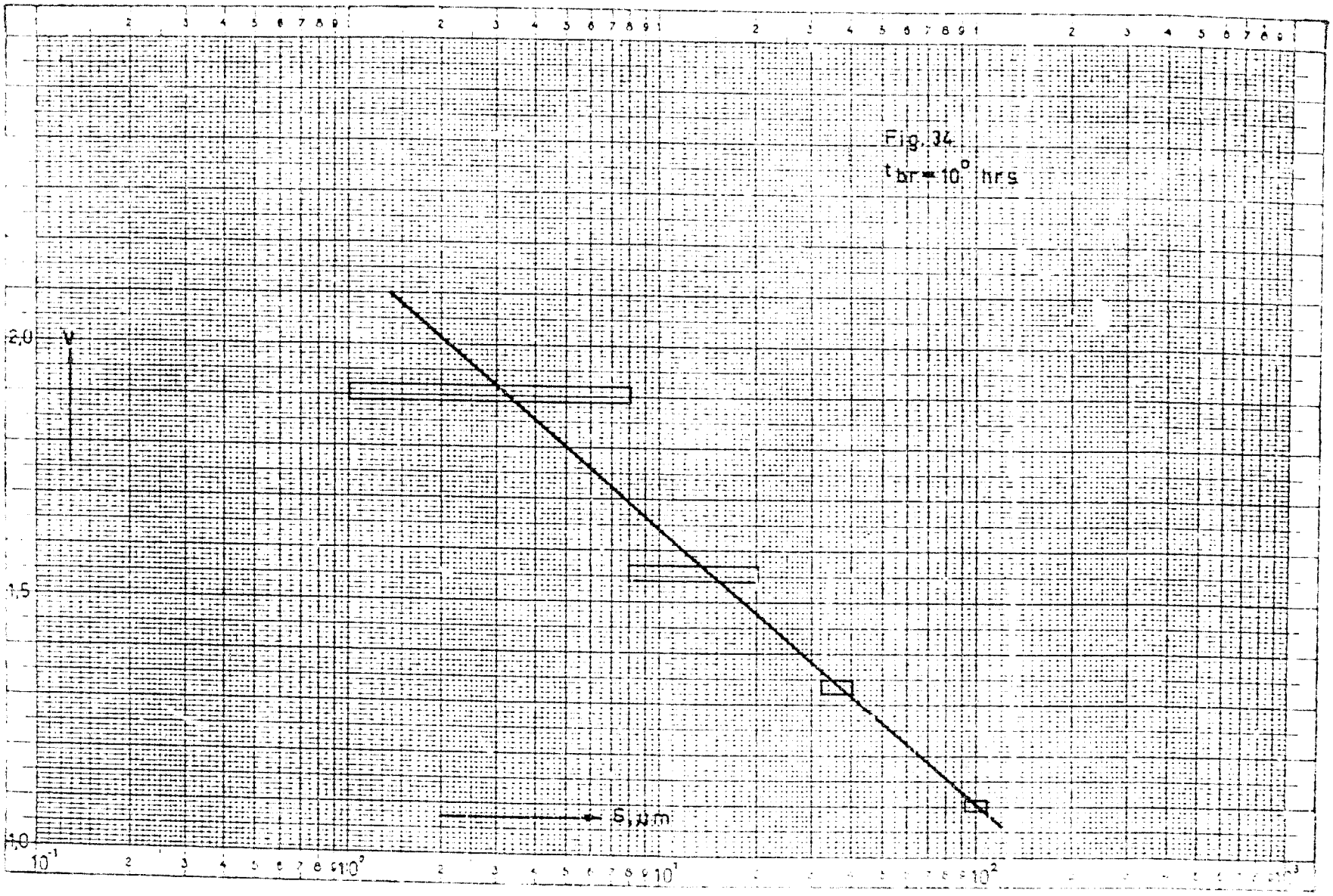

DRUKKERIJ MERCURIUS WORMERVEER NO. 2

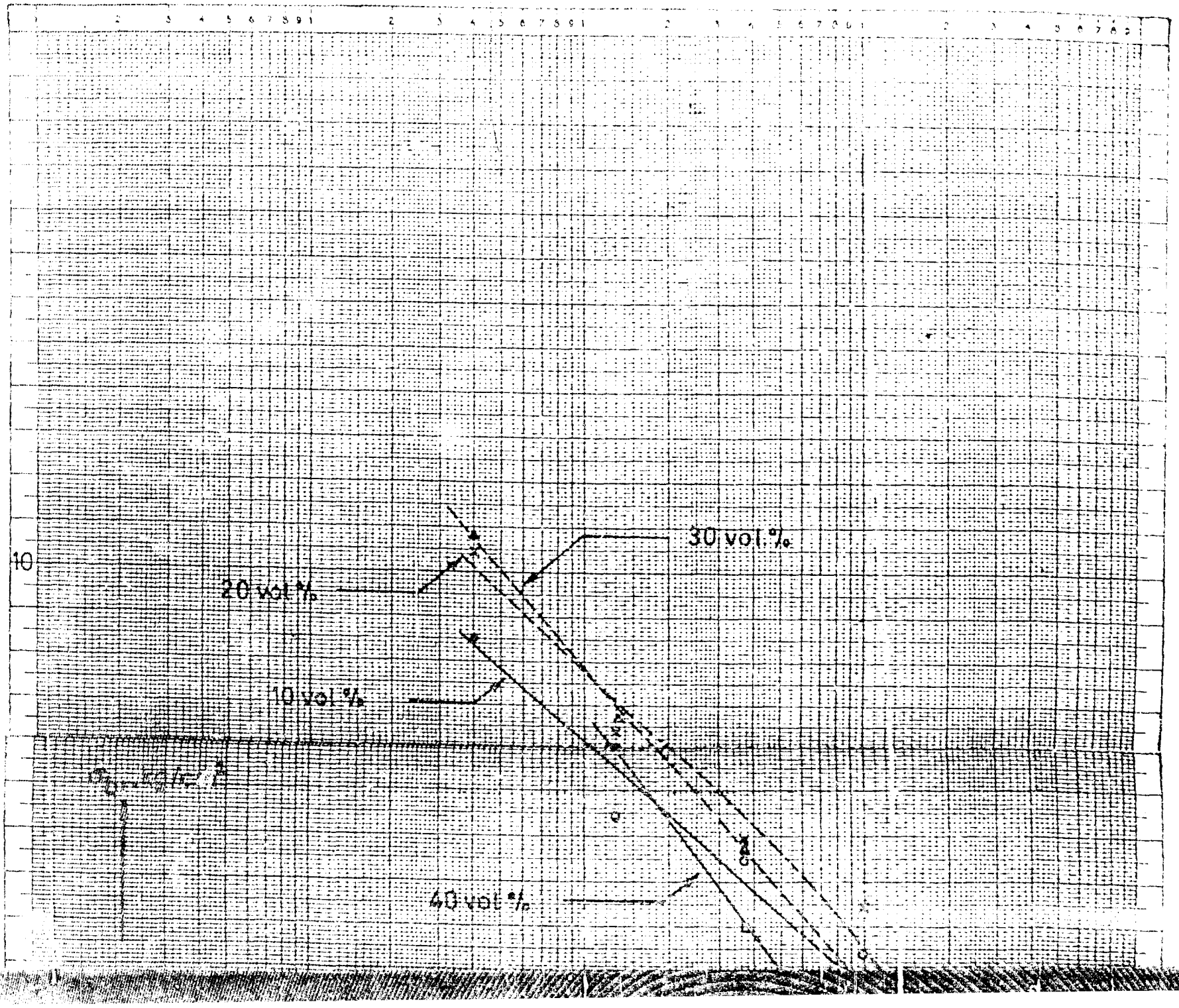
10
30 vol.%
20 vol.%
10 vol.%
40 vol.%

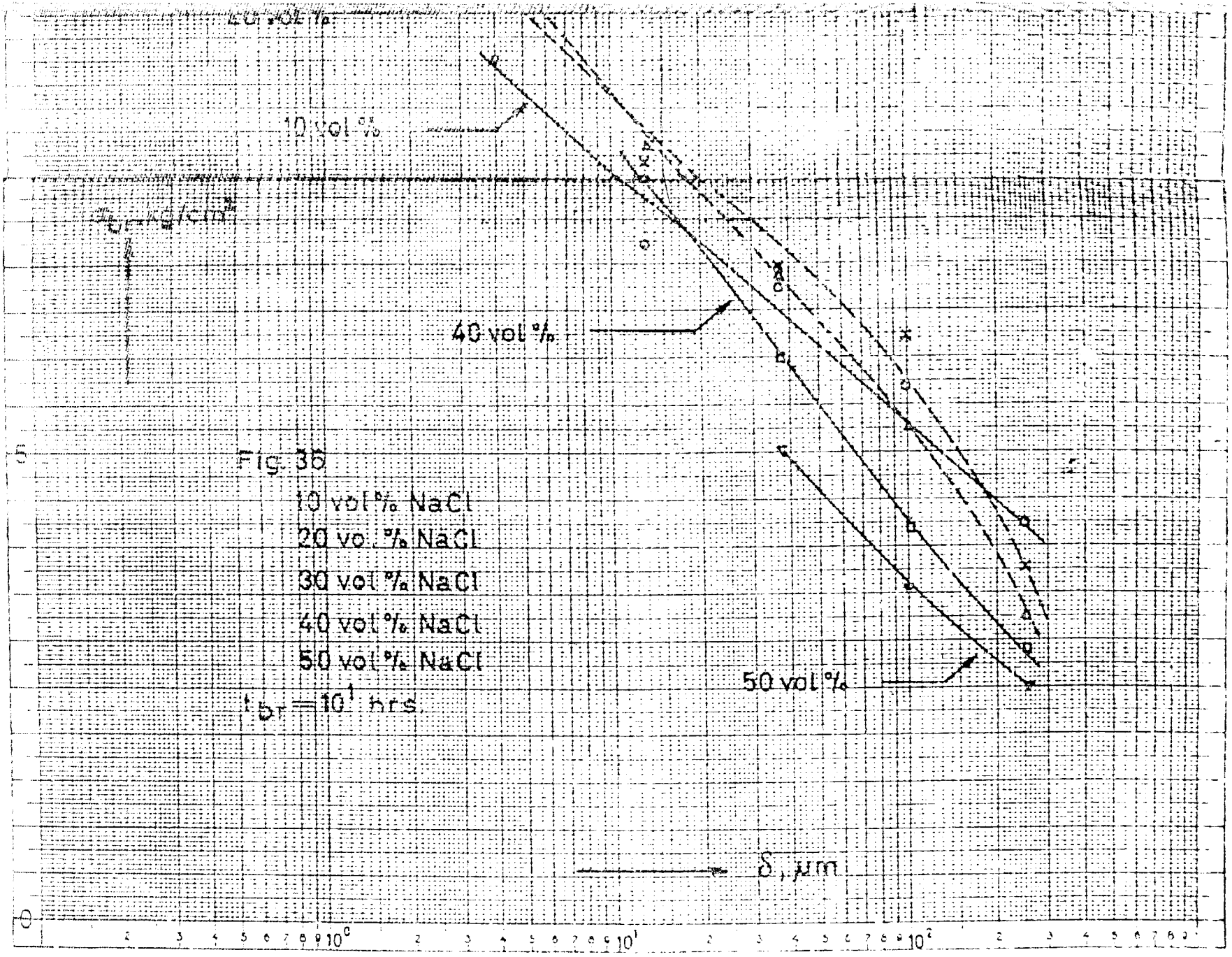

Fig. 36

10 vol % NaCl
20 vo. % NaCl
30 vol % NaCl
40 vol % NaCl
50 vol % NaCl

$t_{br} = 10^1$ hrs.

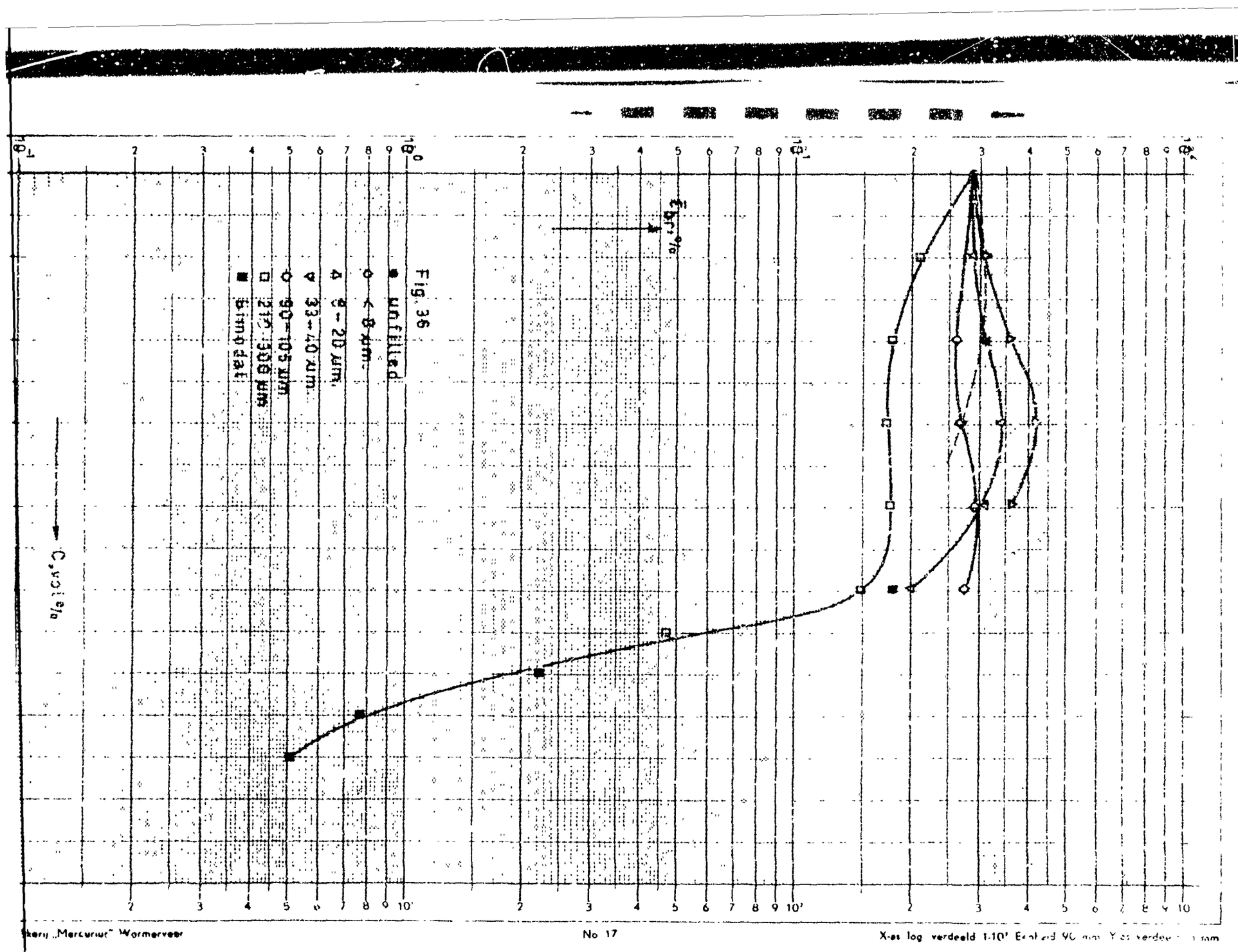
Fig. 36
● unfilled
◇ < 8 µm.
◆ 8 - 20 µm.
▽ 33 - 40 µm.
◇ 90 - 105 µm.
□ 212 - 300 µm.
■ bimodal

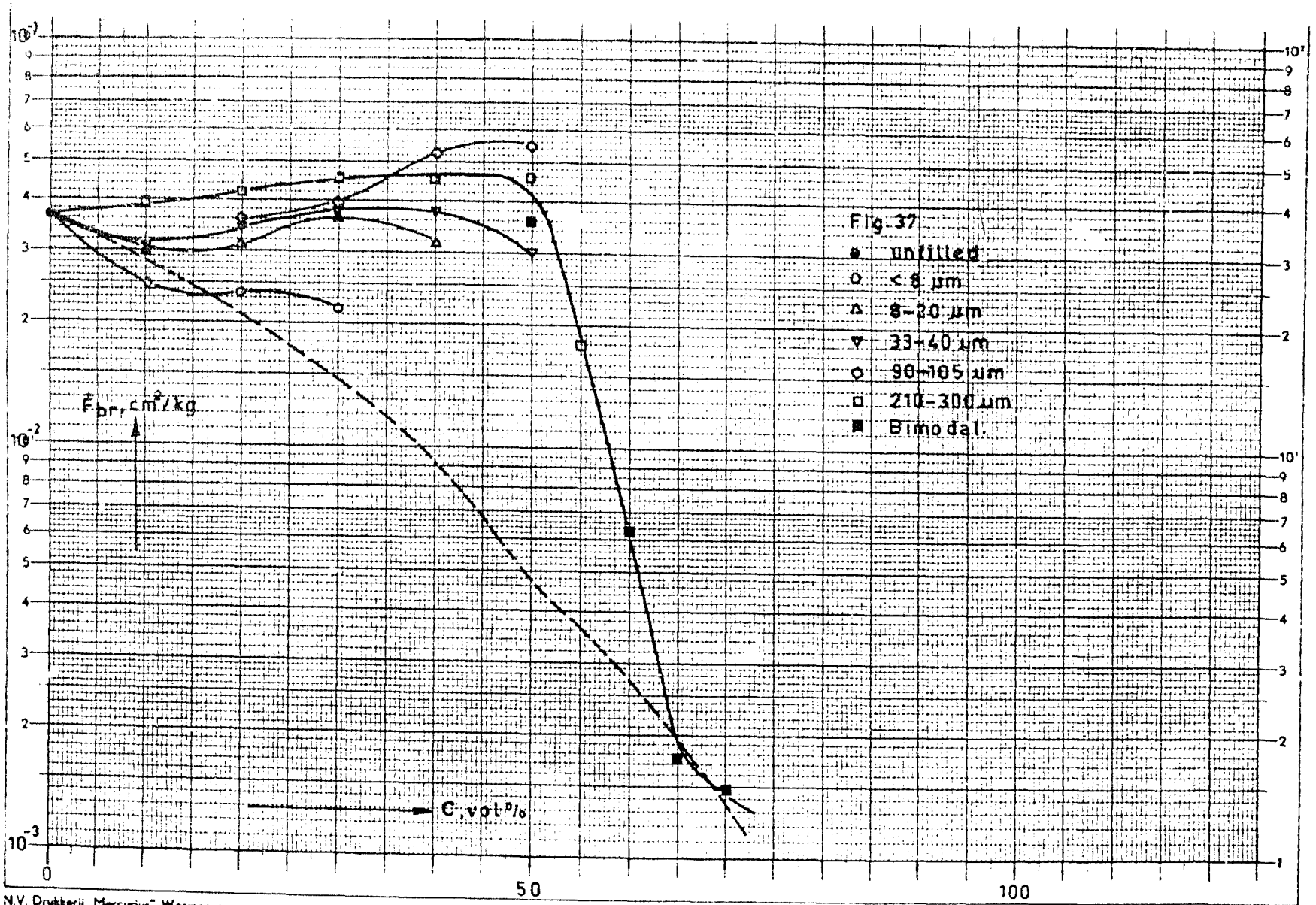

N.V. Drukkerij „Mercurius" Wormerveer

No 16

X-as verdeeld in mm. Y-as log verdeeld 1-10² Eenheid 83.33 mm.

APPENDIX II

NUMERICAL DATA CONCERNING THE TIME-STRESS REDUCTION

Tables II.1 to II.5 summarize numerical data for the time-stress shift for all materials of which creep curves were reduced to master curves (see section 4.5). Each table concerns materials filled with various amounts of the same sodium chloride fraction. The first (upper) row gives filler size, the second filler content, the third the batch number. Values for the time-stress shift log $a(\sigma,\sigma_o)$ are given in time decades as a function of the stress level σ. The reference stress level σ_o in these tables is 6.00 kg/cm^2.

For several materials no creep curves at the reference stress σ_o = 6.00 kg/cm^2 were available. For these materials, initially another reference stress σ_o' was chosen. These levels are indicated in Tables II.1 to II.5 by a cross at the shift number belonging to this stress σ_o'. For instance, a level σ_o' = 3.00 kg/cm^2 was used initially as reference for materials filled with fraction no. 2 (210 - 300 µm); see Table II.1. Afterwards, the shift data were transposed to the reference level σ_o = 6.00 kg/cm^2 by adding a factor found by inter- or extrapolation of the shift function.

Table II.6 gives numerical data of the maximum scatter, S, of the shifted experimental points, around the master curves (see section 4.5). S, concerning Figs 11-15 and Figs 18-22, is given is scale-units. 1 scale-unit for these figures equals 1.5 mm.

Table II.1 Time-stress shift log $a(\sigma,\sigma_o)$; σ_o = 6.00 kg/cm^2

210 - 300 µm									
σ kg/cm^2	10 %	20 %	30 %	40 %			50 %		
	138	123	131	133	122	230 A	134	223	231 A
2.0	- x)	- x)	- x)	- x)		-5.96	-6.69		
2.5			-5.69	-5.65			-5.41	-5.48	-5.39
3.0	-4.50*)	-4.50*)	-4.50*)	-4.50*)	-4.50*)	-4.50*)	-4.50*)	-4.50*)	-4.50*)
3.5		-3.20	-3.55	-3.57			-3.50		-3.82
4.0	-1.7	-1.96			-2.76	-3.05			
4.5									
5.0	-1.1								
5.5									

Table II.2 Time-stress shift log $a(\sigma,\sigma_o)$; σ_o = 6.00 kg/cm^2

90 - 105 µm							
σ kg/cm^2	20 %	30 %		40 %		50 %	
	210	211	214 A	212	216 A	213	215 A
3.0				-4.34	-3.94	-4.70	-4.55
3.5			-2.78	-3.18	-3.09	-2.51	-3.50
4.0		-2.00		-2.09	-2.14		-1.92
4.5	-1.50		-1.50	-1.50*)	-1.50*)	-1.50*)	-1.50*)
5.0	-1.00	-0.84			-1.08		
5.5	-0.50	-0.54	-0.64				
6.0	0.00	0.00					
6.5	0.45		0.68*)				
7.0							
7.5			1.56				

x) creep curves not used for time-stress reduction
*) initial reference stress σ'_o

Table II.3 Time-stress shift log $a(\sigma,\sigma_o)$; σ_o = 6.00 kg/cm^2

33 - 40 µm												
σ kg/cm^2	10 %		20 %		30 %			40 %				50 %
	164	217	166	218	168	219	239 A	170	240 A	220	205 A	206 A
4.0						-2.52						
4.5												-2.65
5.0		-1.22		-1.40	-1.77	-1.22	-1.48		-1.18		-1.35	-2.11
5.5	-0.82							-0.80		-1.13	-0.52	-0.8
6.0	0.00	0.00	0.00	0.00	0.00	0.00	0.00	0.00	0.00	0.00	0.00	
6.5										0.53	0.43	0.5*)
7.0	0.91	0.75	0.60	1.04	1.18	0.81	0.58			1.00		
7.5	1.32		1.11		1.68			1.11				
8.0	1.43	1.00	1.50	1.38	2.00	1.60						

Table II.4 Time-stress shift log $a(\sigma,\sigma_o)$; σ_o = 6.00 kg/cm^2

8 - 20 µm									
σ kg/cm^2	10 %			20 %			30 %		40 %
	178	224	232 A	180	225	233 A	181	234 A	235 A
5.0		-1.00							
5.5									
6.0	0.00		0.00				0.00	0.00	
6.5									0.50*)
7.0								0.90	
7.5	1.00	1.18	1.30	1.25*)		1.25*)			1.60
8.0								2.48	
8.5	2.09			2.90	2.00*)	2.06			2.74
9.0							3.40	3.28	
9.5					3.40	3.25			4.08

Table II.5 Time-stress shift log $a(\sigma,\sigma_o)$; σ_o = 6.00 kg/cm^2

< 8 µm							
σ kg/cm^2	10 %		20 %		30 %		40 %
	185/190	236 A	186	237 A	188	238 A	191 L
4.0				-0.92			
4.5							
5.0					-0.22		-0.48
5.5		-0.57					
6.0	0.00		0.00		0.00		0.00
6.5							
7.0		0.90	0.48	0.48*)	0.34		
7.5	1.12		0.88				
8.0					0.93	0.93*)	
8.5	1.64						
9.0	2.48		1.66				
9.5	2.90	2.90*)					
10.0			2.5	2.59		2.47	
10.5							
11.0			3.11				

Table II.6 Maximum scatter S of shifted experimental points around the master curves; S in scale units (1.5 mm)

content of filler	210 - 300 μm		90 - 105 μm		33 - 40 μm		8 - 20 μm		< 8 μm	
	no.	S sc.un.	no.	S sc.un.	no.	S sc.un.	no.	S sc.un.	no.	S sc.un.
10	138	1.2			164 217	0.9 0.9	178 224 232 A	0.9 0.6 0.6	185/190 236 A	0.6 1.5
20	123	1.5	210	1.8	166 218	1.2 1.5	180 225 233 A	1.2 1.2 1.2	186 237 A	0.9 0.9
30	131	6.3	211 214 A	1.5 3.9	168 219 239 A	3.0 2.4 1.5	181 234 A	1.2 1.2	188 238 A	0.9 0.9
40	133 222 230 A	7.2 1.8 2.1	212 216 A	10.8 5.2	170 220 205 A 240 A	1.2 3.9 4.2 3.3	235 A	5.7	191 L	<0.2
50			213 215 A	7.2 9.0	206 A	2.7				

APPENDIX III

NUMERICAL DATA CONCERNING TENSILE STRAIN RECOVERY

Table III,1 summarizes for each specimen used for tensile strain recovery experiments from left to right:

(a) the specimen number, the number and size of the fraction and the content of filler;

(b) typical data on the primary creep experiment preceding recovery. These data are the stress $\sigma_{pr.creep}$; the elapsed time t_1 and the strain ε_{max} at the moment of unloading; the strain ε_o at the beginning of the primary creep experiment as calculated from the modulus in the non-dewetted state (see section 4.4) and, finally, the contribution $\varepsilon_{max} - \varepsilon_o$ of the de-wetting proces to strain ε_{max};

(c) the strain ε_1' at a recovery time of 1 h.

Table III.1

spec.no.	fraction no.	NaCl vol.%	$\sigma_{pr.cr}$ kg/cm^2	t_1 hrs	ε_{max} (%)	ε_o (%)	$\varepsilon_{max} - \varepsilon_o$ (%)	ε_1' (%)
185/2	8	10	7.5	1480	27.65	15.0	12.7	6.37
185/4	< 8 µm	10	7.0	1440	24.00	14.0	10.0	5.66
185/5		10	6.0	1300	17.52	12.0	5.5	-
236 A/3		10	4.5	1000	14.10	8.8	5.3	2.52
186/1		20	7.5	1200	21.15	9.0	12.2	6.56
186/2		20	7.0	1300	17.40	7.2	10.2	5.80
186/6		20	6.0	1400	13.95	6.1	7.9	5.20
237 A/2		20	4.0	1000	8.43	3.7	4.7	2.74
188/1		30	6.0	1600	10.76	3.4	7.4	5.20
188/2		30	7.0	1500	14.85	4.0	10.9	7.65
188/3		30	8.0	1500	21.9	4.5	17.4	11.00
188/4		30	5.0	1300	8.14	2.8	5.3	4.40
191 L/1		40	5.0	1550	17.8	1.8	16.0	11.60
191 L/2		40	6.0	1500	34.4	2.4	32.0	22.00
224/1	7	10	5.0	980	17.8	11.0	6.8	3.21
232 A/1	8-20 µm	10	6.0	930	23.1	14.5	8.6	2.78
234 A/5		30	6.0	1000	34.2	4.9	29.3	10.15
164/5	6	10	5.5	1340	26.4	14.0	12.4	3.70
217/4	33-40 µm	10		1000	19.6	12.2	7.4	1.80
218/2		20		850	18.7	7.0	11.7	3.20
168/4		30		1030	21.7	4.5	17.2	6.20
219/4		30		980	26.8	4.1	22.7	6.20
175/1		40		1460	7.89	1.8	6.1	3.20

Table III.1 (Continued)

spec.no.	fraction no.	NaCl	$\sigma_{pr.cr.}$	t_1	ε_{max}	ε_o	$\varepsilon_{max} - \varepsilon_o$	ε_1'
		vol.%	kg/cm^2	hrs	(%)	(%)	(%)	(%)
210/5	4	20	4.5	1010	21.2	7.5	13.7	1.8
214 A/5	90 - 105 µm	30	3.5	890	16.5	3.4	13.1	1.4
212/1		40	3.0	1100	15.1	1.7	13.4	2.7
212/3		40	3.5	910	25.1	1.8	23.3	3.8
213/1		50	3.0	1150	13.5	0.7	12.8	3.0
138/2	2	10	3.0	820	12.65	8.0	4.65	0.30
123/1	210 - 300 µm	20	2.0	1000	5.49	4.2	1.29	0.06
131/1		30	2.0	960	4.75	2.2	2.55	0.32
131/3		30	2.5	420	10.50	2.8	7.7	1.1
133/1		40	2.0	850	6.20	1.2	5.0	0.94
204/2		55	2.0	1000	5.90	0.4	5.5	1.26

CENTRAAL LABORATORIU

APPENDIX IV NU

Table IV.1 Rupture
and of

σ_{br}, kg

C vol.%	t_{br} hrs	210 - 300 µm				90 - 105 µm			33 - 40 µm			
		W. A*)		A*)	M*)	W. A	A	M	W. A		A	
10	10^{-1}	5.60			5.60			x	7.85		7.35	
	10^{0}	5.00			5.00			x	7.00	7.50		
	10^{1}	4.25			4.25			x	7.10	6.50		
	10^{2}	3.50			3.50			x	6.10	6.75		
20	10^{-1}	4.70			4.70	6.75		6.75		8.00	8.25	
	10^{0}	4.25			4.25	6.30		6.30		7.50	7.70	
	10^{1}	3.80			3.80	5.80		5.80		6.90	7.10	
	10^{2}	3.30			3.30	5.25		5.25			6.50	
30	10^{-1}	4.30			4.30	6.45	7.25	6.45	8.50		8.00	
	10^{0}	3.80			3.80	5.65	6.50	6.07	7.50	7.70		
	10^{1}	3.30			3.30	4.85	5.60	5.25	6.80	6.90		
	10^{2}	2.75			2.75	4.10	4.75	4.42	-	-	-	-
40	10^{-1}	4.00	4.00	4.20	4.10		5.30	5.30	7.00	7.20		6.90
	10^{0}	3.45	3.50	3.60	3.51	4.40	4.80	4.60	6.50	6.50		6.25
	10^{1}	2.90	2.95	3.00	2.95	4.10	4.25	4.18	6.10	5.75	5.60	5.60
	10^{2}			2.30	2.30	3.90	3.75	3.82	5.70	4.90	4.90	
50	10^{-1}	3.25	3.35	3.50	3.36	4.40	4.35	4.38			6.10	
	10^{0}	3.00	2.80	3.05	2.95	4.00	4.00	4.00			5.55	
	10^{1}	2.60	2.40	2.50	2.50	3.50	3.65	3.57			5.00	
	10^{2}			1.90	1.90	3.00	3.30	3.15			4.45	

*) W.A samples not treated with Asolectin

A: sample treated with Asolectin

Delft, June 8, 1966
Str/K

A

APPENDIX IV NUMERICAL DATA OF RUPTURE PROPERTIES

Table IV.1 Rupture stress σ_{br} at various values of content and size of the filler, and of the rupture time t_{br}.

σ_{br}, kg/cm^2 vs content of filler, t_{br}, particle size

	33 - 40 µm					8 - 20 µm				< 8 µm		
	W. A		A		M	W. A		A	M	W. A	A	M
	7.85		7.35		7.60	8.50			8.50	10.70	10.10	10.40
	7.00	7.50			7.25	7.50		7.70	7.60	10.00	9.35	9.70
	7.10	6.50			6.80	7.25			7.25	9.25		9.25
	6.10	6.75			6.42	6.75			6.75	8.50		8.50
75		8.00	8.25		8.10	9.60	9.00	9.50	9.40			
30		7.50	7.70		7.60	8.60	9.10	8.70	8.80	11.50	10.50	11.00
80		6.90	7.10		7.00	8.10	8.50	8.10	8.20	10.70	9.70	10.20
25			6.50		6.50	7.70	8.00		7.85	9.75		9.75
45	8.50		8.00		8.00			9.65	9.65			x
07	7.50	7.70			7.60			9.00	9.00			x
25	6.80	6.90			6.85			8.20	8.20		10.40	10.40
42	-	-	-	-	x			7.45	7.45			x
30	7.00	7.20		6.90	7.10			9.50	9.50			x
60	6.50	6.50		6.25	6.42			8.75	8.75			x
18	6.10	5.75	5.60	5.60	5.75			8.00	8.00			x
82	5.70	4.90	4.90		5.10			7.25	7.25			x
38			6.10		6.10				x			x
00			5.55		5.55				x			x
57			5.00		5.00				x			x
15			4.45		4.45				x			x

eated with Asolectin M : mean value

B

Unclassified
Security Classification

DOCUMENTATION CONTROL DATA - R & D
(Security classification of title, body of abstract and indexing annotation must be entered when the overall report is classified)

1. ORIGINATING ACTIVITY (Corporate author) F.R. Schwarzl	2a. REPORT SECURITY CLASSIFICATION 2b. GROUP

3. REPORT TITLE
Mechanical Properties of Highly Filled Elastomers V, Influence of Filler Characteristics on Tensile Creep at Large Deformations, on Rupture Properties and on Tensile Strain Recovery

4. DESCRIPTIVE NOTES (Type of report and inclusive dates)
Technical Report No. 5

5. AUTHOR(S) (First name, middle initial, last name)
Leendert C.E. Struik, Hendricus W. Bree, Friedrich R. Schwarzl

6. REPORT DATE April 1966	7a. TOTAL NO. OF PAGES 41	7b. NO. OF REFS 9

8a. CONTRACT OR GRANT NO. N 62558 b. PROJECT NO. 3884 c. 4375 d.	9a. ORIGINATOR'S REPORT NUMBER(S) Technical Report No. 5 9b. OTHER REPORT NO(S) (Any other numbers that may be assigned this report) CL/66/61

10. DISTRIBUTION STATEMENT
Distribution List for Unclassified Technical Reports Issued Under the ONR Contract Research Program in Structural Mechanics

11. SUPPLEMENTARY NOTES	12. SPONSORING MILITARY ACTIVITY Office of Naval Research, Washington DC

13. ABSTRACT

About 60 polyurethane - sodium chloride composites were prepared. The content for materials filled with single fractions ranged from 0 to 55 per cent. by volume; the size of these fractions from 1 μm to 300 μm. Materials with a content of 50 to 70 per cent. by volume were made by using a mixture of a coarse and a fine fraction.

For these materials, primary tensile creep and rupture properties, both at various constantly high stress levels, were determined at room temperature. The filled rubbers showed a typical tensile creep behaviour, related to the growth of vacuoles in the material (de-wetting). Definite relationships were found between respectively:
uniformity of creep over the gauge length and content of filler;
location of considerable creep on time scale and particle size as well as stress level;
shape of the creep curve and content of filler;
rupture stress and particle size, filler content and rupture time;
rupture elongation and content of filler.

Generally, the processes of de-wetting, recovery and rupture were considerably delayed by a decrease in particle size (reinforcement).

DD FORM 1 NOV. 65 1473 (PAGE 1)
S/N 0101-807-6811

Unclassified
Security Classification

A-31408